# A STUDY ON CONTROL OF ACCUMULATORS IN CONTINUOUS WEB PROCESSING LINES

By

INDERPAL SINGH

Bachelor of Science

Thapar Institute of Engineering & Technology

Punjab, India

1998

Submitted to the Faculty of the
Graduate College of the
Oklahoma State University
in partial fulfillment of
the requirements for
the Degree of
MASTER OF SCIENCE
December, 2002

A STUDY ON CONTROL OF ACCUMULATORS IN CONTINUOUS WEB PROCESSING LINES

Thesis Approved:

Prabhakar Pagilla

Thesis Advisor

Gary E. Young

Dean of the Graduate College

## ACKNOWLEDGMENTS

I wish to express my sincerest appreciation to my major advisor, Dr. Prabhakar R. Pagilla for his intelligent supervision, constructive guidance, inspiration, and friendship throughout the development of this investigation.

I would like to extend my warmest thanks to my masters committee members: Dr. Eduardo A. Misawa and Dr. Gary E. Young for their support and suggestions in completion of this research. Their guidance and encouragement made the development of this thesis a positive learning experience.

I would also like to thank my colleagues at Oklahoma State University Ramamurthy V. Dwivedula, Sachin Gupta, Gimkhuan Ng and Yong Liang Zhu for all the help they have provided.

# TABLE OF CONTENTS

## LIST OF TABLES

**Table** **Page**

## LIST OF FIGURES

## NOMENCLATURE

| | | |
|---|---|---|
| $A$ | = | area of cross-section of the strip perpendicular to web travel direction |
| $A_{cyl}$ | = | rod side cylinder area |
| $B_j$ | = | viscous friction coefficient at the j-th roller |
| $C_m$ | = | coefficient of internal leakage of the cylinder |
| $E$ | = | modulus of elasticity of the strip |
| $F_d$ | = | disturbance force |
| $F_h$ | = | controlled force |
| $g$ | = | acceleration due to gravity |
| $I_c$ | = | mass moment of inertia of the carriage |
| $J_j$ | = | moment of inertia of the j-th roller |
| $K_e, K_p$ | = | motor constants |
| $K_q$ | = | flow gain coefficient |
| $k$ | = | spring constant of the web span($\frac{EA}{L_j}$) |
| $L_j$ | = | span length of j-th web span |
| $l_d$ | = | center to center distance between adjacent rollers |
| $M_c$ | = | carriage mass |
| $N$ | = | number of spans |
| $P_c$ | = | cylinder pressure |
| $P_r$ | = | return pressure |
| $P_s$ | = | supply pressure |
| $R_j$ | = | radius of the j-th roller |
| $t_c$ | = | average strip tension in N spans |
| $t_j$ | = | tension in j-th web span |
| $t_r$ | = | downstream and upstream tension of accumulator |

$V_o$ = total control volume in the rod side cylinder chamber

$w_j$ = angular velocity of the j-th roller

$v_c$ = carriage velocity

$x_c$ = carriage position

$x_r$ = ram displacement

$\theta$ = angular rotation of carriage in vertical plane

$\beta$ = bulk modulous of hydraulic fluid

$\rho$ = density of the web material

$\epsilon$ = strain in web span

# CHAPTER 1

# INTRODUCTION

## 1.1 Background

Any continuous material whose width is significantly less than its length and whose thickness is significantly less than its width can be described as a web. Plastic wrap, paper, photographic film, and aluminum strips are all examples of web. It is very important that the tension in a web span be maintained within a close tolerance band during processing of a web. For example, if the tension in the web changes during printing/perforating processes, the print/perforation gets skewed. Further, excessive tension variations may cause wrinkles or may even tear the web. Thus, a good tension control system is an important requirement in a web handling system since any disturbance such as uneven roller or variations in web speed or roll size affect the tension.

As the demand for higher productivity and better performance from the web processing industry increases, better models and more accurate control algorithms for the processes have to be developed. Tension control plays a key role in improving the quality of the finished web. It is essential to keep the web in the process at a required preset tension, which could change throughout the process by many conditions. Poor tension control leads to dishing, coning, and telescoping of the rewind roll, which are undesirable.

A continuous web processing line is a large-scale complex interconnected dynamic system with numerous control zones to transport the web while processing it. A continuous web processing line typically consists of an entry section, a process section, and an exit section. The entry section consists of an unwind stand, a tension leveller, and an entry accumulator. Operations such as wash, coat, and quench on the web are performed in

the process section in the case of aluminum and steel webs, and printing, perforating, and laminating in the case of other consumer products. The exit section consists of an exit accumulator and a rewind stand. Accumulators are primarily used to allow for rewind or unwind core change while the process continues at a constant velocity. Dynamics of the accumulator directly affects the behavior of web tension in the entire process line. Tension disturbance propagation both upstream and downstream of the accumulator has been noticed due to motion of the accumulator carriage.

## 1.2 Literature Review

In [1], a mathematical model for longitudinal dynamics of a web span between two pairs of pinch rolls based on Hooke's law, which are driven by two motors, is given; this model does not predict tension transfer and does not consider tension in the entering span. A modified model that considers tension in the entering span was developed in [3]. The moving web is assumed to be equivalent to a moving continuum in [4] and the general methods of continuum mechanics such as conservation of mass and conservation of momentum were used in the development of a model. A large web process line consists of many rollers for transporting the web, that are driven by electrical motors (DC/AC), while various different operations being performed on the web. The entire system is interconnected through the web. In [5], the authors proposed a decentralized method to decouple an interconnected system. The decentralized decoupling is able to successfully separate the coupling factors between the subsystems, which consists of the roller and the span upstream of the roller. In this study the only subsystem considered is an accumulator. Although sufficient amount of work has been done [1, 2, 3, 4, 6, 7, 8] and is currently being done in tension control of a web but very little published research exists in modelling and control of accumulators in web processing lines. An overview of the lateral and longitudinal behavior and control of moving webs was presented in [6]. A review of the problems in tension control of webs can be found in [7]. Discussions on tension control versus strain control and torque control

versus velocity control were given in [8].

Accumulators in web processing lines constitute an important element in all of the web handling machines. Functional importance of these in web processing lines is quite substantial as they are primarily responsible for continuous operation of web processing lines. A preliminary study on modelling and control of accumulators is given in [9]; characteristics of an accumulator and its operation are explained; throughout the study, discussions are carried out to gain more insight into the dynamic behavior of the accumulator carriage, web spans, and the current methods used in controlling the carriage. A dynamic model for accumulator spans that consider the time-varying nature of the span length was developed in [10].

In this study, control of the accumulator carriage in conjunction with control of the driven rollers both upstream and downstream of the accumulator is considered. The average dynamic model developed in [9] is further simplified based on practical observations and is used for controller design. The design of the control algorithm is carried out based on Lyapunov's second method. An observer for estimating the average web tension in accumulator web spans is also developed in the process. Simulation results on an industrial continuous web process line for a typical operation of an accumulator are conducted using the proposed controller and observer; these results are compared with the simulation results of the current control techniques that are used in the industry.

## 1.3 Thesis Contributions

The following are the thesis contributions.

- Development of average dynamic model for tension in the web spans in the accumulator carriage, process-side driven roller and exit-side driven roller.
- Analysis of accumulator dynamics along with process-side and exit-side driven roller dynamics and a systematic study to analyze tension variation problem in accumula-

tors considering different factors (friction, carriage sway etc.) and disturbances.

- Design and investigation of a controller for the accumulator system and its comparison with a currently used industrial controller.
- Development of necessary simulation software to study the performance of an accumulator system and tension variations in the web spans.

## 1.4 Thesis Outline

The rest of the report is organized as follows. Chapter 2 discusses the modeling of the accumulator system consisting of web dynamics, roller dynamics and hydraulic system dynamics. Chapter 3 describes the methodology to analyze and perform different calculations for accumulator system. Chapter 4 explains the process of control scheme design for the system in investigation and explains the comparison of this proposed controller with industrial control scheme using simulations. Chapter 5 gives conclusions of this research and gives directions for future research.

# CHAPTER 2

# DYNAMIC MODELLING

A line sketch of a typical continuous strip process line layout is given in Figure 2.1. It consists of an entry section that unwinds unprocessed strip, an entry accumulator that releases web into the process section when the entry section (unwind roller) is stopped, a process section where strip processing is performed, an exit accumulator that stores web when the exit section (rewind roller) is stopped for a rewind changeover, and an exit section that winds the processed web into rolls. Bridles shown in the figure are driven rollers and are

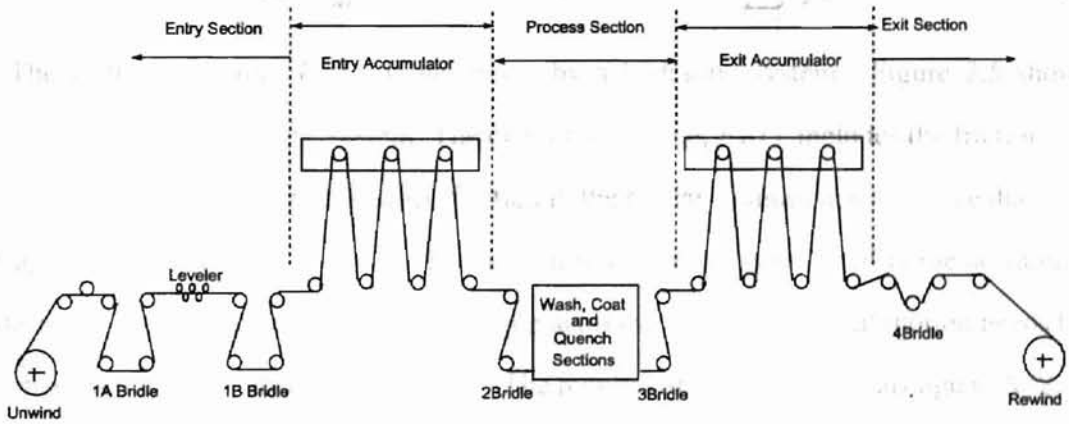


Figure 2.1: Typical process line layout and terminology.

driven by either AC or DC drives. Bridle rollers facilitates the transportation of the web in the web processing line. Both accumulator carriages are controlled by hydraulic systems, ( recently AC motors are used for this purpose) that provide regulation of tension in the strip when the carriage is in motion. This study assumes that a hydraulic system provides control action. This chapter is organized as follows. Section 2.1 presents the dynamics of carriage and web span. Section 2.2 gives the governing equations of the hydraulic system.

Section 2.3 explains equations for entry and exit rollers. Section 2.4 describes the process of incorporating carriage sway dynamics in accumulator system dynamics and Section 2.5 introduces the accumulator dynamics in an average form.

## 2.1 Strip Tension and Carriage Dynamics of Web in Accumulator Spans

In accumulators, length of each web span varies with the motion of the carriage as shown in Figure 2.2. Dynamics of the fixed length span are taken and the length of the span is made time-varying according to the carriage motion to incorporate variable length of the spans in the accumulator dynamics. The dynamics of this variable length is given by the accumulator carriage dynamics by taking the summation of all the forces acting on the carriage. The accumulator carriage dynamics is given by:

$$M_c \frac{d^2 x_c(t)}{dt^2} = F_h(t) - F_d(t) - M_c g - \sum_{j=1}^{N} t_j(t). \tag{2.1}$$

The controlled force, $F_h(t)$, is generated by a hydraulic system. Figure 2.5 shows a schematic of the hydraulic system. The disturbance force, $F_d(t)$, includes the friction in the hydraulic cylinder and the rod seals, friction in the carriage guides and the force due to carriage chain elasticity. The torque shaft shown in Figure 2.2 is included in the accumulator design to synchronize the side to side lifting action so that only vertical motion needs to be considered in the control system design. The number of rollers on the carriage is $N/2$. The number of rollers in the accumulator is $N + 1$. To derive the tension dynamics, consider the sketch of a single roller and two web spans as shown in Figure 2.3. From [10], the law of conservation of mass for a control volume in the first span of Figure 2.3 gives:

$$\frac{d}{dt}\left[\int_{x_1(t)}^{x_2(t)} \rho(x,t)A(x,t)dx\right] = \rho_1(t)A_1(t)v_1(t) - \rho_2(t)A_2(t)v_2(t), \tag{2.2}$$

where $x_1$ and $x_2$ denote the coordinates of roller 1 and roller 2, respectively, from a fixed reference frame. Notice that for the accumulator case, roller 1 is fixed ($x_1(t) = 0$) and roller 2 moves along with the carriage ($x_2(t) = x_c(t)$), where $x_c(t)$ denotes the variable length of the span.

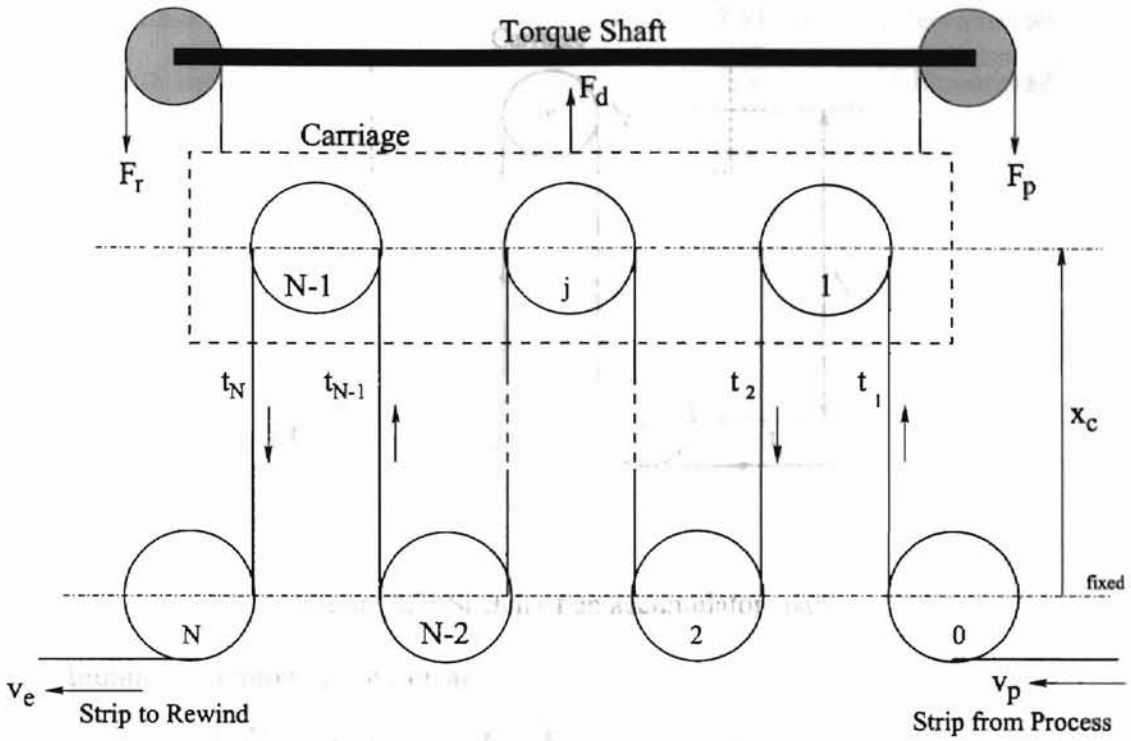


Figure 2.2: Sketch of an exit accumulator.

If we consider an infinitesimal element of the strip in the direction of web travel, the geometric relations between unstretched and stretched element are given by:

$$dx = (1 + \varepsilon_x) dx_u, \tag{2.3}$$

$$w = (1 + \varepsilon_w) w_u, \tag{2.4}$$

$$h = (1 + \varepsilon_h) h_u, \tag{2.5}$$

where subscript $u$ indicates the unstretched state of the element, $w$ and $h$ denote the width and thickness of the web, respectively. The elemental mass, $dm$, in the unstretched and stretched state is equal, and hence:

$$dm = \rho \, dx \, w \, h = \rho_u dx_u w_u h_u. \tag{2.6}$$

Combining equations (2.3)-(2.6), we obtain

$$\frac{\rho(x,t) A(x,t)}{\rho_u(x,t) A_u(x,t)} = \frac{1}{1 + \varepsilon_x(x,t)}. \tag{2.7}$$

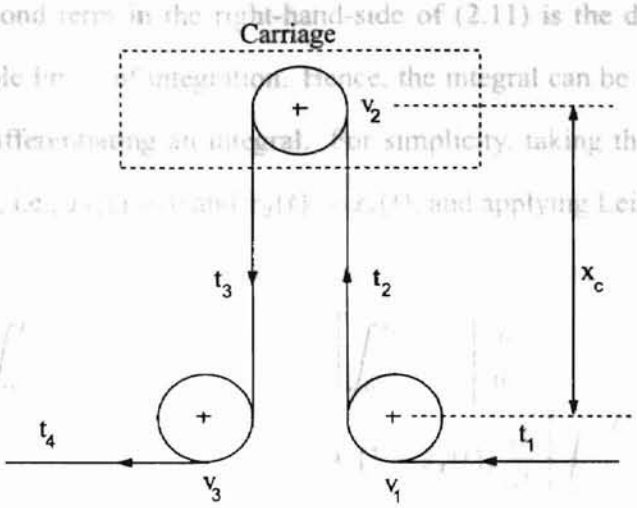


Figure 2.3: Sketch of an accumulator span.

Substituting (2.7) into (2.2), we obtain

$$\frac{d}{dt}\left[\int_{x_1(t)}^{x_2(t)} \frac{\rho_u(x,t)A(x,t)}{1+\varepsilon_x(x,t)}dx\right] = \frac{\rho_{1u}(x,t), A_{1u}(x,t)v_1(t)}{1+\varepsilon_{x1}(x,t)} - \frac{\rho_{2u}(x,t), A_{2u}(x,t)v_2(t)}{1+\varepsilon_{x2}(x,t)}. \tag{2.8}$$

Assuming the density ($\rho$) and the modulus of elasticity ($E$) of the web in the unstretched state are constant over the cross-section, (2.8) can be written as:

$$\frac{d}{dt}\left[\int_{x_1(t)}^{x_2(t)} \frac{1}{1+\varepsilon_x(x,t)}dx\right] = \frac{v_1(t)}{1+\varepsilon_{x1}(x,t)} - \frac{v_2(t)}{1+\varepsilon_{x2}(x,t)}. \tag{2.9}$$

Assuming that the strain is very small, $\varepsilon_x <<< 1$, we can neglect higher order terms and write $1/(1+\varepsilon_x) \approx (1-\varepsilon_x)$. Then, (2.9) can be written as:

$$\frac{d}{dt}\left[\int_{x_1(t)}^{x_2(t)} (1-\varepsilon_x(x,t))dx\right] = v_1(t)[1-\varepsilon_{x1}(x,t)] - v_2(t)[1-\varepsilon_{x2}(x,t)]. \tag{2.10}$$

Assuming that the strain does not vary with $x$, i.e. $\varepsilon_x(x,t) \approx \varepsilon_x(t)$, the left-hand-side of (2.10) can be written as:

$$\frac{d}{dt}\left[\int_{x_1(t)}^{x_2(t)} (1-\varepsilon_x(t))dx\right] = \left[\int_{x_1(t)}^{x_2(t)} dx\right]\frac{d}{dt}(1-\varepsilon_x(t)) + (1-\varepsilon_x(t))\frac{d}{dt}\left[\int_{x_1(t)}^{x_2(t)} dx\right]. \tag{2.11}$$

Notice that the second term in the right-hand-side of (2.11) is the differentiation of an integral with variable limits of integration. Hence, the integral can be differentiated using Leibnitz rule[1] of differentiating an integral. For simplicity, taking the accumulator case given by Figure 2.3, i.e., $x_1(t) = 0$ and $x_2(t) = x_c(t)$, and applying Leibnitz rule for (2.11) gives:

$$\frac{d}{dt}\left[\int_0^{x_c(t)} (1-\varepsilon_x(t))dx\right] = \left[\int_0^{x_c(t)} dx\right]\frac{d}{dt}(1-\varepsilon_x(t)) + (1-\varepsilon_x(t))\frac{d}{dt}\left[\int_0^{x_c(t)} dx\right]. \quad (2.12)$$

Substituting (2.12) into (2.10) and using Hooke's law, i.e., $t_2(t) = AE\epsilon_x(t)$, gives the strip tension in the $j$-th accumulator span as:

$$\frac{dt_j(t)}{dt} = \frac{AER}{x_c(t)}(\omega_j(t) - \omega_{j-1}(t)) + \frac{R}{x_c(t)}[t_{j-1}(t)\omega_{j-1}(t) - t_j(t)\omega_j(t)] + \frac{AE}{x_c(t)}\dot{x}_c(t) - \frac{1}{x_c(t)}t_j(t)\dot{x}_c(t). \quad (2.13)$$

Also the dynamics of j-th roller is given by

$$J_j\frac{d\omega_j(t)}{dt} = -B_j\omega_j + R_j(t_{j+1}(t) - t_j(t)). \quad (2.14)$$

### 2.1.1 Speed Changes During Rewind Roll Change

A continuous aluminum strip processing line consists of an entry section, a process section, and an exit section. The entry section consists of an unwind stand and an entry accumulator. The process section consists of several stations where washing, coating, and drying operations are performed on the strip. The exit section consists of an exit accumulator and a rewind stand. The process speed and exit speed are relative to the exit accumulator as shown in Figure 2.2.

[1]Leibnitz rule

$$\frac{d}{dt}\left[\int_{\phi(t)}^{\psi(t)} f(x,t)dx\right] = \int_{\phi(t)}^{\psi(t)} \frac{\partial f(x,t)}{\partial t}dx - \frac{d\phi}{dt}f(\phi(t),t) + \frac{d\psi}{dt}f(\psi(t),t)$$

A typical scenario of the exit speed and the carriage speed during a rewind roll change is depicted in Figure 2.4. The following steps describe a rewind roll change-over scenario when the strip velocity in the process section is maintained at a constant value: (i) AB – velocity of the strip in the rewind side is decelerated to zero, as a result of this the accumulator starts collecting strip and the carriage accelerates upwards; (ii) BC – rewind stops and the carriage is moving up with constant velocity; (iii) CD – after rewind roll change, exit side is accelerated up to the process speed, in this period the carriage is moving up while decelerating; (iv) DE – exit side is accelerated up to a speed above the process speed; (v) EF – exit speed is maintained at a constant speed; (vi) FG – exit speed is reduced to the process speed. The carriage after this cycle returns to its original position. Notice that carriage returns to its original position when the area under the carriage speed graph of Figure 2.4 is zero. Since there are $N$ spans in the accumulator, carriage velocity can be obtained based

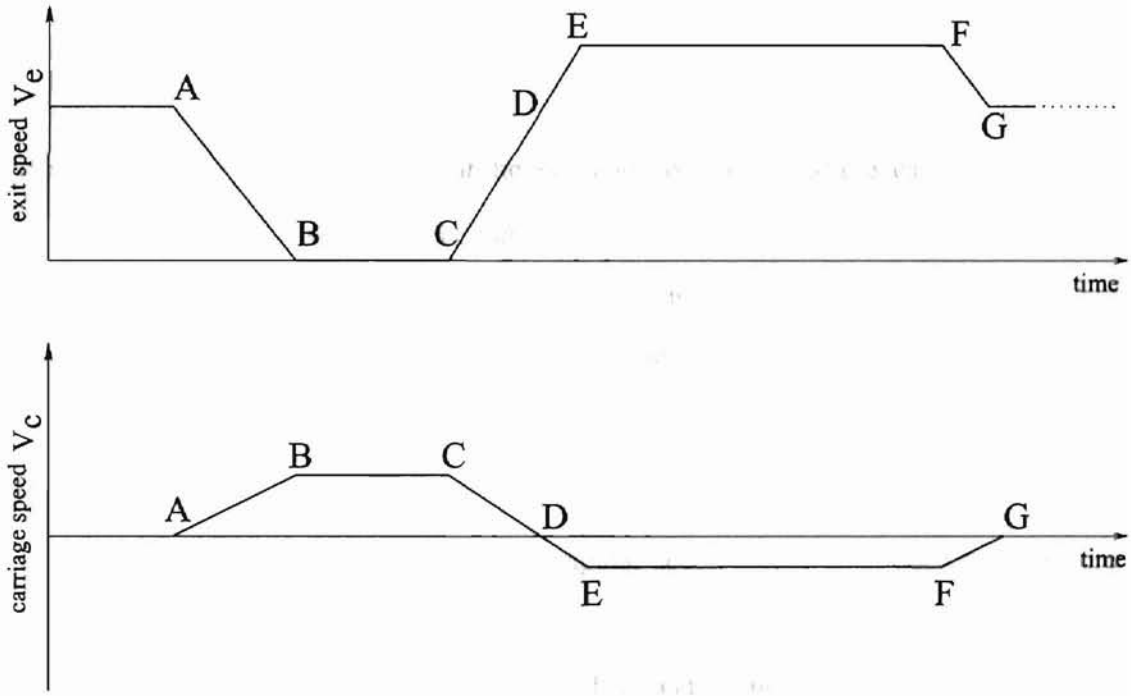


Figure 2.4: Exit and carriage speed profiles during roll-change.

on the process speed and the exit speed, under the assumption that there is no web slippage on the rollers. The relationship between the process speed, $v_p$, the exit speed, $v_e$, and the

carriage speed, $v_c$, in an ideal situation is given by the following equation

$$v_c = \frac{v_p - v_e}{N}, \tag{2.15}$$

$$\omega_j = \frac{v_p - j v_c}{R}. \tag{2.16}$$

It is assumed that the process speed is the speed of the strip in the span just upstream of the exit accumulator, as shown in Figure 2.2, and the exit speed is the speed of the strip in the span just downstream of the accumulator. The carriage speed as given by equation (2.15), depends on the speed variation between the process section and the exit section. Generally, the process speed is kept constant and the exit speed varies according to the sketch shown in Figure 2.4. When the strip is stationary at the exit side of the accumulator, $v_e = 0$, then equations (2.15) and (2.16) become:

$$v_c = \frac{v_p}{N}, \tag{2.17}$$

$$\omega_j = \frac{v_c}{R}(N - j). \tag{2.18}$$

Using this notion of speed changes at the exit side, some observations can be drawn from the dynamics of the carriage given by equation (2.1). Assume that the external disturbance force, $F_d(t)$, is zero. If the web is stationary at the exit side then the carriage is moving up with a constant velocity $v_c$ thus, carriage acceleration $\frac{dv_c}{dt}$ is zero, then (2.1) becomes:

$$F_{h0}(t) = M_c g + \sum_{j=1}^{N} t_j(t).$$

Further, it can be seen from (2.18) that the angular acceleration $\frac{d\omega_j}{dt}$ of each roller is zero. Thus equation (2.14) gives $t_j = t_{j+1}$ for all $j = 1 : N$. This is true under the assumption that the roller bearing friction, $B_j$, is very small and can be ignored ($B_j \approx 0$). Thus, when the exit side is stationary, the tension in all the spans is equal and the controlled force is required to overcome the weight of the carriage, sum of the tensions in the spans, and other force disturbances. Now consider the case of constant acceleration or deceleration of the

exit side and constant process speed. The carriage dynamics, (2.1), can be re-written as:

$$F_h(t) = M_c\frac{dv_c}{dt} + M_c g + \sum_{j=1}^{N} t_j(t), \tag{2.19}$$

where $F_{hd}(t)$ is the control force required when the exit side is accelerating or decelerating. It should be observed that during deceleration of the exit side, the carriage is accelerating up, i.e., $dv_c/dt$ is positive. Hence, the controlled force, $F_h(t)$, in this case should be larger than the controlled force in the case of stationary exit side. However, in the event of acceleration of the exit side, $dv_c/dt$ is negative, and hence the controlled force $F_h(t)$ in this case is smaller than the one required for the case of stationary exit side. To sum up,

$$F_h^{acc}(t) > F_{h0}(t)$$

$$F_h^{dec}(t) < F_{h0}(t)$$

Therefore, variations in the hydraulic force are required to account for acceleration/deceleration of the carriage, as well as for compensating the friction loss between the ram and the cylinder. The friction between the ram and the cylinder during carriage motion plays a major role in the strip tension change through the accumulator. Friction for up and down motion of the ram is different. Seal design and rod lubrication are big factors affecting the friction coefficients.

## 2.2 Hydraulic System

A schematic of the accumulator hydraulic system and the carriage is shown in Figure 2.5. It consists of two symmetrically placed cylinders, a directional proportional valve, and a pressure compensated pump. The pressure in each cylinder is regulated by the same directional proportional valve. Even though the pipe length from the proportional valve (point A) to the entry point of the cylinder (point $P_c$) is generally large, pressure drop due to friction in the pipe length and bends is comparatively small, as discussed in [9]. The

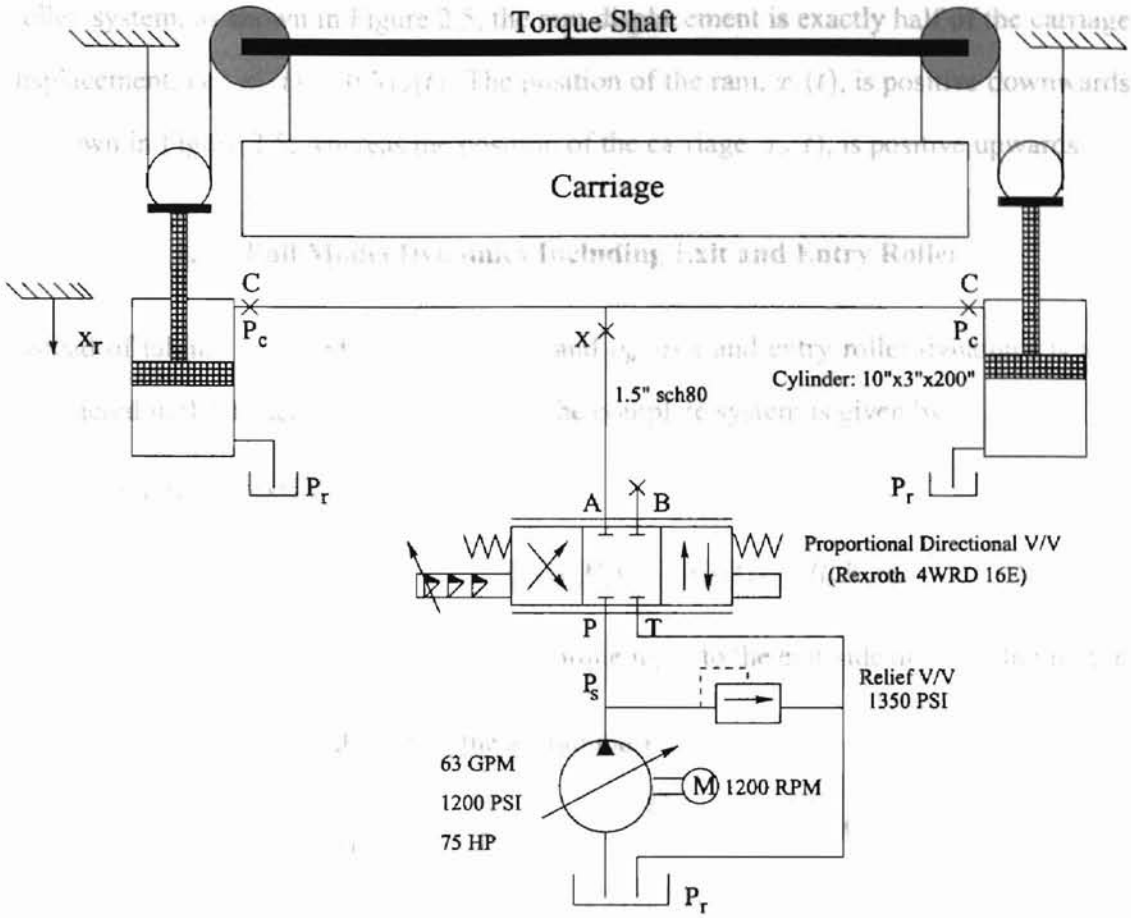


Figure 2.5: Sketch of carriage and accumulator hydraulic system.

cylinder pressure dynamics for the setup shown in Figure 2.5, in a simplified way, is given by:

$$\frac{V_o}{\beta}\frac{dP_c(t)}{dt} = Q_c(t) - C_m(P_c(t) - P_r) - A_{cyl}\dot{x}_r(t), \tag{2.20}$$

where $Q_c(t)$ is the flow rate to and from the cylinder, which is related to the proportional spool valve displacement, $x_v$, by:

$$Q_c(t) = K_q x_v \sqrt{P_s - P_c(t)} \quad \text{for} \quad x_v > 0, \tag{2.21}$$

$$Q_c(t) = K_q x_v \sqrt{P_c(t) - P_r} \quad \text{for} \quad x_v < 0. \tag{2.22}$$

The total cylinder control volume is $V_0(t) = V_{in} + A_{cyl}x_r(t)$, where $V_{in}$ is the initial clearance volume of the cylinder when the ram is fully extended, i.e., when $x_r = 0$. Due to the

pulley system, as shown in Figure 2.5, the ram displacement is exactly half of the carriage displacement, i.e., $x_r(t) = 0.5x_c(t)$. The position of the ram, $x_r(t)$, is positive downwards as shown in Figure 2.5, whereas the position of the carriage, $x_c(t)$, is positive upwards.

### 2.3 Full Model Dynamics Including Exit and Entry Roller

Instead of taking a defined function for $v_e$ and $v_p$, exit and entry roller dynamics is also considered in the system. The dynamics of the complete system is given by:

- Dynamics of exit-side driven roller:

$$\dot{v}_e = \frac{1}{J_e}(-B_{fe}v_e(t) + R_e^2(t_r - t_N(t)) + R_eK_eu_e) \tag{2.23}$$

  where $K_e$ is motor constant and $u_e$ is torque input to the exit-side driven roller motor.

- Span dynamics of j-th span in the accumulator:

$$\begin{aligned}\frac{dt_j(t)}{dt} = &\frac{AER}{x_c(t)}(\omega_j(t) - \omega_{j-1}(t)) + \frac{R}{x_c(t)}[t_{j-1}(t)\omega_{j-1}(t) - t_j(t)\omega_j(t)] \\ &+ \frac{AE}{x_c(t)}\dot{x}_c(t) - \frac{1}{x_c(t)}t_j(t)\dot{x}_c(t),\end{aligned} \tag{2.24}$$

- Accumulator carriage dynamics:

$$\dot{x}_c = v_c(t), \tag{2.25}$$

$$\dot{v}_c = \frac{1}{M_c}(-\sum_{j=1}^{N} t_j(t) + A_{cyl}P_c - F_d(t)) - g, \tag{2.26}$$

- Hydraulic system dynamics:

$$\frac{dP_c(t)}{dt} = \frac{\beta}{V_o}(Q_c(t) - C_m(P_c(t) - P_r) - A_{cyl}\dot{x}_r(t)), \tag{2.27}$$

- Dynamics of process-side driven roller:

$$\dot{v}_p = \frac{1}{J_p}(-B_{fp}v_p(t) + R_p^2(t_1(t) - t_r) + R_pK_pu_p) \tag{2.28}$$

  where $K_p$ is motor constant and $u_p$ is torque input to the process-side driven roller motor.

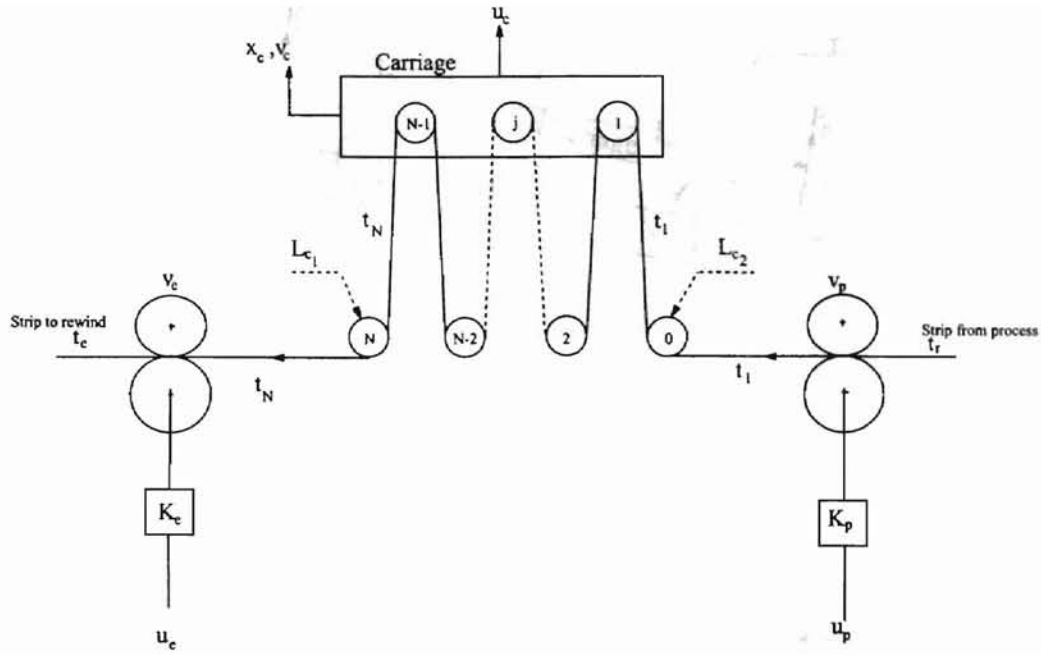


Figure 2.6: Exit accumulator with process-side and exit-side driven roller.

Accumulator can be represented as shown in Figure 2.6. The system has three control inputs, i.e., two motor inputs to the exit and entry rollers and the third is spool valve displacement to the hydraulic system.

## 2.4 System with Carriage Sway Dynamics

Even though it is required that the carriage slots and the guide ways mate properly to give smooth motion, there will invariably be sway and cocking reaction due to inherent limitations on manufacturing processes. The manufacturing tolerances, which are necessary to compensate for manufacturing process capabilities will generate clearance in the guide ways. In general, this sway will be in both planes; plane parallel to the travel of the web and plane perpendicular to the travel of the web and will affect tension in the web spans. The effect of carriage sway in the vertical plane is incorporated in the following analysis. For simplicity even number of spans are considered in this analysis. The web strand length

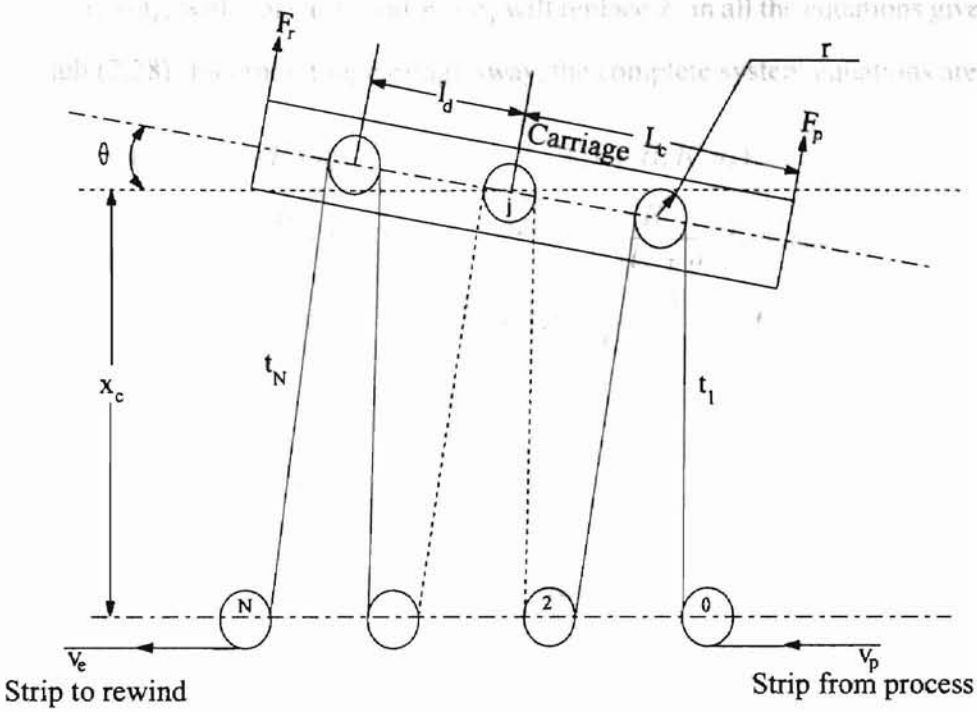


Figure 2.7: Illustration of carriage during sway.

($\delta$) due to carriage rotation is given by:

$$\delta_j = \begin{cases} \vdots & \\ -2l_d\theta & \text{for } j = \frac{N}{2} - 3, \frac{N}{2} - 4 \\ -l_d\theta & \text{for } j = \frac{N}{2} - 1, \frac{N}{2} - 2 \\ 0 & \text{for } j = \frac{N}{2}, \frac{N}{2} + 1 \\ l_d\theta & \text{for } j = \frac{N}{2} + 2, \frac{N}{2} + 3 \\ 2l_d\theta & \text{for } j = \frac{N}{2} + 4, \frac{N}{2} + 5 \\ \vdots & \end{cases}$$

Thus, $(x_c+\delta_j)$ will replace $x_c$ and $\dot{x}_c+\dot{\delta}_j$ will replace $\dot{x}_c$ in all the equations given by (2.23) through (2.28). Incorporating carriage sway, the complete system equations are given by:

$$\dot{v}_e = \frac{1}{J_e}(-B_{fe}v_e(t) + R_e^2(t_r - t_N(t)) + R_eK_eu_e), \tag{2.29}$$

$$\frac{dt_j(t)}{dt} = \frac{AER}{x_c(t)+\delta_j}(\omega_j(t) - \omega_{j-1}(t)) + \frac{R}{x_c(t)+\delta_j}[t_{j-1}(t)\omega_{j-1}(t) - t_j(t)\omega_j(t)] + \frac{AE}{(x_c(t)+\delta_j)}(\dot{x}_c(t)+\dot{\delta}_j) - \frac{1}{(x_c(t)+\delta_j)}t_j(t)(\dot{x}_c(t)+\dot{\delta}_j), \tag{2.30}$$

$$\dot{x}_c = v_c(t) + \dot{\delta}_j, \tag{2.31}$$

$$\dot{v}_c = \frac{1}{M_c}(-\sum_{j=1}^{N} t_j(t) + A_{cyl}P_c - F_d(t)) - g, \tag{2.32}$$

$$\frac{v_o}{\beta}\frac{dP_c(t)}{dt} = Q_c(t) - C_m(P_c(t) - P_r) - A_{cyl}\dot{x}_r(t), \tag{2.33}$$

$$\dot{v}_p = \frac{1}{J_p}(-B_{f1}v_p(t) + R_1^2(t_1(t) - t_r) + R_pK_pu_p). \tag{2.34}$$

There will be one more equation for carriage dynamics due to rotational moment. This equation can be written in following form

$$I_c\ddot{\theta} = f(t_j, \delta_j) + L_c(F_r - F_p), \tag{2.35}$$

where

$$f(t_j,\delta_j) = \sum \begin{cases} \vdots & \\ (t_j + k\delta_j)(2l_d + r) & \text{for } j = \frac{N}{2} - 4 \\ (t_j + k\delta_j)(2l_d - r) & \text{for } j = \frac{N}{2} - 3 \\ (t_j + k\delta_j)(l_d + r) & \text{for } j = \frac{N}{2} - 2 \\ (t_j + k\delta_j)(l_d - r) & \text{for } j = \frac{N}{2} - 1 \\ -(t_j + k\delta_j)(-r) & \text{for } j = \frac{N}{2} \\ -(t_j + k\delta_j)(r) & \text{for } j = \frac{N}{2} + 1 \\ -(t_j + k\delta_j)(l_d - r) & \text{for } j = \frac{N}{2} + 2 \\ -(t_j + k\delta_j)(l_d + r) & \text{for } j = \frac{N}{2} + 3 \\ -(t_j + k\delta_j)(2l_d - r) & \text{for } j = \frac{N}{2} + 4 \\ \vdots & \end{cases}$$

and $A_{cyl}P_c = F_r + F_p$; $F_r$ and $F_p$ are forces acting on the two ends of the carriage. The $k\delta_j$ term is there to account for elastic force due to web span. The effect of the carriage rotation will be a important factor in designing a controller to control tension in accumulator web spans.

## 2.5 Average Dynamic Model

Analysis and controller design for large scale nonlinearly interconnected systems is challenging task even with the help of design/analysis techniques available at present. A comprehensive study is required to implement these controllers. The web handling process is a large scale multi-input multi-output system. Analysis of the models discussed in Sections 2.1 or Section 2.3 requires knowledge of all the states for each and every web span in the accumulator. The motivation for using average dynamics is that practically it is not feasible to control tension variations in each and every span as variation in one span affects tension in next span and vice versa. Also, installing load cells on all the rollers is not a feasible approach. The motivation for averaging the tension dynamics of $N$ web spans in the accumulator is to obtain a simpler dynamic model for all the accumulator spans in an average sense. With aggregation of dynamics, the system is equivalent to a dynamic system with one roller on the carriage, as shown in Figure 2.8. Therefore, a simpler dynamic model for all the accumulator spans in an average sense can be obtained and implementation of control scheme requires, perhaps only two load cells at each end of the accumulator, i.e., first $(0^{th})$ and last roller $(N^{th})$ of the accumulator. Consider a new variable $t_c$, which denotes an average sum of the tensions in the accumulator web spans and is given by:

$$t_c(t) = \frac{1}{N}\sum_{j=1}^{N} t_j(t). \tag{2.36}$$

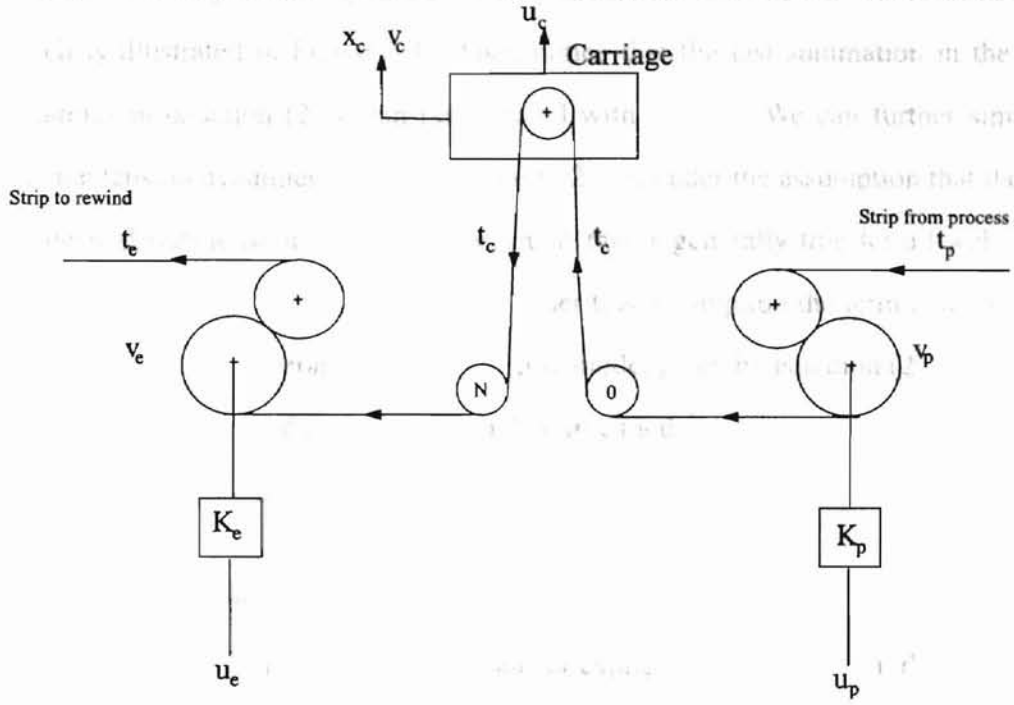


Figure 2.8: Equivalent of exit accumulator for average model, i.e., with one span.

Taking the sum from $j = 1$ to $j = N$ of both sides of equation (2.13) and dividing by $N$ results in

$$\frac{dt_c(t)}{dt} = \frac{AER}{x_c(t)}\frac{1}{N}\sum_{j=1}^{N}(\omega_j(t) - \omega_{j-1}(t)) + \frac{1}{N}\sum_{j=1}^{N}\frac{R}{x_c(t)}(t_{j-1}(t)\omega_{j-1}(t) - t_j(t)\omega_j(t)) + \frac{1}{N}\sum_{j=1}^{N}\frac{AE}{x_c(t)}\dot{x}_c(t) - \frac{1}{N}\sum_{j=1}^{N}\frac{1}{x_c(t)}t_j(t)\dot{x}_c(t). \tag{2.37}$$

Evaluating the sum on the right-hand-side results in

$$\frac{dt_c(t)}{dt} = \underbrace{\frac{AER}{x_c(t)}\frac{1}{N}(\omega_N(t) - \omega_0(t))}_{term_1} + \underbrace{\frac{1}{N}\frac{R}{x_c(t)}(t_0(t)\omega_0(t) - t_N(t)\omega_N(t))}_{term_2} + \underbrace{\frac{AE}{x_c(t)}\dot{x}_c(t)}_{term_3} - \underbrace{\frac{1}{x_c(t)}t_c(t)\dot{x}_c(t)}_{term_4}. \tag{2.38}$$

Using this approach, the average dynamics in terms of $t_c(t)$ simplifies the dynamics of $N$ spans given by $N$ equations of (2.13). Notice that the average dynamics, (2.38), simply

looks like the strip tension dynamics of an accumulator with a single roller on its carriage, which is illustrated in Figure 2.8. Also, notice that the last summation in the carriage dynamics in equation (2.1), can be replaced with $Nt_c(t)$. We can further simplify the average tension dynamics given by equation (2.38), under the assumption that the ratio of the desired web tension to $AE$ is very small; this is generally true for all web materials processed in web processing machines. Under this assumption the term 2 and term 4 can be ignored from the average tension dynamic model given by equation (2.38), resulting in the following simplified average tension dynamic model:

$$\frac{dt_c(t)}{dt} = \frac{AER}{x_c(t)}\frac{1}{N}\left(\omega_N(t) - \omega_0(t)\right) + \frac{AE}{x_c(t)}\dot{x}_c(t). \tag{2.39}$$

In the average dynamics given by equation (2.39), the angular velocities of the 0-th and $n$-th stationary rollers of the accumulator appear explicitly. Assuming that there is no slip on the entry and exit rollers of the accumulator, the process velocity $v_p$ and the exit velocity $v_e$ are given by $v_p(t) = R\omega_0(t)$ and $v_e(t) = R\omega_N(t)$. Therefore, the average tension dynamics given by equation (2.39) becomes

$$\frac{dt_c(t)}{dt} = \frac{AE}{x_c(t)}\frac{1}{N}\left(v_e(t) - v_p(t)\right) + \frac{AE}{x_c(t)}\dot{x}_c(t). \tag{2.40}$$

Notice that the average tension dynamics (2.40) clearly reflects variations in the process and exit velocities on the average tension in the accumulator spans. The driven roller angular dynamics at the process side and the exit side of the accumulator are given by the following equations:

$$J_e\dot{\omega}_e(t) = -B_{fe}\omega_e(t) + R_e(t_e(t) - t_c(t)) + K_e u_e(t), \tag{2.41}$$

$$J_p\dot{\omega}_p(t) = -B_{fp}\omega_p(t) + R_p(t_c(t) - t_p(t)) + K_p u_p(t), \tag{2.42}$$

where $\omega_e(t)$ and $\omega_p(t)$ are the exit side and process side driven roller angular velocities, respectively, $B_{fe}$ and $B_{fp}$ are the viscous friction coefficients in the exit side roller and process side roller, respectively, $t_e(t)$ and $t_p(t)$ are the web tension in the span downstream of the exit-side roller and in the span upstream of the process-side roller, $K_e$ and $K_p$ are

positive gains, and $u_e(t)$ and $u_p(t)$ are exit side and process side driven roller control inputs. Notice that $t_e(t)$ and $t_p(t)$ are given by the tension dynamics downstream of the exit-side driven roller and upstream of the process-side driven roller; since in this work we are interested in the web tension behavior in the accumulator region, we assume that $t_e(t)$ and $t_p(t)$ are maintained close to the desired web tension, that is, $t_e(t) = t_r + \delta_e(t)$ and $t_p(t) = t_r + \delta_p(t)$, where $t_r$ is the desired web tension in the process line, and $\delta_e(t)$ and $\delta_p(t)$ are disturbances. Assuming that there is sufficient web wrap on the driven rollers which will ensure that there is no web slip, we have $v_e(t) = R_e\omega_e(t)$ and $v_p(t) = R_p\omega_p(t)$, the equations for exit-side and process-side web velocities are:

$$\dot{v}_e(t) = \frac{1}{J_e}\left(-B_{fe}v_e(t) + R_e^2(t_r - t_c(t)) + R_eK_eu_e(t) + R_e^2\delta_e(t)\right), \tag{2.43}$$

$$\dot{v}_p(t) = \frac{1}{J_p}\left(-B_{fp}v_p(t) + R_p^2(t_c(t) - t_r) + R_pK_pu_p(t) - R_p^2\delta_p(t)\right). \tag{2.44}$$

The carriage dynamics, (2.1), can be re-written as:

$$M_c\frac{d^2x_c(t)}{dt^2} = F_h(t) - F_d(t) - M_cg - Nt_c(t). \tag{2.45}$$

Together, equations (2.40) and (2.45) characterize the dynamics of the accumulator carriage and its spans in an average sense. This dynamic model is suitable for design of the controller force, $F_h(t)$, to provide a desired regulation of the average tension in the accumulator spans. The control force $F_h(t)$ is generated by a hydraulic system. Considering the pressure ($P_c(t)$) in each cylinder to be the same, the force on the carriage is obtained from

$$F_h(t) = P_c(t)A_{cyl}.$$

Using this expression for controlled force, equations (2.40), (2.45) and (2.20) can be combined into the state space form by choosing the state variables and input as follows:

$$\begin{aligned}
\xi_1(t) &= t_c(t), \\
\xi_2(t) &= x_c(t), \\
\xi_3(t) &= v_c(t), \\
\xi_4(t) &= P_c(t), \\
\xi_5(t) &= v_e(t), \\
\xi_6(t) &= v_p(t), \\
u &= x_v.
\end{aligned}$$

Then the state space form of the complete system dynamics in a simplified form is

$$\dot{\xi}_1(t) = \frac{AE}{\xi_2(t)}\left(\xi_3(t) + \frac{1}{N}(\xi_5(t) - \xi_6(t))\right), \tag{2.46}$$

$$\dot{\xi}_2(t) = \xi_3(t), \tag{2.47}$$

$$\dot{\xi}_3(t) = \frac{1}{M_c}\left(-N\xi_1(t) - F_f(\xi_3(t)) + A_{cyl}\xi_4(t)\right) - g, \tag{2.48}$$

$$\dot{\xi}_4(t) = \alpha(\xi_2)(-\frac{A_{cyl}}{2}\xi_3 - C_m(\xi_4 - P_r)) + h(\xi_4, u)u, \tag{2.49}$$

$$\dot{\xi}_5(t) = \frac{1}{J_e}\left(-B_{fe}\xi_5(t) + R_e^2(t_r - \xi_1(t)) + R_e K_e u_e(t) + R_e^2\delta_e(t)\right), \tag{2.50}$$

$$\dot{\xi}_6(t) = \frac{1}{J_p}\left(-B_{fp}\xi_6(t) + R_p^2(\xi_1(t) - t_r) + R_p K_p u_p(t) - R_p^2\delta_p(t)\right), \tag{2.51}$$

where

$$\begin{aligned}
\alpha(\xi_2) &= \frac{\beta}{(V_{in} + A_{cyl}\xi_2)}, \\
h(\xi_4, u) &= \frac{K_q}{2}(1 + \mathrm{sgn}(u))\sqrt{P_s - \xi_4} + \frac{K_q}{2}(1 - \mathrm{sgn}(u))\sqrt{\xi_4 - P_r},
\end{aligned}$$

and $V_{in}$ is the initial volume of the cylinder when the ram is fully extended. The function sgn is defined as:

$$\text{sgn}(u) = \begin{cases} +1 & \text{if } u > 0 \\ 0 & \text{if } u = 0 \\ -1 & \text{if } u < 0 \end{cases}$$

## 2.6 Synopsis

In this chapter the dynamics of a web span, carriage and driven roller are developed. The effect of carriage sway is also considered and a mathematical equation is developed for the same. To simplify the dynamics averaging is performed. This transfers a system with $N$ web spans into a system with one web span. This average model is used for further analysis in the following chapters.

# CHAPTER 3

# DYNAMIC BEHAVIOR OF SYSTEM

This chapter concentrates on the analysis of dynamic behavior of accumulator system under different approaches. Such systematic study of accumulator system is of utmost use in designing a controller. The remainder of the chapter is organized as follows. Section 3.1 describes the process of calculating initial states of system parameters. This section also explains the fact that with movement of the carriage, the weight of web spans that is being acted on the carriage will be in significant proportion to the weight of the carriage for certain web materials. Section 3.2 explains the open loop behavior of tension variations in the system. Section 3.3 analyze the carriage dynamics along with dynamics of driven rollers on exit and process-side to establish groundwork for controller design.

## 3.1 System Parameter Calculations

### 3.1.1 Required Reference Pressure to Maintain Carriage Position and Reference Tension in Web Spans

This section explains the calculation for the reference pressure to maintain carriage position and reference tension in web spans throughout the operating range of the system, irrespective of the case whether the carriage is moving or not. The calculations are performed for an ALCOA continuous processing line (CPL). The following numerical values are used in

the calculations.

Reference tension to be maintained: $t_{ref} = 1165\ lbs.$

Number of spans: $N = 34.$

Rod side cylinder area: $A_{cyl} = 71.47\ in^2.$

Weight of the carriage: $W_c = 16134\ lbs.$

Accumulator carriage dynamics is given by:

$$M_c \frac{d^2 x_c(t)}{dt^2} = F_h(t) - F_d(t) - M_c g - N t_c(t).$$

When carriage is not in motion

$$\frac{d^2 x_c(t)}{dt^2} = 0,$$
$$t_c(t) = t_{ref}.$$

So

$$P_c = \frac{W_c + N t_{ref}}{A_{cyl}}$$
$$= 779.96\ psi.$$

This is the reference pressure the hydraulic system has to maintain irrespective of the motion of the carriage. To compensate for acceleration or deceleration of carriage, pressure boost as discussed in [9] is required.

### 3.1.2 Calculation of Spool Valve Position for any Forced Equilibrium Point

This section explains the calculations performed to calculate the position of spool valve to maintain reference pressure calculated in previous section. The hydraulic dynamics is given by (2.49). Calculations are performed for an ALCOA continuous process line (CPL),

for which hydraulic parameters are:

$$\beta = 100000\ psi, \qquad C_m = 0.01,$$
$$P_r = 200\ psi, \qquad P_s = 1200\ psi,$$
$$V_{in} = 0\ in^2, \qquad K_q = 0.7.$$

The lowest point of the carriage is taken as the forced equilibrium point for calculation. At this point

$$\bar{\xi}_2 = 71\ in, \qquad \bar{\xi}_3 = 0,$$
$$\dot{\bar{\xi}}_4 = 0\ psi.$$

In this scenario the spool valve will always be moving in the positive direction. The value of functions $\alpha(\bar{\xi}_2)$ and $h(\bar{\xi}_4, \bar{u})$ at a given forced equilibrium point are:

$$\alpha(\bar{\xi}_2) = 19.707, \qquad h(\bar{\xi}_4, \bar{u}) = 14.346.$$

From equation (2.49)

$$\bar{u} = -\frac{\alpha(\bar{\xi}_2)(-\frac{A_{cyl}}{2}\bar{\xi}_3 - C_m(\bar{\xi}_4 - P_r))}{h(\bar{\xi}_4, \bar{u})}$$

which is the reference value of spool valve position $u$ and is 7.9 in. This is the reference value of spool valve position to maintain reference pressure which in turn will compensate for weight of the carriage and reference tension in all the accumulator web spans.

### 3.1.3 Calculations for Weight Change of Web Spans during Carriage Motion

This section explains the fact that, when carriage is in motion, the length of each web span in the accumulator changes and thus the weight of the web material acting on the carriage changes. The hydraulic system has to compensate for this changing weight of the web spans. If the web thickness is quite significant, in the range of $1/8^{th}$ to $1/4^{th}$ of an inch, the weight of the web material is comparable to that of the carriage as shown in Figure 3.2. Figure 3.1 shows the weight change for the aluminium strip of thickness 0.01 inches, which is the case used for the simulation study in the next chapter.

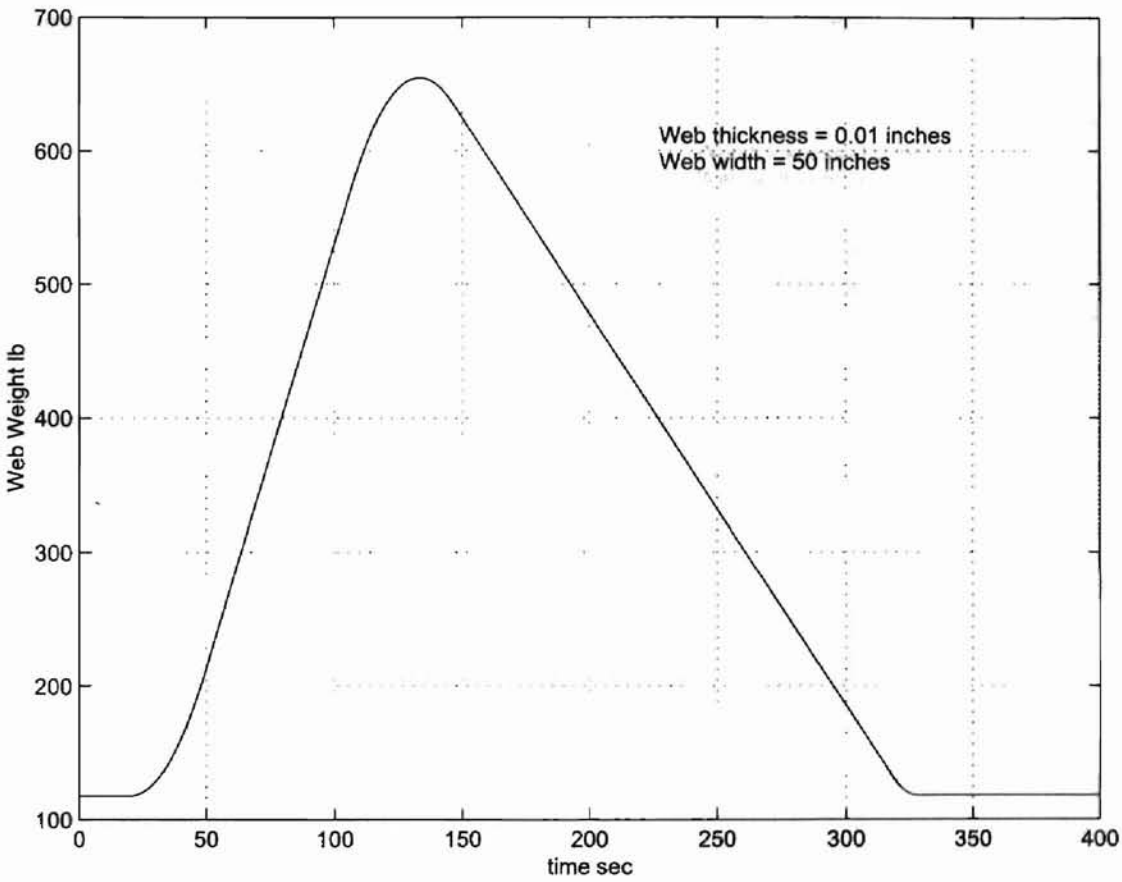


Figure 3.1: Change in web weight during carriage motion for 0.01 inches thick aluminium web.

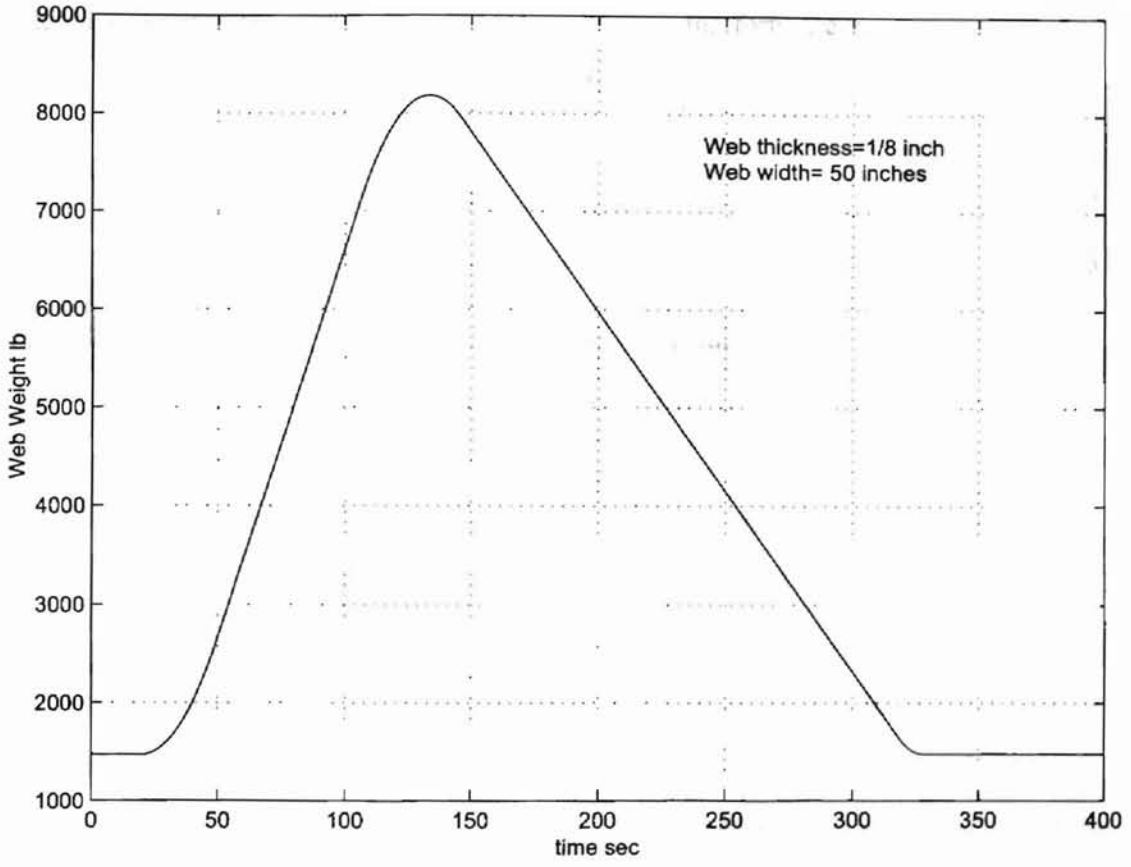


Figure 3.2: Change in web weight during carriage motion for 0.125 inches thick aluminium web.

## 3.2 Study of Dynamic Behavior of System

This section considers the study of the dynamic behavior of the system using some simplifying approximations. To simplify the analysis, initially the hydraulic dynamics is not considered in the simulation process. Also the effect of viscous and coulomb friction is ignored. It is assumed that there is no pressure dynamics, therefore hydraulic force is considered as input to the system. Equations in the following form are used:

$$\dot{\xi}_1 = \frac{AE - \xi_1}{\xi_2}\xi_3 + \frac{AE}{\xi_2}\frac{1}{N}(v_e(t) - v_p(t)), \tag{3.1}$$

$$\dot{\xi}_2 = \xi_3, \tag{3.2}$$

$$\dot{\xi}_3 = \frac{1}{M_c}(-N\xi_1 + u_c) - g. \tag{3.3}$$

The input $u_c$ is chosen to consist of feed forward terms only, i.e.,

$$u_c = M_c g + N t_{ref}.$$

The results obtained from the simulation of this simplified system are shown in Figure 3.3. A defined pattern of exit velocity as shown in Figure 2.4 is used to govern the motion of the carriage. The carriage movement is confined, with a lower limit of 71 inches and a upper limit of 400 inches. After each cycle the carriage will return back to its original position if the area under the carriage velocity curve is zero. Large variations in the web tension can be noticed and the reference tension value returns to 1165 lb after every cycle and stays there if the carriage is not in motion.

In the second step, friction term is added in (2.48) and simulations are performed. The variations in average tension are higher than the previous case as shown in Figure 3.4.

In the third step, a small sinusoidal disturbance is added in equation (2.48) and simulation is performed. Figure 3.5 shows that in the absence of feedback control, this sinusoidal disturbance will generate large variations in the tension.

In the fourth step, a compensator (a PI controller) is incorporated by using the error signal, because of the difference in reference position and the actual position, as feedback.

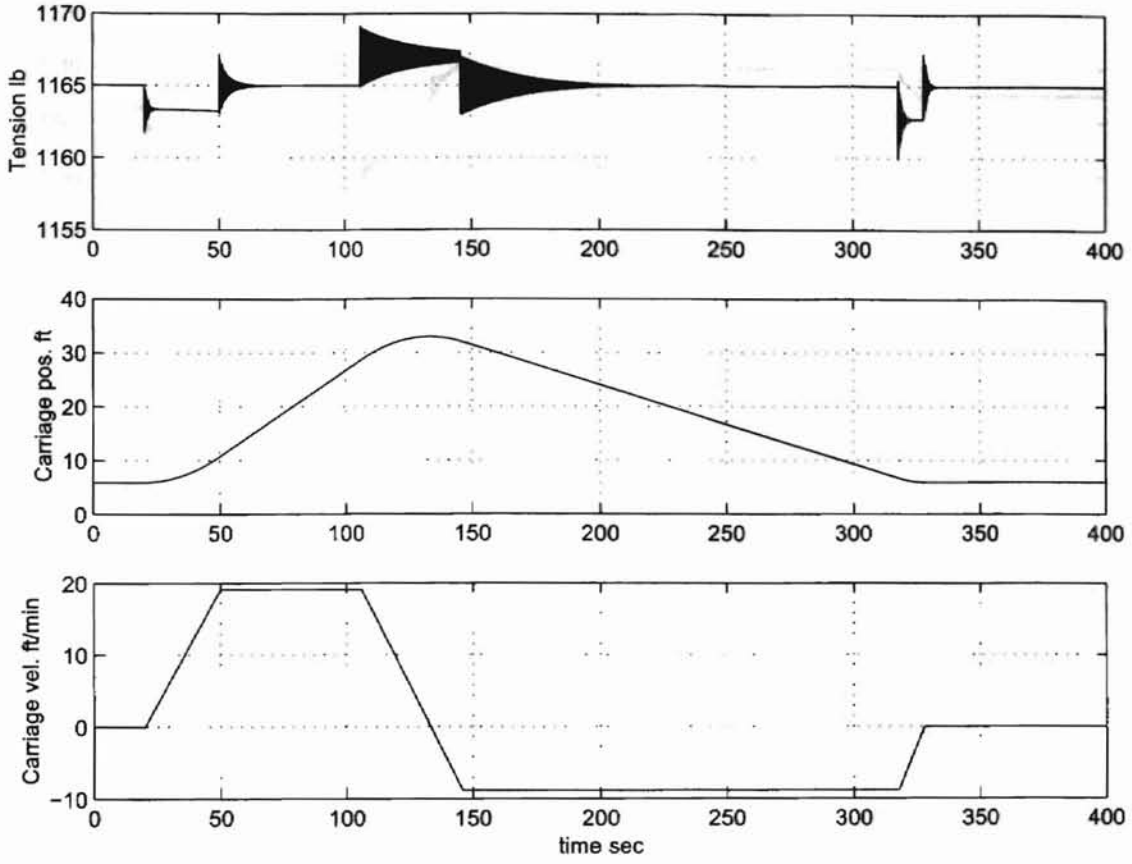


Figure 3.3: Uncompensated system states ignoring friction term.

The results from simulation is shown in Figure 3.6.

This study shows that variations in the hydraulic force are required to account for acceleration/deacceleration of the carriage, as well as for compensating the friction loss between the ram and the cylinder. The model described in the previous chapter is highly nonlinear. Besides the friction, the nonlinearities present in the hydraulic system make controller design a challenging task. A detailed analysis of the system is required to design a controller for the system.

### 3.2.1 Reachability and Observability Analysis for the Accumulator System

The system given by (2.46) through (2.51) is a nonlinear system. Before designing a controller one must first analyze the question of reachability and observability. For this analysis

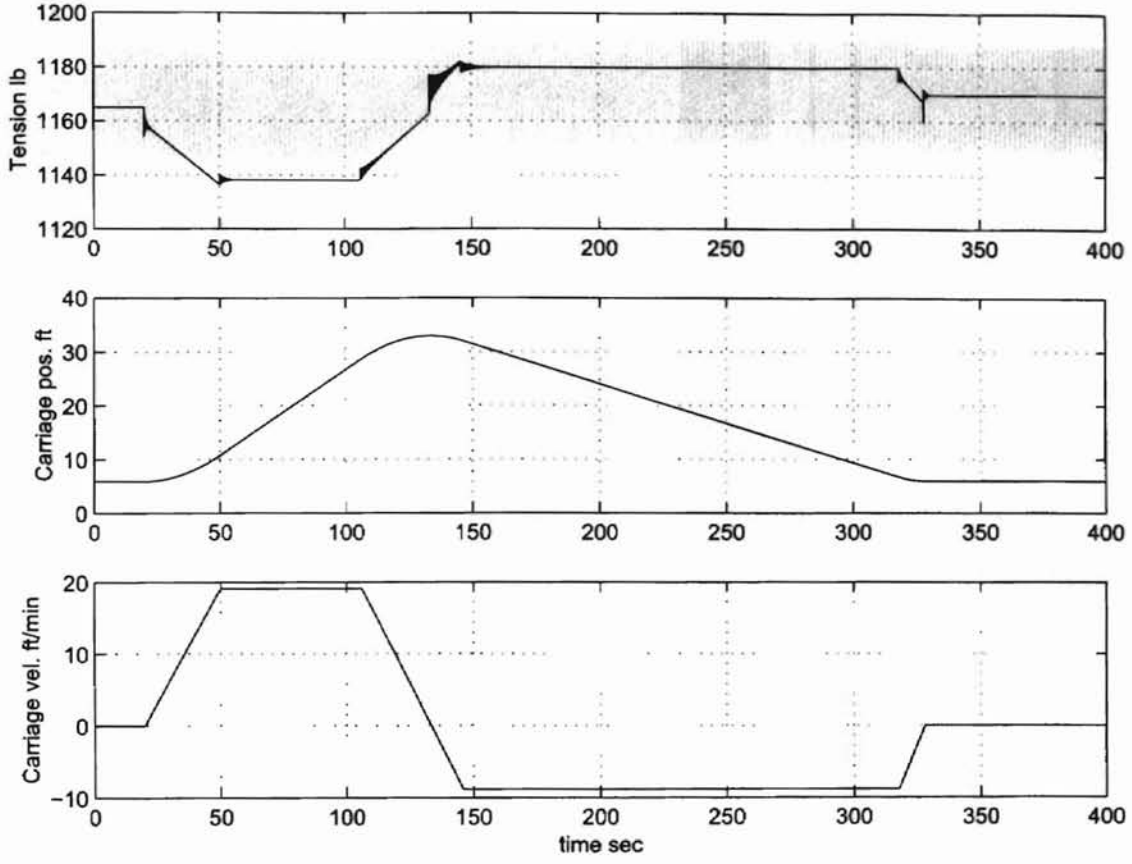


Figure 3.4: Uncompensated system states incorporating friction term.

dynamics of $\xi_1, \xi_2$ and $\xi_3$ are considered. Among these three states the last two states can be measured and thus are available for feedback. These three state equations can be written in the following form as those are linear in the input, i.e.,

$$\dot{\xi} = f(\xi) + g(\xi)u, \tag{3.4}$$

where $f(\xi)$ and $g(\xi)$ are smooth vector functions of $\xi(t)$ and are given by:

$$f(\xi) = \begin{bmatrix} (\frac{AE-\xi_1}{\xi_2})(\xi_3 + \frac{1}{N}(v_e(t) - v_p(t)) \\ \xi_3 \\ \frac{1}{M_c}(-N\xi_1 - F_f(\xi_3)) - g \end{bmatrix}, \qquad g(\xi) = \begin{bmatrix} 0 \\ 0 \\ \frac{1}{M_c} \end{bmatrix}. \tag{3.5}$$

Also the output equation can be written as:

$$y = \begin{bmatrix} h_1(\xi) & h_2(\xi) \end{bmatrix}. \tag{3.6}$$

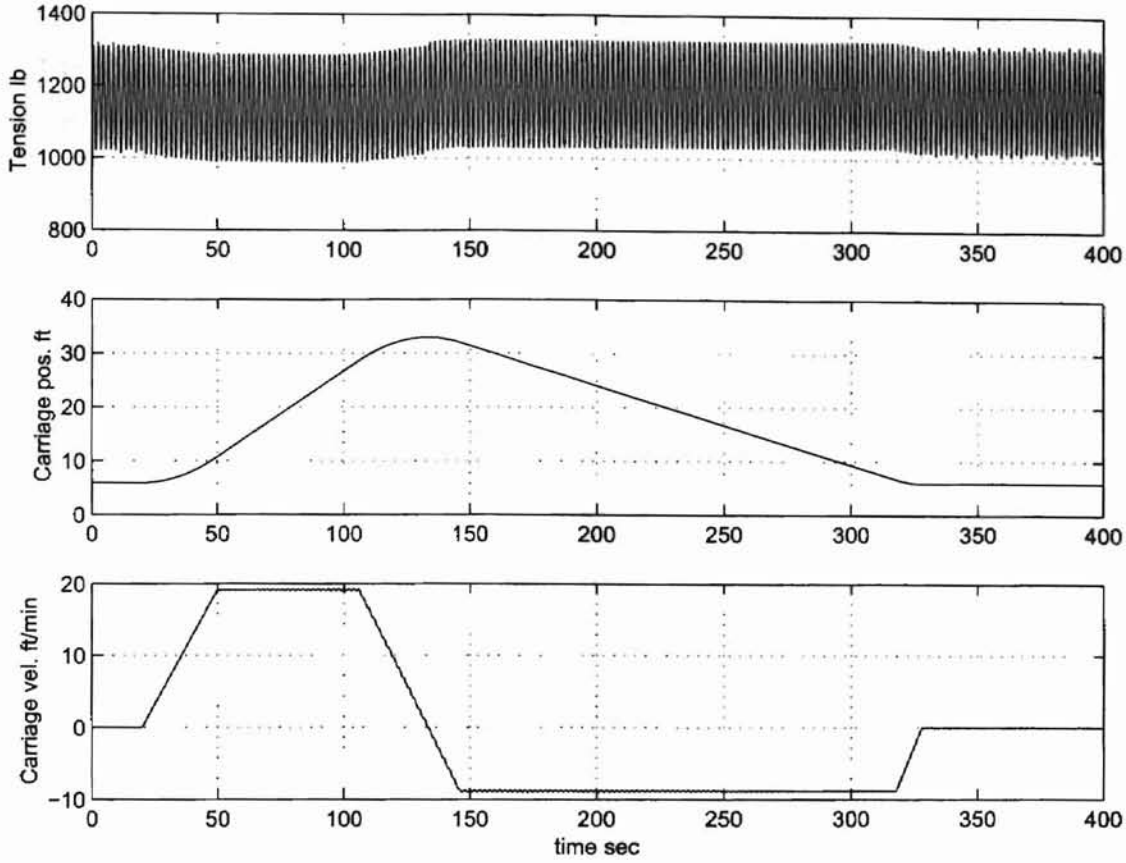


Figure 3.5: Uncompensated system states incorporating friction term and sinusoidal disturbance.

A system given by (3.4), is said to be locally reachable around a state $x_0 \in X$ if there exists a neighborhood $U$ of $x_0$ such that for each $x_f \in U$, $\exists\, T > 0$ and $\exists\, u(t), t \in [0, T]$, such that if the system starts in $x_0$ at time $t = 0$, then it reaches the state $x_f$ at time $t = T$. Define

$$\zeta = \begin{bmatrix} g & ad_f g & ad_f^2 g \end{bmatrix}$$

where $ad_f^i g$ is the i-th Lie bracket. The nonlinear system given by (3.4) is locally reachable if $\zeta$ has 3 linearly independent columns. $\zeta$ is evaluated as:

$$\zeta = \begin{bmatrix} 0 & -\frac{1}{M_c}\frac{AE-\xi_1}{\xi_2} & -\frac{1}{M_c}\frac{AE-\xi_1}{\xi_2^2}(\xi_3 + \frac{v_c - v_p}{N}) + \frac{1}{M_c}\frac{AE-\xi_1}{\xi_2}(\frac{\xi_3}{\xi_2} - \frac{v_f}{M_c}) \\ 0 & -\frac{1}{M_c} & -\frac{1}{M_c}\frac{v_f}{M_c} \\ \frac{1}{M_c} & \frac{1}{M_c}\frac{v_f}{M_c} & -\frac{N}{M_c}\frac{1}{M_c}\frac{AE-\xi_1}{\xi_2} + v_f^2\frac{1}{M_c^3} \end{bmatrix}.$$

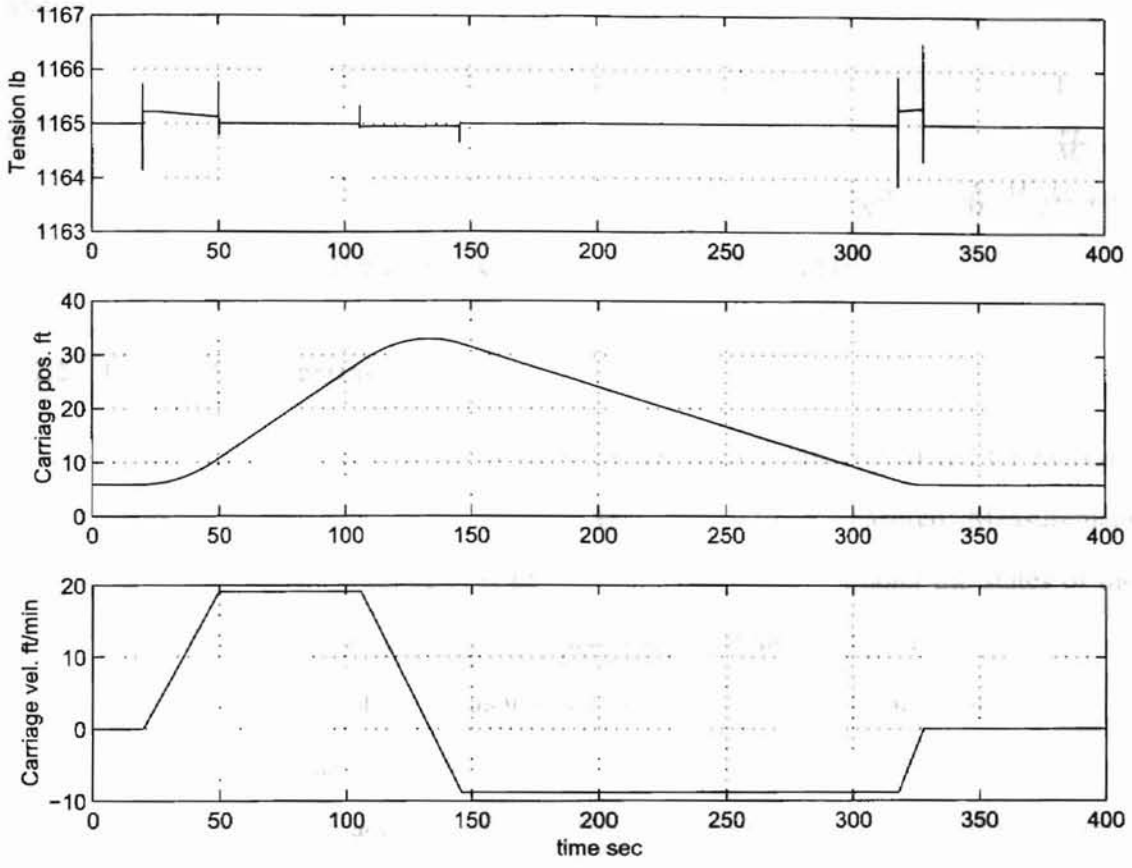


Figure 3.6: Compensated system with friction term and PI controller.

The column rank of this matrix is three. Therefore the system is locally reachable. After this the local observability of the system is checked. The system given by (3.4) and (3.6) is said to be locally observable at $x_0 \in X$ if there exists a deleted neighborhood $N$ of $x_0$ such that each $x \in N$ is distinguishable from $x_0$. The system is locally observable if it is locally observable at each $x_0 \in X$. If $G$ denotes the set of all finite linear combinations of the Lie derivatives of $h_1$ and $h_2$ with respect to $f$ and $dG$ denotes the set of all their gradients, then the system is said to be locally observable if one can find 3 linearly independent vectors within $dG$. In the present case of the accumulator system, $G$ and $dG$ are given by:

$$G = \begin{bmatrix} \xi_2 & \xi_3 \\ \xi_3 & \frac{1}{M_c}(-N\xi_1 - F_f(\xi_3)) - g \\ \frac{1}{M_c}(-N\xi_1 - F_f(\xi_3)) - g & -\frac{N(AE-\xi_1)}{\xi_2 M_c}(\xi_3 + \frac{v_e - v_p}{N}) - \frac{v_f}{M_c}(\frac{-N\xi_1 - F_f}{M_c} - g) \end{bmatrix},$$

and

$$dG = \begin{bmatrix} 0 & 1 & 0 & 0 & 0 & 1 \\ 0 & 0 & 1 & -\frac{N}{M_c} & 0 & -\frac{v_f}{M_c} \\ -\frac{N}{M_c} & 0 & -\frac{v_f}{M_c} & \frac{N}{M_c}(\frac{1}{\xi_2}(\xi_3 + \frac{v_e - v_p}{N}) + \frac{v_f}{M_c}) & \frac{N}{M_c}\frac{AE-\xi_1}{\xi_2^2}(\xi_3 + \frac{v_e-v_p}{N}) & -\frac{N}{M_c}\frac{AE-\xi_1}{\xi_2} + (\frac{v_f}{M_c})^2 \end{bmatrix}.$$

The rank of $dG$ is three. Therefore the system is locally observable.

### 3.2.2 Feedback Linearization

In this section, the dynamics of the web spans and the carriage are considered for analysis. Only the position and velocity of the carriage are assumed to be measured. Measurement of tension in each accumulator span is practically not feasible. Among the states of the system given by (2.46), (2.47), and (2.48), only position of the carriage and velocity of the carriage are directly available as measured signals. Full knowledge of the mathematical model of system can be used to estimate the unknown state. For this purpose the feedback linearization is used. Displacement of the carriage is considered as output of the system. The output equation can be written as:

$$y = h(\xi) = \xi_2. \tag{3.7}$$

The derivatives of the output equation are given by:

$$\dot{y} = \dot{\xi}_2 = \xi_3,$$

$$\ddot{y} = \dot{\xi}_3 = \frac{1}{M_c}(-N\xi_1 - F_f(\xi_3) + u_c) - g.$$

Hence, the system has relative degree of 2 in $R^3$. Now let

$$u_c = M_c(u_p + g) + N\xi_1 + F_f(\xi_3). \tag{3.8}$$

This gives the transformed, linearized system as:

$$\ddot{y} = u_p. \tag{3.9}$$

Now let

$$f(\xi) = \begin{bmatrix} \frac{AE-\xi_1}{\xi_2}\left(\xi_3 + \frac{v_e - v_p}{N}\right) \\ \xi_3 \\ \frac{1}{M_c}(-N\xi_1 - F_f(\xi_3)) - g \end{bmatrix}, \quad p(\xi) = \begin{bmatrix} 0 \\ 0 \\ \frac{1}{M_c} \end{bmatrix}. \tag{3.10}$$

Then

$$\psi_1 = h(\xi) = \xi_2,$$
$$\psi_2 = \frac{\partial \psi_1}{\partial \xi} f(\xi) = \xi_3.$$

The third function required to complete the transformation should satisfy

$$\frac{\partial \phi}{\partial \xi} p(\xi) = 0,$$

which gives

$$\frac{\partial \phi}{\partial \xi_3} = 0.$$

The state $\phi$ is independent of $\xi_3$ and it is a function of $\xi_1$ and $\xi_2$ only. To complete the transformation let

$$\phi = \xi_1 \xi_2.$$

The associated state transformation is given by:

$$\mathbf{z} = \begin{bmatrix} \phi \\ \psi_1 \\ \psi_2 \end{bmatrix}. \tag{3.11}$$

After transformation the final state space form is given by:

$$\dot{\phi} = AE\psi_2 + \frac{AE}{N}(v_e(t) - v_p(t)), \tag{3.12}$$

$$\dot{\psi}_1 = \psi_2, \tag{3.13}$$

$$\dot{\psi}_2 = u_p, \tag{3.14}$$

$$y = \psi_1, \tag{3.15}$$

$$u_c = M_c(u_p + g) + N(AE + \frac{\phi}{\psi_1}) + F_f(\psi_2). \tag{3.16}$$

This is the transformed state space model of the system. This system is equivalent to a system with a unit mass and a controller can be designed for this system. The control input $u_p$ can be obtained from this analysis, which will further govern the hydraulic force profile $u_c$. In equation (3.16), the control input $u_p$ is being multiplied by $M_c$ to amplify its effect. With this exercise of state transformation, the tension control problem is converted into a position and velocity tracking problem.

**Observability and Controllability of Feedback Linearized System**

The question of controllability and observability for the transformed system given by equations (3.12) through (3.16) is briefly considered in this section. In matrix form the system can be written as:

$$\begin{bmatrix} \dot{\phi} \\ \dot{\psi}_1 \\ \dot{\psi}_2 \end{bmatrix} = \begin{bmatrix} 0 & 0 & AE \\ 0 & 0 & 1 \\ 0 & 0 & 0 \end{bmatrix} \begin{bmatrix} \phi \\ \psi_1 \\ \psi_2 \end{bmatrix} + \begin{bmatrix} 0 \\ 0 \\ 1 \end{bmatrix} u_p, \tag{3.17}$$

and output equation can be written as:

$$\begin{bmatrix} y_1 \\ y_2 \end{bmatrix} = \begin{bmatrix} 0 & 1 & 0 \\ 0 & 0 & 1 \end{bmatrix} \begin{bmatrix} \phi \\ \psi_1 \\ \psi_2 \end{bmatrix}. \tag{3.18}$$

The controllability matrix is given by

$$W_c = \begin{bmatrix} B & AB & A^2B \end{bmatrix} = \begin{bmatrix} 0 & AE & 0 \\ 0 & 1 & 0 \\ 1 & 0 & 0 \end{bmatrix}. \tag{3.19}$$

Rank of this matrix is 2. From this a conclusion can be made that the system is not controllable. Similarly the observability matrix is given by

$$W_o = \begin{bmatrix} C' & A'C' & A'^2C' \end{bmatrix} = \begin{bmatrix} 0 & 0 & 0 & 0 & 0 & 0 \\ 1 & 0 & 1 & 0 & 1 & 0 \\ 0 & 1 & 0 & 0 & 0 & 0 \end{bmatrix}. \tag{3.20}$$

Again the rank is 2. All the states of the system are not observable. The first state i.e product of position and tension in the web spans, is not observable.

### 3.2.3 Controllability and Observability Analysis for Jacobi Linearized System

In this section Jacobi linearization is performed on the system considered in the previous section. The linearized system will be in the form

$$\dot{\delta x} = A\delta x + B\delta u,$$

$$y = C\delta x.$$

In this particular system there are forced equilibrium points. Linearization is performed about the point defined by:

$$\dot{\xi}_1 = 0,$$

$$\xi_1 = t_{ref} = 1165,$$

$$\xi_2 = \xi_2^{eq} = 71,$$

$$\dot{\xi}_3 = \xi_3 = 0,$$

$$v_e^{eq} = v_p^{eq} = 130,$$

$$u_c^{eq} = Nt_{ref} + M_c g.$$

Matrices $A$, $B$ and $C$ are computed as:

$$A = \begin{bmatrix} -\frac{1}{\xi_2}(\xi_3 + \frac{v_e - v_p}{N}) & -\frac{AE-\xi_1}{\xi_2^2}(\xi_3 + \frac{v_e - v_p}{N}) & \frac{AE-\xi_1}{\xi_2} \\ 0 & 0 & 1 \\ -\frac{N}{M_c} & 0 & -\frac{v_f}{M_c} \end{bmatrix},$$

$$B = \begin{bmatrix} 0 \\ 0 \\ \frac{1}{M_c} \end{bmatrix}, \quad and \quad C = \begin{bmatrix} 0 & 1 & 0 \\ 0 & 0 & 1 \end{bmatrix}.$$

The controllability matrix is given by:

$$W_c = \begin{bmatrix} B & AB & A^2B \end{bmatrix}$$

$$= \begin{bmatrix} 0 & \frac{1}{M_c}\frac{AE-\xi_1}{\xi_2} & -\frac{2}{M_c}\frac{AE-\xi_1}{\xi_2^2}(\xi_3 + \frac{v_e-v_p}{N}) - \frac{1}{M_c}\frac{v_f}{M_c}\frac{AE-\xi_1}{\xi_2} \\ 0 & \frac{1}{M_c} & -\frac{1}{M_c}\frac{v_f}{M_c} \\ \frac{1}{M_c} & -\frac{1}{M_c}\frac{v_f}{M_c} & -\frac{N}{M_c}\frac{1}{M_c}\frac{AE-\xi_1}{\xi_2} + (\frac{v_f}{M_c})^2\frac{1}{M_c} \end{bmatrix}.$$

Rank of this matrix is 2. Therefore the system is not controllable. Similarly the Observability matrix is given by:

$$W_o = \begin{bmatrix} C \\ CA \\ CA^2 \end{bmatrix}$$

$$= \begin{bmatrix} 0 & 1 & 0 \\ 0 & 0 & 1 \\ 0 & 0 & 1 \\ -\frac{N}{M_c} & 0 & -\frac{v_f}{M_c} \\ -\frac{N}{M_c} & 0 & -\frac{v_f}{M_c} \\ \frac{N}{M_c}\frac{1}{\xi_2}(\xi_3 + \frac{v_e-v_p}{N}) + \frac{v_f}{M_c}\frac{N}{M_c} & \frac{N}{M_c}\frac{AE-\xi_1}{\xi_2^2}(\xi_3 + \frac{v_e-v_p}{N}) & -\frac{N}{M_c}\frac{AE-\xi_1}{\xi_2} + (\frac{v_f}{M_c})^2 \end{bmatrix}.$$

The rank of this matrix is 3. Therefore the system is observable as concluded in previous section.

### 3.3 System Dynamics Including Exit and Entry Roller Dynamics

In the previous two sections, only the dynamics of $\xi_1$, $\xi_3$ and $\xi_3$ are considered and $v_e$, $v_p$ are taken as known perturbations to the system. In this section dynamics of exit and entry

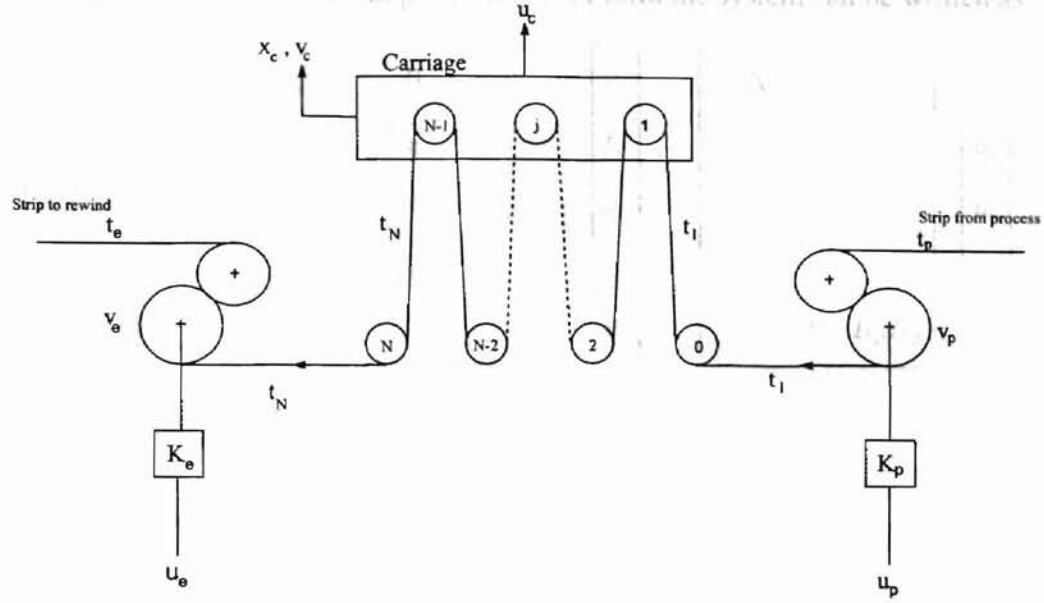


Figure 3.7: Exit accumulator with process-side and exit-side driven roller.

roller to accumulator are also considered for analysis. The final system is given by:

$$\dot{v}_e = \frac{1}{J_e}(-B_{fe}v_e(t) + R_e^2(t_r - t_c(t)) + R_e K_e u_e), \tag{3.21}$$

$$\dot{t}_c = \frac{AE - t_c(t)}{x_c(t)}\left(v_c(t) + \frac{(v_e(t) - v_p(t))}{N}\right), \tag{3.22}$$

$$\dot{x}_c = v_c(t), \tag{3.23}$$

$$\dot{v}_c = \frac{1}{M_c}(-Nt_c(t) + u_c - F_d(t)) - g, \tag{3.24}$$

$$\dot{v}_p = \frac{1}{J_p}(-B_{f1}v_p(t) + R_p^2(t_c(t) - t_r) + R_p K_p u_p). \tag{3.25}$$

Accumulator can be represented as shown in Figure 3.7, i.e. a system with three control inputs. An assumption has been made here that both entry and exit spans to accumulator

have tension $t_c$. With this assumption, in matrix form the system can be written as:

$$\begin{bmatrix} \dot{v}_e \\ \dot{t}_c \\ \dot{x}_c \\ \dot{v}_c \\ \dot{v}_p \end{bmatrix} = \underbrace{\begin{bmatrix} -\frac{B_{fe}}{J_e} & -R_e^2 & 0 & 0 & 0 \\ \frac{AE-t_c}{Nx_c} & 0 & 0 & \frac{AE-t_c}{N} & \frac{AE-t_c}{Nx_c} \\ 0 & 0 & 0 & 1 & 0 \\ 0 & -\frac{N}{M_c} & 0 & 0 & 0 \\ 0 & R_p^2 & 0 & 0 & -\frac{B_{fp}}{J_p} \end{bmatrix}}_{A} \begin{bmatrix} v_e \\ t_c \\ x_c \\ v_c \\ v_p \end{bmatrix} + \underbrace{\begin{bmatrix} R_eK_e & 0 & 0 \\ 0 & 0 & 0 \\ 0 & 0 & 0 \\ 0 & 1 & 0 \\ 0 & 0 & R_pK_p \end{bmatrix}}_{B} \begin{bmatrix} u_e \\ u_c \\ u_p \end{bmatrix}, \quad (3.26)$$

and the output matrix is given by

$$\begin{bmatrix} y_1 \\ y_2 \\ y_3 \\ y_4 \end{bmatrix} = \underbrace{\begin{bmatrix} 1 & 0 & 0 & 0 & 0 \\ 0 & 0 & 1 & 0 & 0 \\ 0 & 0 & 0 & 1 & 0 \\ 0 & 0 & 0 & 0 & 1 \end{bmatrix}}_{C} \begin{bmatrix} v_e \\ t_c \\ x_c \\ v_c \\ v_p \end{bmatrix}.$$

### 3.3.1 Analysis of the Accumulator System Ignoring Nonlinearities

In this section the system is written in following form for analysis:

$$\dot{x} = Ax + Bu + f(x), \quad (3.27)$$

$$y = Cx. \quad (3.28)$$

Considering the equations (2.46), (2.47),(2.48), (2.50), and (2.51), the matrices $A$, $B$, $C$, and the term $f(x)$ are given by:

$$A = \begin{bmatrix} 0 & 0 & 0 & 0 & 0 \\ 0 & 0 & 1 & 0 & 0 \\ -\frac{N}{M_c} & 0 & -\frac{v_f}{M_c} & 0 & 0 \\ -R_e^2 & 0 & 0 & -\frac{B_{fe}}{J_e} & 0 \\ R_p^2 & 0 & 0 & 0 & -\frac{B_{fp}}{J_p} \end{bmatrix}, \qquad B = \begin{bmatrix} 0 & 0 & 0 \\ 0 & 0 & 0 \\ 0 & 1 & 0 \\ R_eK_e & 0 & 0 \\ 0 & 0 & R_pK_p \end{bmatrix},$$

$$C = \begin{bmatrix} 1 & 0 & 0 & 0 & 0 \\ 0 & 0 & 1 & 0 & 0 \\ 0 & 0 & 0 & 1 & 0 \\ 0 & 0 & 0 & 0 & 1 \end{bmatrix}, \qquad f(x) = \begin{bmatrix} (\frac{AE-\xi_1}{\xi_2})(\xi_3 + \frac{1}{N}(v_e(t) - v_p(t)) \\ 0 \\ 0 \\ 0 \\ 0 \end{bmatrix}.$$

Using these matrices the controllability and observability matrices can be calculated as per:

$$W_c = \begin{bmatrix} B & AB & A^2B & A^3B & A^4B \end{bmatrix},$$
$$W_o = \begin{bmatrix} C' & A'C' & A'^2C' & A'^3C' & A'^4C' \end{bmatrix}.$$

Due to construction of the matrix $A$, the column rank of $W_c$ and $W_o$ can not be five. Therefore the system is not controllable as well as not observable. In the next step, state equations are written using a new state vector defined as:

$$\mathbf{x} = \begin{bmatrix} v_e \\ \xi_1\xi_2 \\ \xi_2 \\ \xi_3 \\ v_p \end{bmatrix} = \begin{bmatrix} x_1 \\ x_2 \\ x_3 \\ x_4 \\ x_5 \end{bmatrix}. \tag{3.29}$$

This transformation is equivalent to feedback linearized system along with exit-side and process-side driven roller dynamics. The system can be rewritten in terms of new state variables as:

$$\dot{x}_1 = \frac{1}{J_e}(-B_{fe}x_1 + R_e^2(t_{ref} - \frac{x_2}{x_3})) + R_eK_eu_e, \tag{3.30}$$

$$\dot{x}_2 = AE(\frac{x_1}{N} + x_4 - \frac{x_5}{N}) - \frac{x_2}{x_3}(\frac{x_1}{N} - \frac{x_5}{N}), \tag{3.31}$$

$$\dot{x}_3 = x_4, \tag{3.32}$$

$$\dot{x}_4 = \frac{1}{M_c}(-N\frac{x_2}{x_3} - v_fx_4 + u_c) - g, \tag{3.33}$$

$$\dot{x}_5 = \frac{1}{J_p}(-B_{fp}x_5 + R_p^2(\frac{x_2}{x_3} - t_{ref})) + R_eK_eu_e. \tag{3.34}$$

The new matrices $A$, $B$, $C$, and the term $f(x)$ are given by:

$$A = \begin{bmatrix} -\frac{B_{fe}}{J_e} & 0 & 0 & 0 & 0 \\ \frac{AE}{N} & 0 & 0 & AE & -\frac{AE}{N} \\ 0 & 0 & 0 & 1 & 0 \\ 0 & 0 & 0 & -\frac{v_f}{M_c} & 0 \\ 0 & 0 & 0 & 0 & -\frac{B_{fp}}{J_p} \end{bmatrix}, \quad B = \begin{bmatrix} R_e K_e & 0 & 0 \\ 0 & 0 & 0 \\ 0 & 0 & 0 \\ 0 & \frac{1}{M_c} & 0 \\ 0 & 0 & R_p K_p \end{bmatrix}$$

$$C = \begin{bmatrix} 1 & 0 & 0 & 0 & 0 \\ 0 & 0 & 1 & 0 & 0 \\ 0 & 0 & 0 & 1 & 0 \\ 0 & 0 & 0 & 0 & 1 \end{bmatrix}, \quad f(x) = \begin{bmatrix} -R_e^2 \frac{x_2}{x_3} \\ -\frac{x_2}{x_3}\left(\frac{x_1}{N} - \frac{v_p}{N}\right) \\ 0 \\ -\frac{N}{M_c}\frac{x_2}{x_3} \\ R_p^2 \frac{x_2}{x_3} \end{bmatrix}.$$

Using these matrices the controllability matrix ($W_c$)and observability matrix ($W_o$) are calculated again and rank of these matrices is less than five. Thus the system is not controllable as well as not observable.

### 3.3.2 Analysis of the Accumulator System

Considering the nonlinearities along with the fact that the position of the carriage and reference average tension in the web spans is always a positive number, the controllability and observability matrices are calculated using matrix form system given by (3.26). Rank of the controllability as well as observability matrix comes out to be 5, which makes the system controllable and observable. As discussed in a earlier section, the exit velocity is zero for some part of the core change cycle. When the exit velocity is zero, the first control

input is lost. Therefore, matrix B is given by:

$$B = \begin{bmatrix} 0 & 0 & 0 \\ 0 & 0 & 0 \\ 0 & 0 & 0 \\ 0 & 1 & 0 \\ 0 & 0 & R_p K_p \end{bmatrix}, \tag{3.35}$$

and matrix C is given by

$$C = \begin{bmatrix} 0 & 0 & 1 & 0 & 0 \\ 0 & 0 & 0 & 1 & 0 \\ 0 & 0 & 0 & 0 & 1 \end{bmatrix}. \tag{3.36}$$

Again the matrices $W_c$ and $W_o$ have rank 5, which keeps the system controllable and observable. The system is controllable and observable if considered in its nonlinear form, without neglecting any nonlinear terms. A nonlinear controller has to be designed for this system as linear control schemes may not be feasible.

### 3.3.3 Jacobi Linearization of the Accumulator System

To analyze the system about some equilibrium point Jacobi linearization can be very helpful. In this particular system there are many different forced equilibrium points. Linearization is performed about the point, when the carriage is at its lowest position and it is not in motion. At this equilibrium point following identities will be true,

$$\begin{aligned} \dot{v}_p = \dot{v}_e = 0, \qquad & v_p = v_e = v = 130, \\ \dot{t}_c = 0, \qquad & t_c = t_{ref} = 1165, \\ \dot{x}_c = 0, \qquad & x_c = x_{eq} = 71, \\ u_e^{eq} = \frac{B_{fe} v}{J_e K_e}, \qquad & u_c^{eq} = \frac{N t_{rcf} + M_c g}{A_{cyl}}, \\ u_p^{eq} = \frac{B_{fp} v}{J_p K_p}. & \end{aligned}$$

From matrices defined in previous section, this system in linear form can be represented as:

$$\dot{\delta x} = \begin{bmatrix} -\frac{B_{fe}}{J_e} & -\frac{R_e^2}{J_e} & 0 & 0 & 0 \\ -\frac{AE}{Nx_{eq}} & 0 & 0 & \frac{AE-t_{ref}}{x_{eq}} & \frac{AE}{Nx_{eq}} \\ 0 & 0 & 0 & 1 & 0 \\ 0 & -\frac{N}{M_c} & 0 & 0 & 0 \\ 0 & -\frac{R_p^2}{J_p} & 0 & 0 & -\frac{B_{fp}}{J_p} \end{bmatrix} \delta\mathbf{x} + \begin{bmatrix} \frac{R_e K_e}{J_e} & 0 & 0 \\ 0 & 0 & 0 \\ 0 & 0 & 0 \\ 0 & \frac{1}{M_c} & 0 \\ 0 & 0 & \frac{R_p K_p}{J_p} \end{bmatrix} \delta\mathbf{u}.$$

This final representation is in the form of

$$\dot{x} = Ax + Bu.$$

The roller bearing friction for entry and exit roller, $B_j$, is very small and can be ignored ($B_j \approx 0$). For that case, the eigen values of this matrix $A$, using parameters for ALCOA CPL, are given by:

$$\lambda_{1--5} = 0,\ \pm 69.1197i,\ 0,\ 0.$$

Also the rank of Jacobi matrix $A$ is 3 in this case. All the eigen values are at origin or at the imaginary axis. So linearization about this forced equilibrium point does not suggest any thing new in understanding the system. This system is a real time system and practically it is stable. So it can be concluded that because of the nature of the process of linearization about a single point cannot guarantee the same characteristics of the system, in the whole space.

### 3.4 Synopsis

In all the previous sections, the system given by equations (2.46) through (2.51), is analyzed after performing different state transformations. The system given by equations (2.46) through (2.48) along with exit-side driven roller dynamics (2.50) and process-side driven roller (2.51), is controllable and observable. The system loses its controllability and observability if any transformation is performed ,therefore, a linear control scheme can not

be designed. The nonlinearities in the system are responsible for the controllability and observability of this system. This nonlinear system is used for further analysis in following chapters. A nonlinear controller scheme is designed and investigated for this system.

# CHAPTER 4

# CONTROLLER AND OBSERVER DESIGN

## 4.1 Controller Design

This chapter considers the design of control algorithms for the accumulator carriage, the exit-side driven roller and the process-side driven roller such that the average web tension, the carriage position, the carriage velocity, the exit-side web velocity and process-side web velocity track their desired trajectories. It is assumed that all the state variables are measurable except for the average web tension, $\xi_1(t)$. An observer will be designed to estimate the average web tension.

Consider the following error variables: $e_1(t) = \xi_1(t) - \xi_1^d$, $e_2(t) = \xi_2(t) - \xi_2^d(t)$, $e_3(t) = \xi_3(t) - \xi_3^d(t)$, $e_e(t) = \xi_5(t) - \xi_5^d(t)$,and $e_p(t) = \xi_6(t) - \xi_6^d(t)$, where $\xi_1^d$ is the desired web tension, $\xi_2^d(t)$ and $\xi_3^d(t)$ are the desired accumulator position and velocity, respectively and $\xi_5^d(t)$ and $\xi_6^d(t)$ are desired exit and process-side velocities, respectively. Choose the following control inputs for the accumulator carriage, exit-side driven roller, and the process-side driven roller:

$$u_c(t) = M_c(\dot{\xi}_3^d(t) + g + \frac{v_f}{M_c}\xi_3^d(t) + \frac{N}{M_c}\xi_1^d + u_{ca}(t)), \tag{4.1}$$

$$u_e(t) = \frac{J_e}{R_e K_e}\left(u_{ea}(t) + \frac{B_{fe}}{J_e}\xi_5^d(t) + \dot{\xi}_5^d(t)\right), \tag{4.2}$$

$$u_p(t) = \frac{J_p}{R_p K_p}\left(u_{pa}(t) + \frac{B_{fp}}{J_p}\xi_6^d(t) + \dot{\xi}_6^d(t)\right), \tag{4.3}$$

where $u_{ca}(t)$, $u_{ea}(t)$, and $u_{pa}(t)$ are auxiliary control inputs that will be designed later. Substituting the control input and using the error definitions, the error dynamics is given

by:

$$\dot{e}_1(t) = \frac{AE}{\xi_2(t)} e_3(t) + \frac{AE}{N\xi_2(t)} \left(e_e(t) - e_p(t)\right), \tag{4.4}$$

$$\dot{e}_2(t) = e_3(t), \tag{4.5}$$

$$\dot{e}_3(t) = -\frac{N}{M_c} e_1(t) - \frac{v_f}{M_c} e_3(t) + u_{ca}(t), \tag{4.6}$$

$$\dot{e}_e(t) = \frac{1}{J_e}\left(-B_{fe} e_e(t) - R_e^2 e_1(t) + R_e^2 \delta_e(t)\right) + u_{ea}(t), \tag{4.7}$$

$$\dot{e}_p(t) = \frac{1}{J_p}\left(-B_{fp} e_p(t) + R_p^2 e_1(t) - R_p^2 \delta_p(t)\right) + u_{pa}(t). \tag{4.8}$$

Consider the following observer for estimating the average tension dynamics:

$$\dot{\widehat{\xi}}_1(t) = \frac{AE}{\xi_2(t)} e_3(t) + \frac{AE}{N\xi_2(t)}(e_e(t) - e_p(t)) + \widehat{f}_{\xi_1}, \;\; \widehat{\xi}_1(0) = \widehat{\xi}_{10}, \tag{4.9}$$

where $\widehat{\xi}_1(t)$ is the estimate of $\xi_1(t)$, and $\widehat{f}_{\xi_1}$ will be chosen later during the stability analysis. Define the observation error as $\widetilde{e}_1(t) = \xi_1(t) - \widehat{\xi}_1(t)$. Also, define $\widehat{e}_1(t) = \widehat{\xi}_1(t) - \xi_1^d$. Therefore, the observer error dynamics is

$$\dot{\widetilde{e}}_1(t) = -\widehat{f}_{\xi_1}. \tag{4.10}$$

Notice that we have used the fact that $\xi_3^d(t) = (\xi_6^d(t) - \xi_5^d(t))/N$, that is, the difference between the desired process velocity and the desired exit velocity divided by the number of spans gives the desired carriage velocity.

Consider the following Lyapunov function candidate for the accumulator carriage system:

$$V_c(t) = \frac{1}{2} e_1^2(t) + \frac{1}{2} e_2^2(t) + \frac{1}{2} e_3^2(t) + \frac{1}{2} \widetilde{e}_1^2(t). \tag{4.11}$$

The derivative of the Lyapunov function candidate along the trajectories of the error dynamics is given by:

$$\begin{aligned} \dot{V}_c(t) &= e_1\dot{e}_1 + e_2\dot{e}_2 + e_3\dot{e}_3 + \widetilde{e}_1\dot{\widetilde{e}}_1 \\ &= \frac{AE}{\xi_2} e_1 e_3 + \frac{AE}{N\xi_2(t)}\left(e_e - e_p\right) e_1 + e_2 e_3 - \frac{N}{M_c} e_1 e_3 - \frac{v_f}{M_c} e_3^2 + u_{ca}(t) e_3 - \widehat{f}_{\xi_1}\widetilde{e}_1. \end{aligned} \tag{4.12}$$

Choose the following auxiliary control input for the carriage:

$$u_{ca}(t) = -\frac{AE}{\xi_2(t)}\widehat{e}_1(t) - e_2(t) + \frac{N}{M_c}\widehat{e}_1(t) - \gamma_3 e_3(t), \tag{4.13}$$

where $\gamma_3$ is a positive gain.

Substituting (4.13) into (4.12), the derivative of the Lyapunov function candidate becomes

$$\dot{V}_c(t) = -\left(\gamma_3 + \frac{v_f}{M_c}\right)e_3^2 + \frac{AE}{N\xi_2(t)}\left(e_e - e_p\right)e_1 + \left(\frac{AE}{\xi_2} - \frac{N}{M_c}\right)\widetilde{e}_1 e_3 - \widehat{f}_{\xi_1}\widetilde{e}_1. \tag{4.14}$$

Consider the following Lyapunov function candidate for the exit and the process-side roller dynamics:

$$V_{ep}(t) = \frac{1}{2}e_e^2(t) + \frac{1}{2}e_p^2(t). \tag{4.15}$$

The derivative of $V_{ep}(t)$ along the trajectories of the error dynamics, (4.7) and (4.8), is

$$\begin{aligned}\dot{V}_{ep}(t) = {} & \frac{1}{J_e}\left(-B_{fe}e_e^2 - R_e^2 e_1 e_e + R_e^2\delta_e(t)e_e\right) + e_e u_{ea} \\ & + \frac{1}{J_p}\left(-B_{fp}e_p^2 + R_p^2 e_1 e_p - R_p^2\delta_p(t)e_p\right) + e_p u_{pa}.\end{aligned} \tag{4.16}$$

Consider the following Lyapunov function candidate for the combined system of the accumulator carriage, exit-side driven roller, and the process-side driven roller:

$$V(t) = V_c(t) + V_{ep}(t). \tag{4.17}$$

The derivative of $V(t)$ is:

$$\begin{aligned}\dot{V}(t) &= \dot{V}_c(t) + \dot{V}_{ep}(t) \\ &= -\left(\gamma_3 + \frac{v_f}{M_c}\right)e_3^2 + \frac{AE}{N\xi_2(t)}\left(e_e - e_p\right)e_1 + \left(\frac{AE}{\xi_2} - \frac{N}{M_c}\right)\widetilde{e}_1 e_3 - \widehat{f}_{\xi_1}\widetilde{e}_1 \\ &\quad + \frac{1}{J_e}\left(-B_{fe}e_e^2 - R_e^2 e_1 e_e + R_e^2\delta_e(t)e_e\right) + e_e u_{ea} \\ &\quad + \frac{1}{J_p}\left(-B_{fp}e_p^2 + R_p^2 e_1 e_p - R_p^2\delta_p(t)e_p\right) + e_p u_{pa}.\end{aligned} \tag{4.18}$$

Assuming that $\delta_e(t)$ and $\delta_p(t)$ are bounded by some known constants, that is, $|\delta_e(t)| \leq \bar{\delta}_e$ and $|\delta_p(t)| \leq \bar{\delta}_p$, we choose the following auxiliary control inputs:

$$u_{ea}(t) = -\gamma_e e_e(t) - \left(\frac{AE}{N\xi_2(t)} - \frac{R_e^2}{J_e}\right)\widehat{e}_1(t) - \frac{R_e^2}{J_e}\bar{\delta}_e \text{sgn}(e_e), \tag{4.19}$$

$$u_{pa}(t) = -\gamma_p e_p(t) + \left(\frac{AE}{N\xi_2(t)} - \frac{R_p^2}{J_p}\right)\widehat{e}_1(t) - \frac{R_p^2}{J_p}\bar{\delta}_p \text{sgn}(e_p), \tag{4.20}$$

where $\gamma_e$ and $\gamma_p$ are positive gains. As all the rollers are of same size and inertia in real industries, therefore $J_e = J_p = J$ and $R_e = R_p = R$ is used in further analysis.

Using these auxiliary control inputs and re-arranging terms, we obtain

$$\begin{aligned}\dot{V}(t) \leq & -\left(\gamma_3 + \frac{v_f}{M_c}\right)e_3^2 - \left(\gamma_e + \frac{B_{fe}}{J}\right)e_e^2 - \left(\gamma_p + \frac{B_{fp}}{J}\right)e_p^2 \\ & - \frac{R^2}{J}|e_e|(\bar{\delta}_e - |\delta_e(t)|) - \frac{R^2}{J}|e_p|(\bar{\delta}_p - |\delta_p(t)|) \\ & + \left(\frac{AE}{\xi_2} - \frac{N}{M_c}\right)\widetilde{e}_1 e_3 + \left(\frac{AE}{N\xi_2} - \frac{R^2}{J}\right)\widetilde{e}_1 e_e - \left(\frac{AE}{N\xi_2} - \frac{R^2}{J}\right)\widetilde{e}_1 e_p - \widehat{f}_{\xi_1}\widetilde{e}_1.\end{aligned} \tag{4.21}$$

Choosing

$$\widehat{f}_{\xi_1} = \left(\frac{AE}{\xi_2} - \frac{N}{M_c}\right)e_3 + \left(\frac{AE}{N\xi_2} - \frac{R^2}{J}\right)(e_e - e_p), \tag{4.22}$$

we get

$$\dot{V}(t) \leq -\left(\gamma_3 + \frac{v_f}{M_c}\right)e_3^2 - \left(\gamma_e + \frac{B_{fe}}{J}\right)e_e^2 - \left(\gamma_p + \frac{B_{fp}}{J}\right)e_p^2. \tag{4.23}$$

Therefore, $V(t) \geq 0$ is a non increasing function of time for all $t \geq 0$. Hence, $V(t) \in \mathcal{L}_\infty$ and $\lim_{t\to\infty} V(t) = V_\infty < \infty$. Also, $e_1(t), \widetilde{e}_1(t), e_2(t), e_3(t),\ e_e(t), e_p(t) \in \mathcal{L}_\infty$ and $e_2(t), e_3(t), e_e(t), e_p(t) \in \mathcal{L}_2$. From the error dynamics, (4.5)–(4.8), $\dot{e}_2(t), \dot{e}_3(t), \dot{e}_e(t), \dot{e}_p(t) \in \mathcal{L}_\infty$. Therefore, using Barbalat's lemma, we have $e_2(t), e_3(t), e_e(t), e_p(t) \to 0$ as $t \to \infty$.

The following theorem summarizes the results of this section.

**Theorem 4.1.1** *For the dynamics of the accumulator carriage and the driven rollers upstream and downstream of the accumulator given by equations* (2.46) *through* (2.51)*, the*

*following control inputs*

$$u_c(t) = M_c(\dot{\xi}_3^d(t) + g + \frac{v_f}{M_c}\xi_3^d(t) + \frac{N}{M_c}\xi_1^d - \frac{AE}{\xi_2(t)}\widehat{e}_1(t) - e_2(t) + \frac{N}{M_c}\widehat{e}_1(t) - \gamma_3 e_3(t)), \tag{4.24}$$

$$u_e(t) = \frac{J}{RK_e}\left(-\gamma_e e_e(t) - \left(\frac{AE}{N\xi_2(t)} - \frac{R^2}{J}\right)\widehat{e}_1(t) - \frac{R^2}{J}\bar{\delta}_e sgn(e_e) + \frac{B_{fe}}{J}\xi_5^d(t) + \dot{\xi}_5^d(t)\right), \tag{4.25}$$

$$u_p(t) = \frac{J}{RK_p}\left(-\gamma_p e_p(t) + \left(\frac{AE}{N\xi_2(t)} - \frac{R^2}{J}\right)\widehat{e}_1(t) - \frac{R^2}{J}\bar{\delta}_p sgn(e_p) + \frac{B_{fp}}{J}\xi_6^d(t) + \dot{\xi}_6^d(t)\right), \tag{4.26}$$

*and the average tension observer*

$$\dot{\widehat{\xi}}_1(t) = \left(\frac{2AE}{\xi_2(t)} - \frac{N}{M_c}\right)e_3(t) + \left(\frac{2AE}{N\xi_2(t)} - \frac{R^2}{J}\right)(e_e(t) - e_p(t)), \quad \widehat{\xi}_1(0) = \widehat{\xi}_{10}, \tag{4.27}$$

*will result in the signals* $e_1(t), \widetilde{e}_1(t), e_2(t), e_3(t), e_e(t), e_p(t)$ *being bounded and further, the signals* $e_3(t), e_e(t), e_p(t)$ *asymptotically converge to zero.*

Equations (4.24), (4.25), (4.26), and (4.27) give the accumulator carriage input, exit-side driven roller input, process-side driven roller input, and the observer dynamics, respectively. The proof of the theorem follows from the prior analysis. Notice that the control inputs given by equations (4.24), (4.25) and (4.26) are dependent on $\widehat{e}_1$, which in turn depends upon $e_e$ and $e_p$. Therefore, in the proposed control scheme all the control algorithms are coupled, i.e., it is centralized control as compared to what is presently used in industry, which is decentralized control.

### 4.1.1 Simulation Study

In this section, the proposed control scheme is investigated by conducting simulations on an industrial continuous web process line. The simulations are performed using the parameters of an ALCOA continuous process line (CPL) and its exit accumulator. Different values of the parameters of the accumulator used in the simulations are given in Table 4.1. The

| Description | Symbol | Value |
|---|---|---|
| Mass of the carriage | Mc | 501.06 slugs |
| Cross-section area of web | A | 0.5 $in^2$ |
| Modulus of elasticity | E | $10^7$psi |
| Number of web spans | N | 34 |
| Viscous friction coefficient | $v_f$ | 20000 lb/(in/sec) |
| Radius of exit and process-side roller | R | 6 in |
| Moment of inertia | J | 228.8448 slugs-$in^2$ |
| Bearing friction coefficient | $B_f$ | 0.02 |

Table 4.1: Parameters of the accumulator.

desired tension in the web spans is 1165 lbs. The desired process speed is 650 fpm. A typical case of the exit speed and the carriage speed during a rewind roll change is depicted in Figure 4.1. The rewind roll change-over scenario, when the web velocity in the process section is maintained at a constant value, is described in the following steps by referring to Figure 4.1: (i) AB – velocity of the web in the rewind side is decelerated to zero from a value of 650 fpm, as a result of this the accumulator starts collecting the web and the carriage accelerates upwards; (ii) BC – rewind stops and the carriage is moving up with constant velocity; (iii) CD – after rewind roll change, exit side is accelerated up to the process speed, in this period the carriage is moving up while decelerating; (iv) DE – exit side is accelerated up to a speed above the process speed, 950 fpm in this case; (v) EF – exit speed is maintained at this constant speed; (vi) FG – exit speed is reduced to the process speed. The desired profile for carriage velocity is given by:

$$\xi_3^d(t) = \frac{\xi_6^d(t) - \xi_5^d(t)}{N}.$$

From this velocity profile the desired carriage position profile is calculated. After each cycle of rewind roll-change operation the carriage will return to its original position; this means that the area under the carriage velocity curve is zero. The goal is to track the

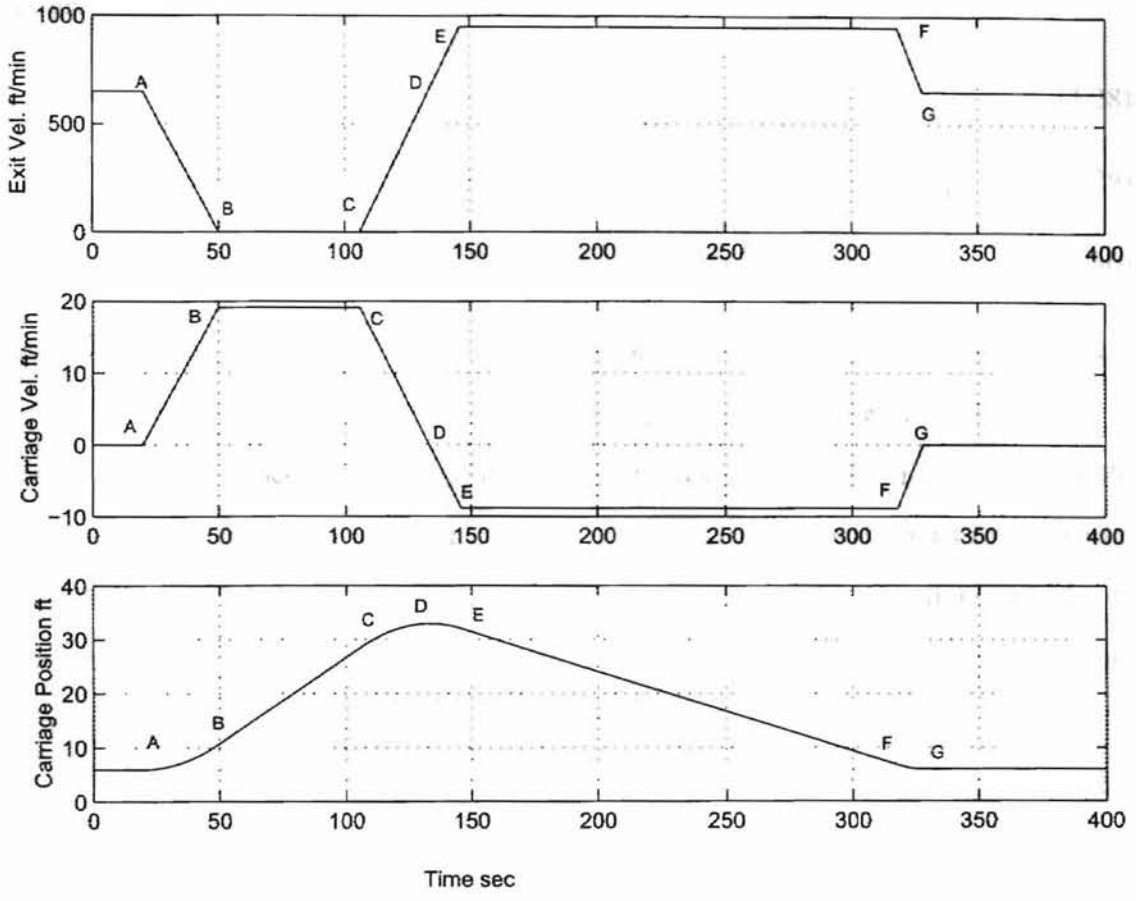


Figure 4.1: Desired exit speed, carriage speed and carriage position during rewind roll-change.

desired profiles of the carriage position and speed, exit velocity and process velocity while maintaining the desired level of the average web tension. The simulations are conducted using the system model given by equations (2.46)-(2.51) and the control algorithms given by (4.24), (4.25), (4.26), and the observer given by equation (4.27).

Two types of controllers are considered for comparative study via simulations: (1) Currently used industrial controller, and (2) the controller proposed in this paper. Currently, the industrial controller uses only feed forward of the desired profile for the accumulator carriage and PI controllers for the exit and process-side driven rollers. The industrial controllers for the accumulator carriage, exit-side driven roller, and process-side driven roller

are given by:

$$u_{cI}(t) = M_c(\dot{\xi}_3^d(t) + g + \frac{v_f}{M_c}\xi_3^d(t) + \frac{N}{M_c}\xi_1^d), \tag{4.28}$$

$$u_{eI}(t) = \frac{J}{RK_e}\left(\frac{B_{fe}}{J}\xi_4^d(t) + \dot{\xi}_4^d(t) - k_{pe}e_e(t) - k_{ie}\int e_e(t)d\tau\right), \tag{4.29}$$

$$u_{pI}(t) = \frac{J}{RK_p}\left(\frac{B_{fp}}{J}\xi_5^d(t) + \dot{\xi}_5^d(t) - k_{pp}e_p(t) - k_{ip}\int e_p(t)d\tau\right), \tag{4.30}$$

where $k_{pe}$ and $k_{pp}$, and $k_{ie}$ and $k_{ip}$ are the proportional and integral gains, respectively. Notice that if same control gains are considered for proposed control scheme and for industrial controller, the proposed controller expressions given by equations (4.24), (4.25) and (4.26) have few additional terms, as auxiliary input, in comparison to expressions for industrial controllers given by equations (4.28), (4.29) and (4.30). Later with simulations, it is shown that with this little extra effort at each instant, the tension variations can be controlled more effectively.

The disturbances $\delta_e$, present on the exit-side driven roller tension system, and $\delta_p$, present on the process-side driven roller tension system, considered in equations (2.50) and (2.51), are of sinusoidal nature with a frequency of 0.2 Hz and amplitude 10 lbs. For comparing the results of the two types of controllers, three types of sinusoidal disturbances are introduced into the accumulator carriage dynamics, that is, into equation (2.48). The amplitude of these disturbances is 10 in/sec$^2$ and the frequency is 0.5 Hz. Low frequency disturbances are used because they are typical disturbances on the accumulator carriage; the accumulator carriage does not have the ability to respond to high frequency disturbances due to its large mass. We consider the three time profiles shown in Figure 4.2 for introducing sinusoidal disturbances into the accumulator carriage. In the first case the sinusoidal disturbance is introduced throughout the time duration of 400 seconds. In the second case the sinusoidal disturbance is introduced at specific time intervals of 20 to 30 seconds, 106 to 126 seconds, and then from 318 to 328 seconds. In the third case the disturbance is introduced at specific time intervals of 20-30 seconds, 40-60 seconds, 96-116 seconds, 136-156 seconds, and 308-328 seconds. The time durations in the second and third case are picked

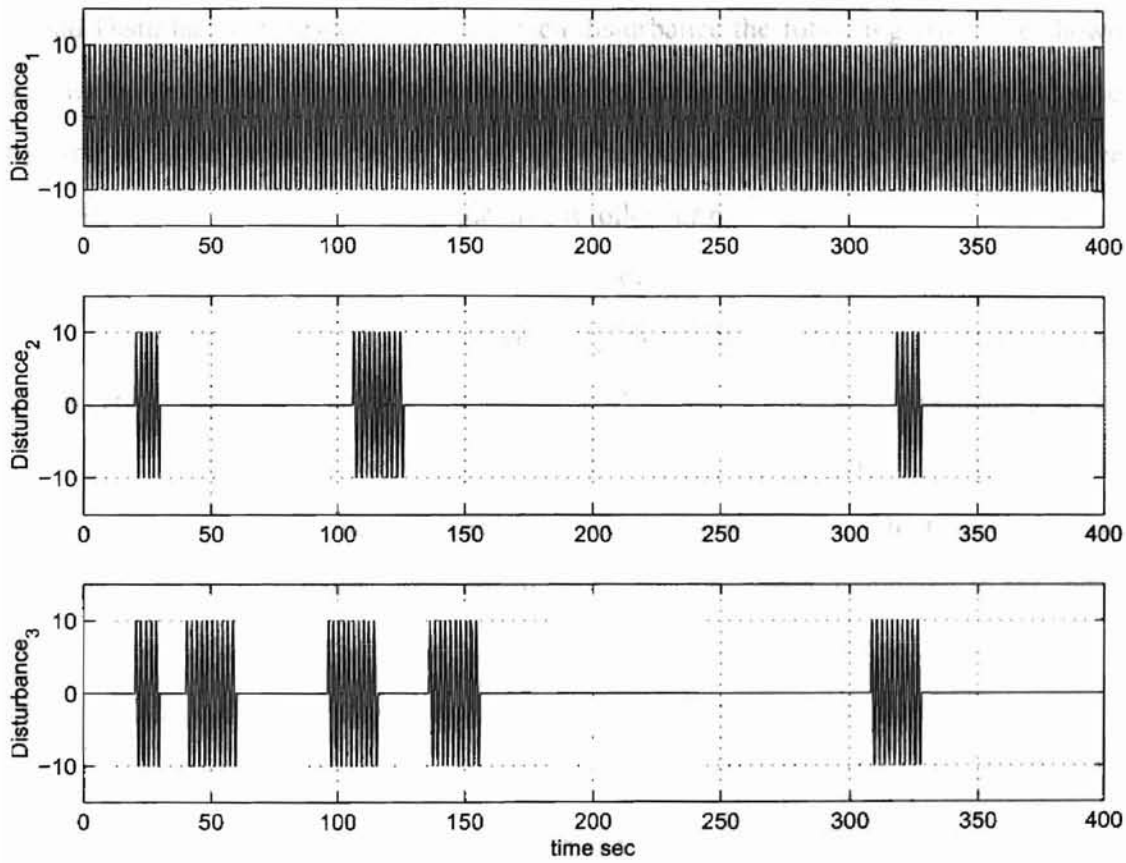


Figure 4.2: Three cases of sinusoidal disturbances.

to reflect observations made on an industrial process line that periodic disturbances occur during the initiation of carriage motion from its stationary state and when the exit velocity starts to accelerate or decelerate. The simulations are performed for these three cases of disturbances and for both types of controllers. All the gains that are common to both controllers are chosen to be the same. The results are shown in Figures 4.3 through 4.14. The three cases of disturbances shown in Figure 4.2 are labelled as Disturbance 1, Disturbance 2, and Disturbance 3, respectively. For each disturbance the following errors are shown: web tension error ($e_1$), carriage position error ($e_2$), carriage velocity error ($e_3$), exit velocity error ($e_e$), and process velocity error ($e_p$). The control signals of accumulator carriage, exit-side driven roller, and process-side driven roller for both controllers are also shown.

Figures 4.3 and 4.4 show the errors for the industrial controller and the proposed controller, respectively. From the results we can gather that the proposed controller does a much better job at the sinusoidal disturbances. As tension variations propagate both upstream and downstream of the accumulator, these variations in tension and process speed will affect the web in the entire process line, which is undesirable. The magnitude of all the error signals for the proposed control scheme is very small compared to the industrial controller. Figures 4.5 and 4.6 show the plots for control effort required for the two schemes. The control effort required for accumulator carriage is similar in both schemes but the control effort for both driven rollers for the proposed controller is smaller than the industrial controller. Overall, the performance of the proposed controller is much improved compared to the industrial controller with no additional control effort.

Figures 4.7 through 4.10 and Figures 4.11 through 4.14 show results corresponding to Disturbance 2 and Disturbance 3, respectively. Similar observations as made in the case of Disturbance 1 can also be made for Disturbance 2 and Disturbance 3.

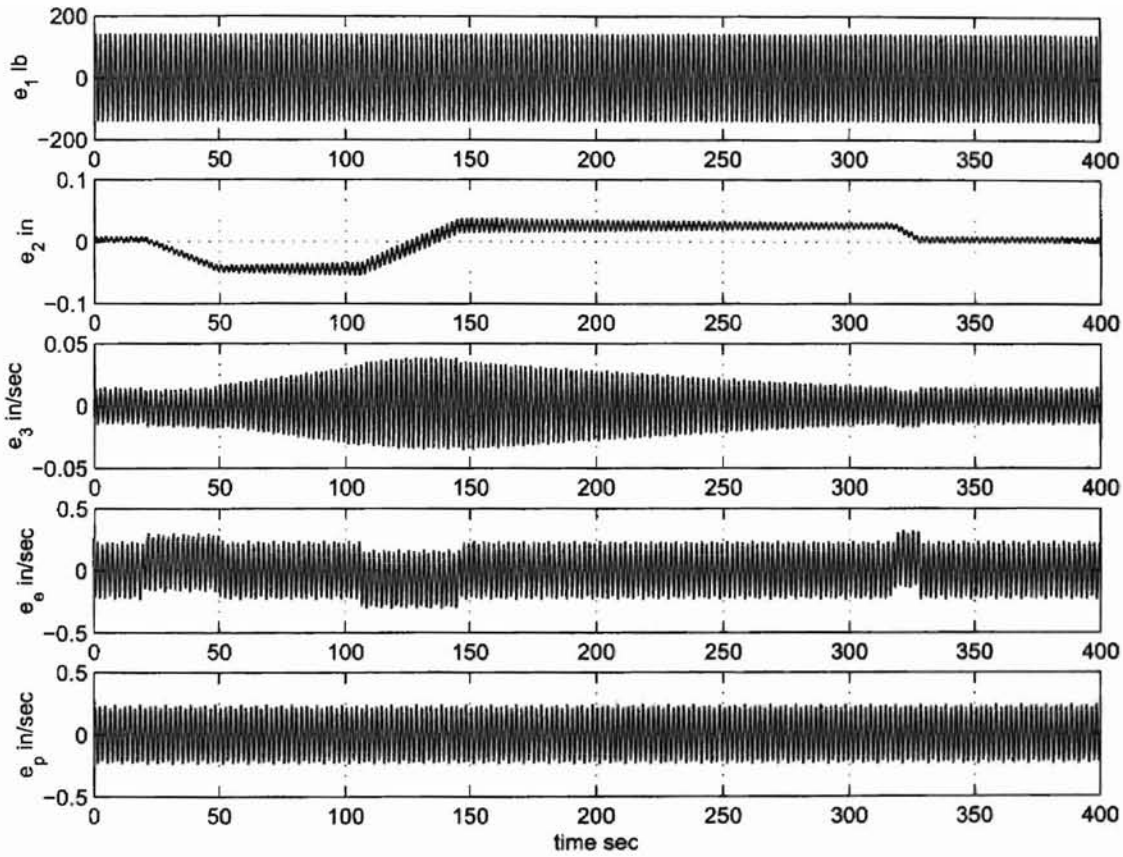


Figure 4.3: State errors of the industrial controller: Disturbance 1.

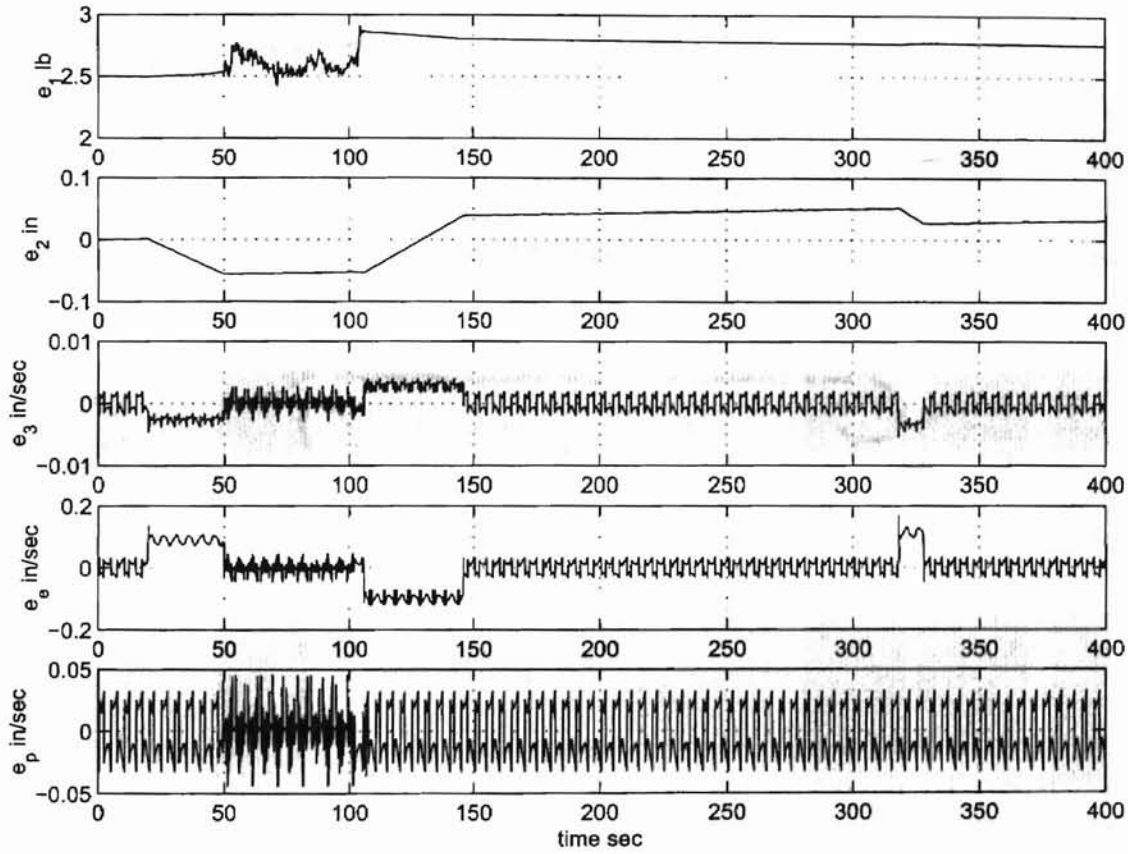


Figure 4.4: State errors of the proposed controller: Disturbance 1.

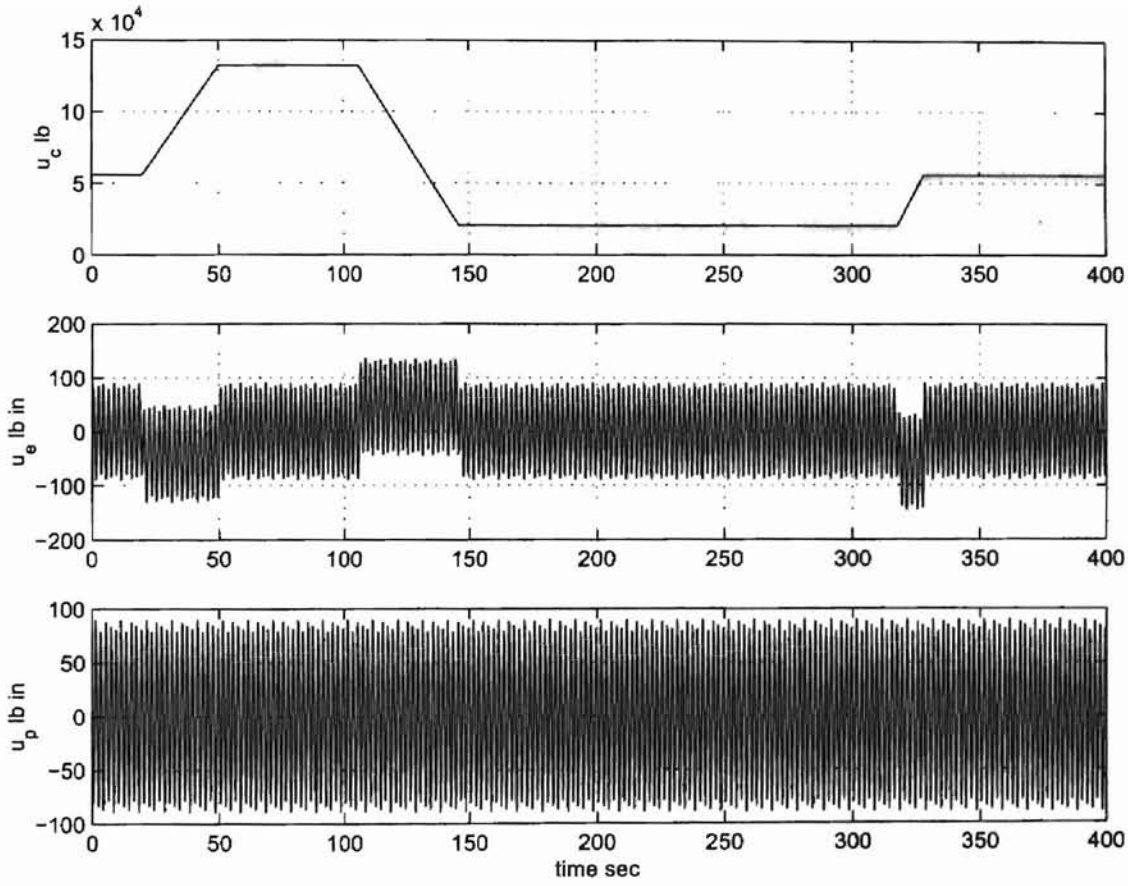


Figure 4.5: Control inputs for the industrial controller: Disturbance 1.

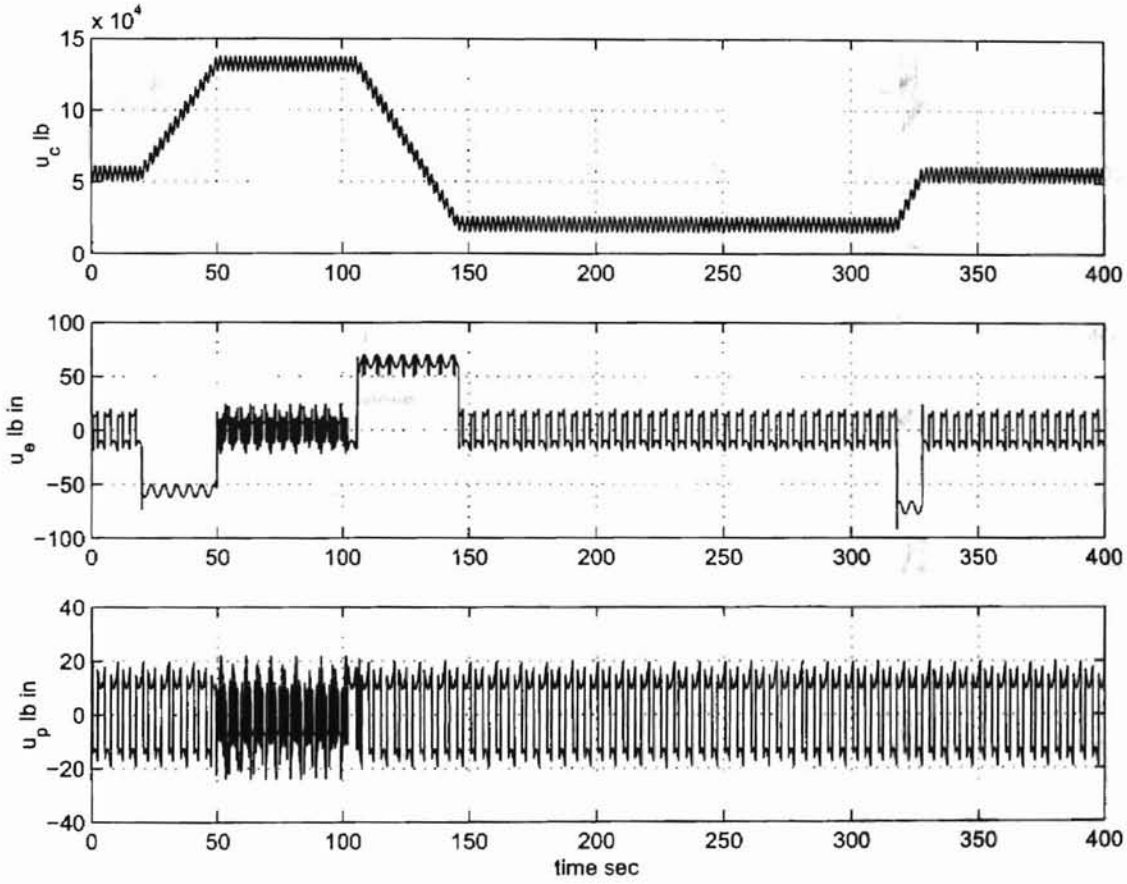


Figure 4.6: Control inputs for the proposed controller: Disturbance 1.

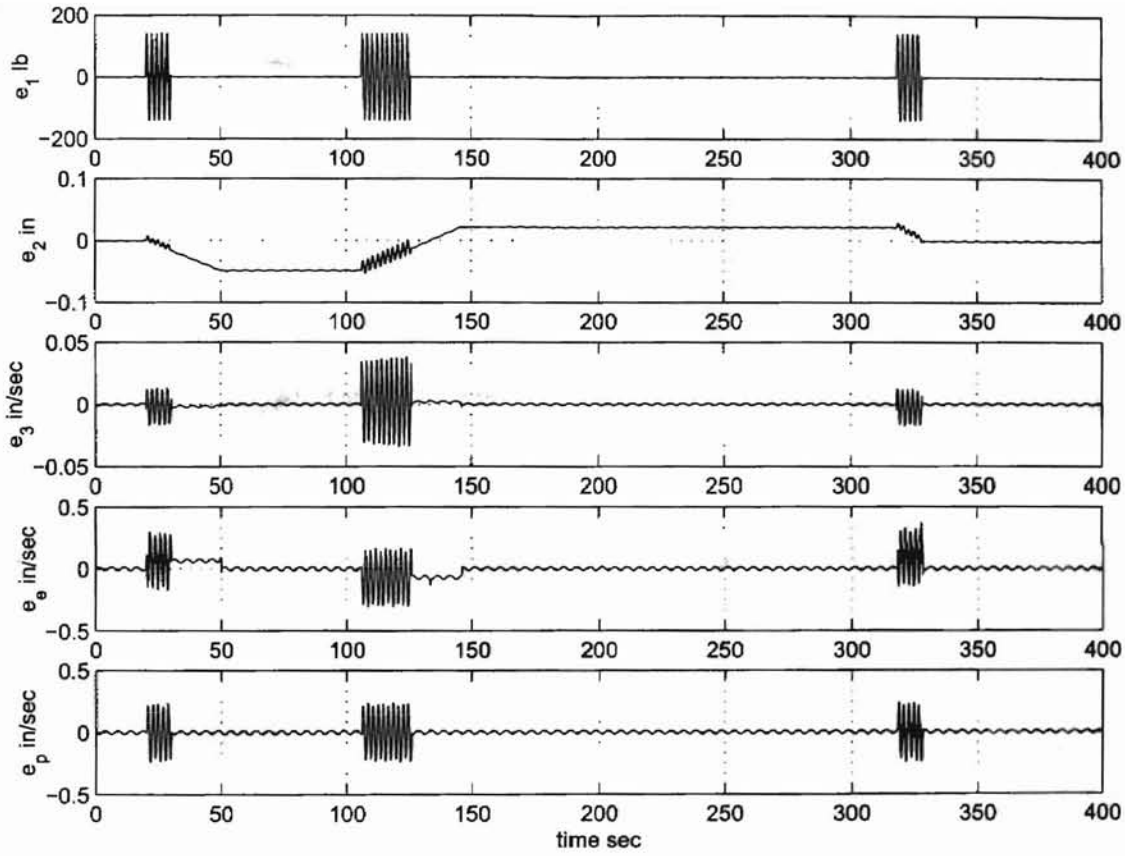


Figure 4.7: State errors of the industrial controller: Disturbance 2.

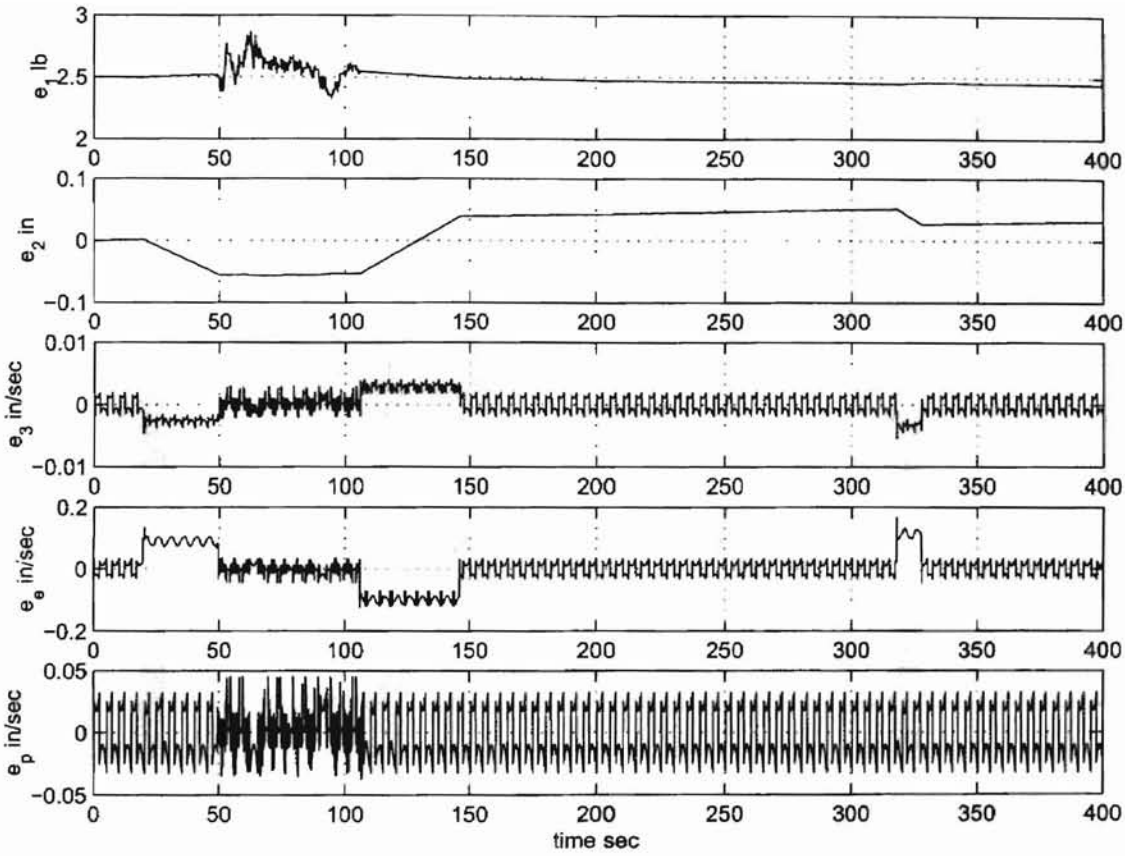


Figure 4.8: State errors of the proposed controller: Disturbance 2.

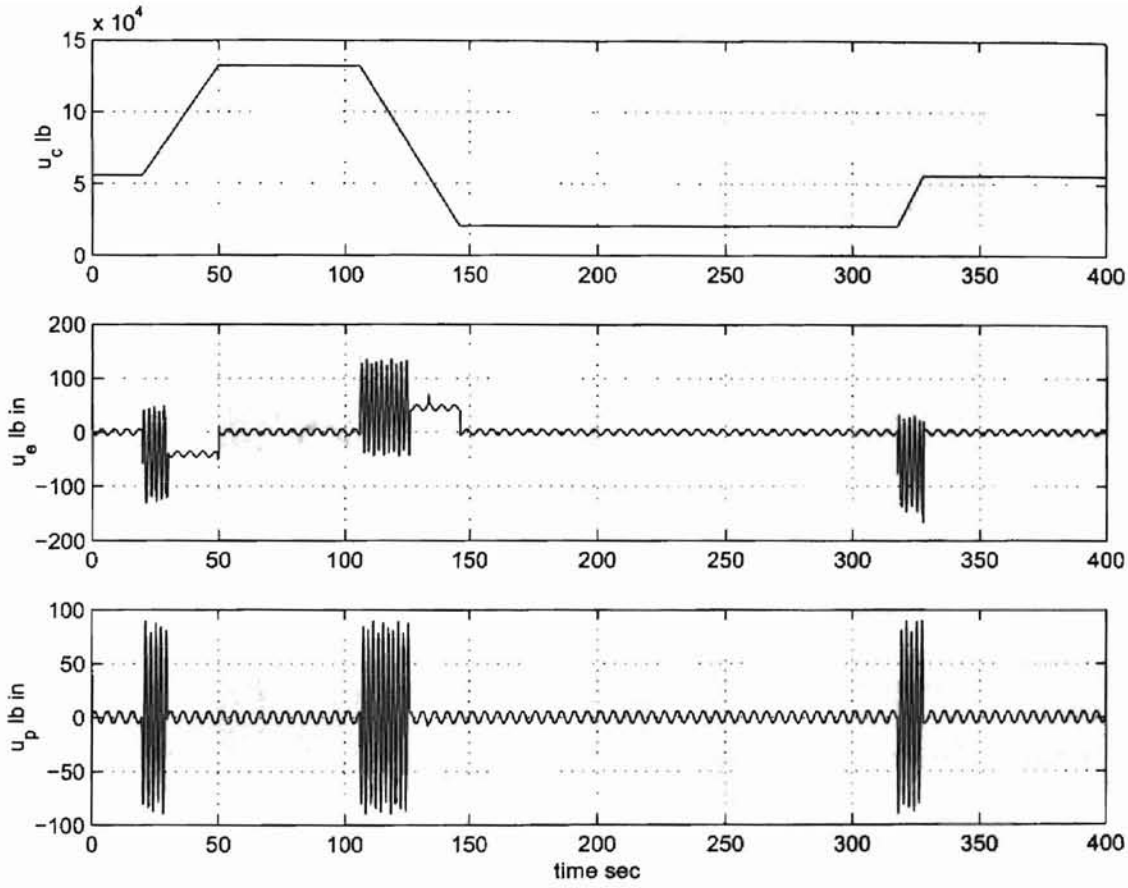


Figure 4.9: Control inputs for the industrial controller: Disturbance 2.

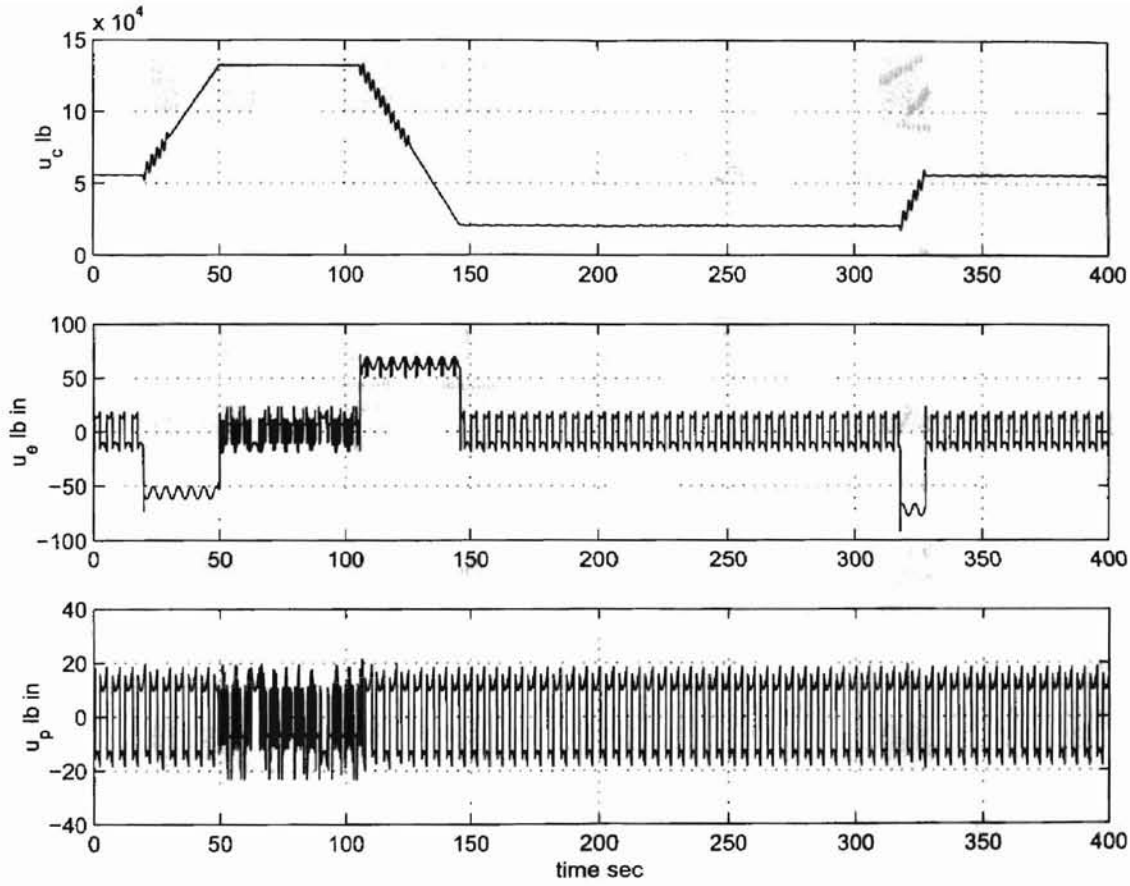


Figure 4.10: Control inputs for the proposed controller: Disturbance 2.

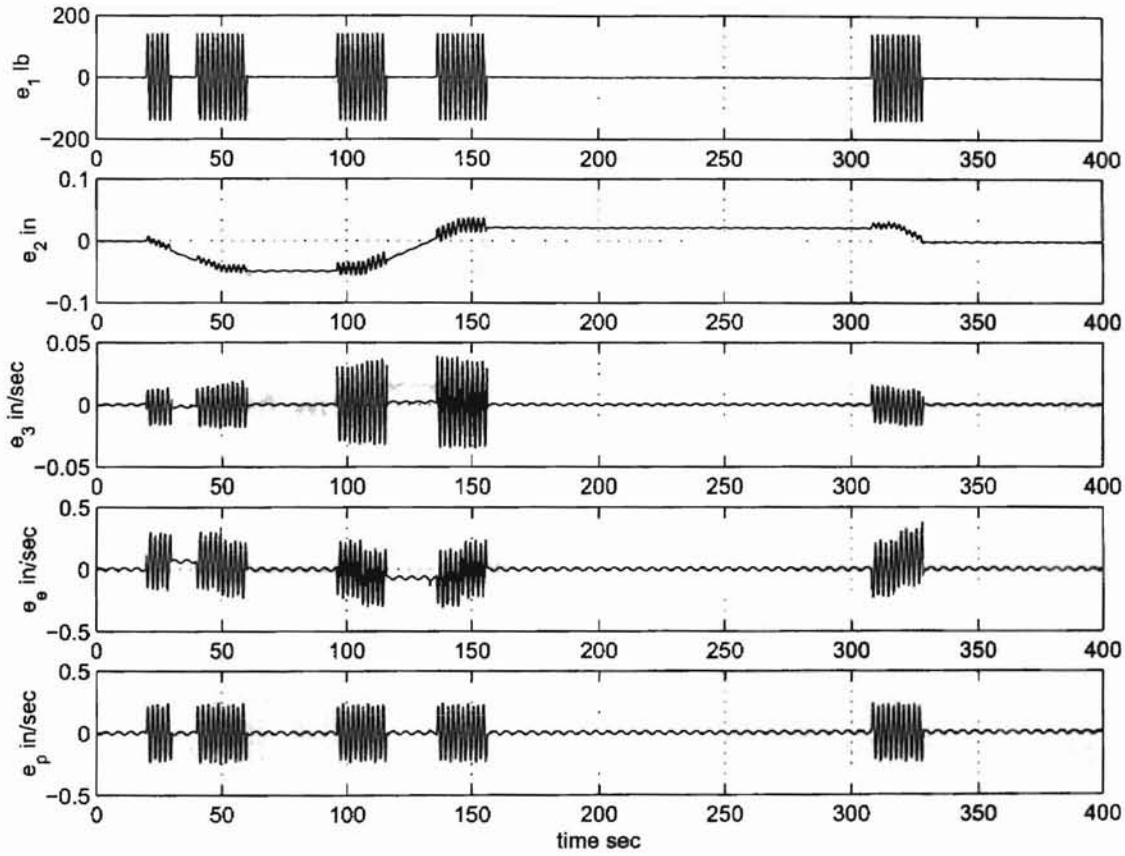


Figure 4.11: State errors of the industrial controller: Disturbance 3.

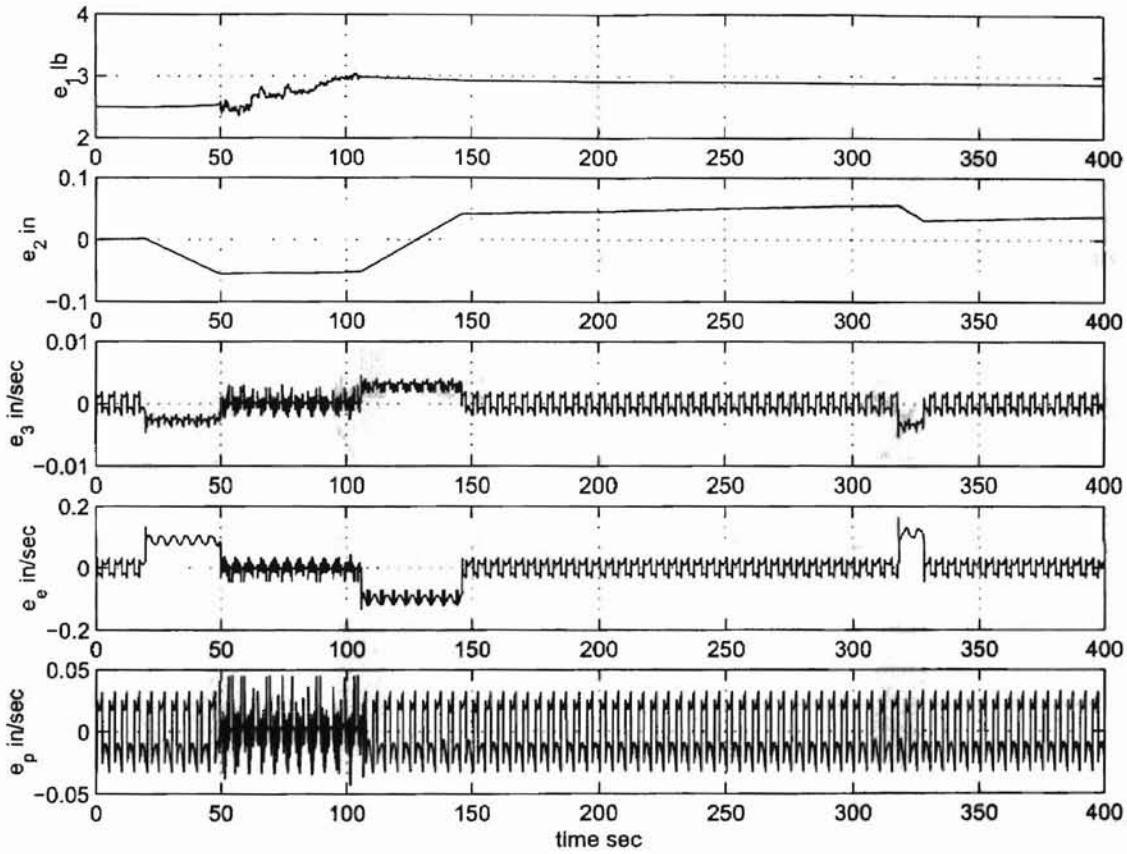


Figure 4.12: State errors of the proposed controller: Disturbance 3.

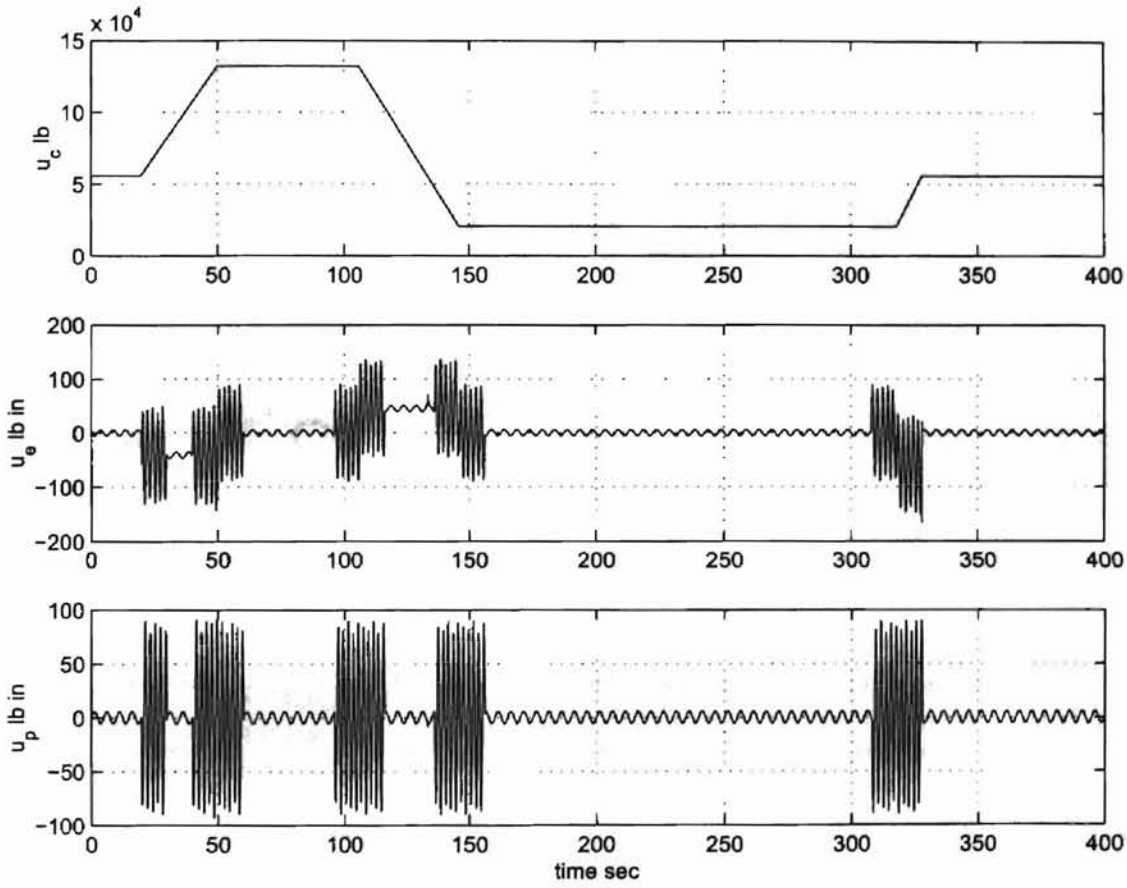


Figure 4.13: Control inputs for the industrial controller: Disturbance 3.

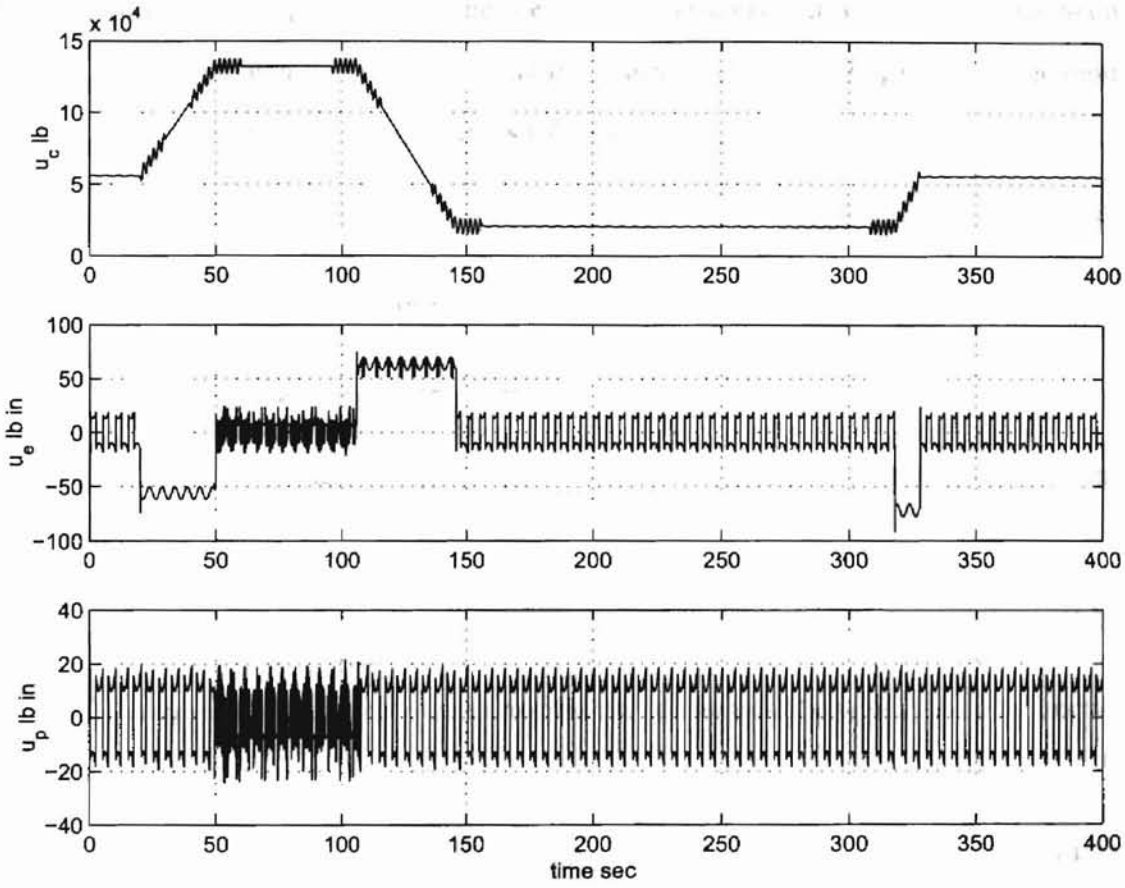


Figure 4.14: Control inputs for the proposed controller: Disturbance 3.

## 4.2 Controller Design Incorporating Adaptation Law for Friction Coefficient

Friction is a complicated phenomenon, which exists in all mechanical systems. Knowledge of the friction coefficients is essential for a stable controller design, which may not be practically feasible. High accuracy control cannot be achieved if friction effect is not considered properly. Therefore, an adaptation law is designed for friction coefficient along with a stable closed loop controller. The coefficient of viscous friction will be estimated online. Considering the same error definitions and control inputs $u_e$ and $u_p$ given by equations (4.2) and (4.3), as in section 4.1 and $u_c$ as follows:

$$u_c(t) = M_c(\dot{\xi}_3^d(t) + g + \frac{\widehat{v}_f}{M_c}\xi_3^d(t) + \frac{N}{M_c}\xi_1^d + u_{ca}(t)), \tag{4.31}$$

gives the same error dynamics for $e_1$, $e_2$, $e_e$, $e_p$ and new error dynamics for $e_3$:

$$\dot{e}_3(t) = -\frac{N}{M_c}e_1(t) - \frac{v_f}{M_c}\xi_3(t) + \frac{\widehat{v}_f}{M_c}\xi_3^d + u_{ca}(t). \tag{4.32}$$

By adding and subtracting the term $\frac{v_f}{M_c}\xi_3^d$ from equation (4.32) and rearranging term this equation can be written as:

$$\dot{e}_3(t) = -\frac{N}{M_c}e_1(t) - \frac{v_f}{M_c}e_3(t) + \frac{\widetilde{v}_f}{M_c}\xi_3^d + u_{ca}(t), \tag{4.33}$$

where $\widetilde{v}_f = \widehat{v}_f - v_f$. Considering the same observer dynamics, the new Lyapunov function candidate will be:

$$V_c^{mod}(t) = V_c(t) + \frac{1}{2}\alpha\widetilde{v}_f^2(t), \tag{4.34}$$

where $\alpha$ is a positive gain. The new derivative of the Lyapunov function candidate along the trajectories of the error dynamics is given by:

$$\dot{V}_c^{mod}(t) = \dot{V}_c(t) + \frac{\widetilde{v}_f}{M_c}\xi_3^d e_3 + \alpha\widetilde{v}_f\dot{\widetilde{v}}_f. \tag{4.35}$$

Following the same process to choose $u_{ca}(t)$, $u_{ea}(t)$, $u_{pa}(t)$, as per equations (4.13), (4.19), (4.20) and if we let

$$\frac{\widetilde{v}_f}{M_c}\xi_3^d e_3 + \alpha\widetilde{v}_f\dot{\widetilde{v}}_f = 0, \tag{4.36}$$

then the adaptation law is given as follows:

$$\dot{\widetilde{v}}_f = -\frac{1}{\alpha}\frac{\xi_3^d}{M_c}e_3. \tag{4.37}$$

Since actual parameter $v_f$ is not varying, $\dot{\widetilde{v}}_f = \dot{\widehat{v}}_f$. So above equation can be rewritten as:

$$\dot{\widehat{v}}_f = -\frac{1}{\alpha}\frac{\xi_3^d}{M_c}e_3. \tag{4.38}$$

Using these auxiliary control inputs and the term $\widehat{f}_{\xi_1}$ as per equation (4.22), the same conclusion can be made as in section 4.1. Therefore, $V^{mod}(t) \geq 0$ is a non increasing function of time for all $t \geq 0$. Hence, $V^{mod}(t) \in \mathcal{L}_\infty$ and $\lim_{t\to\infty} V^{mod}(t) = V_\infty < \infty$. Also, $e_1(t), \widetilde{e}_1(t), e_2(t), e_3(t), e_e(t), e_p(t), \widetilde{v}_f(t) \in \mathcal{L}_\infty$ and $e_2(t), e_3(t), e_e(t), e_p(t) \in \mathcal{L}_2$. From the error dynamics, (4.5)–(4.8), $\dot{e}_2(t), \dot{e}_3(t), \dot{e}_e(t), \dot{e}_p(t) \in \mathcal{L}_\infty$. Therefore, using Barbalat's lemma, we have $e_2(t), e_3(t), e_e(t), e_p(t) \to 0$ as $t \to \infty$.

The following theorem summarizes the results of this section.

**Theorem 4.2.1** *For the dynamics of the accumulator carriage and the driven rollers upstream and downstream of the accumulator given by equations* (2.46) *through* (2.51)*, the following control inputs,*

$$u_c(t) = M_c(\dot{\xi}_3^d(t) + g + \frac{\widehat{v}_f(t)}{M_c}\xi_3^d(t) + \frac{N}{M_c}\xi_1^d - \frac{AE}{\xi_2(t)}\widehat{e}_1(t) - e_2(t) + \frac{N}{M_c}\widehat{e}_1(t) - \gamma_3 e_3(t)), \tag{4.39}$$

$$u_e(t) = \frac{J}{RK_e}\left(-\gamma_e e_e(t) - \left(\frac{AE}{N\xi_2(t)} - \frac{R^2}{J}\right)\widehat{e}_1(t) - \frac{R^2}{J}\bar{\delta}_e sgn(e_e) + \frac{B_{fe}}{J}\xi_4^d(t) + \dot{\xi}_4^d(t)\right), \tag{4.40}$$

$$u_p(t) = \frac{J}{RK_p}\left(-\gamma_p e_p(t) + \left(\frac{AE}{N\xi_2(t)} - \frac{R^2}{J}\right)\widehat{e}_1(t) - \frac{R^2}{J}\bar{\delta}_p sgn(e_p) + \frac{B_{fp}}{J}\xi_5^d(t) + \dot{\xi}_5^d(t),\right) \tag{4.41}$$

*the average tension observer and the adaptation law*

$$\dot{\widehat{\xi}}_1(t) = \left(\frac{2AE}{\xi_2(t)} - \frac{N}{M_c}\right)e_3(t) + \left(\frac{2AE}{N\xi_2(t)} - \frac{R^2}{J}\right)(e_e(t) - e_p(t)),\ \widehat{\xi}_1(0) = \widehat{\xi}_{10} \tag{4.42}$$

$$\dot{\widehat{v}}_f(t) = -\frac{1}{\alpha}\frac{\xi_3^d(t)}{M_c}e_3(t), \tag{4.43}$$

*will result in the signals* $e_1(t), \widetilde{e}_1(t), e_2(t), e_3(t), e_e(t), e_p(t), \widetilde{v}_f(t)$ *being bounded and further, the signals* $e_3(t), e_e(t), e_p(t)$ *asymptotically converge to zero.*

The simulations are conducted using the system model given by equations (2.46)-(2.51) and the control algorithms given by (4.39), (4.40), (4.41), the observer given by equation (4.42) and adaptation law given by equation (4.43). The simulations are performed for first case of disturbance. The results are shown in Figures 4.15 through 4.17. For this disturbance the following errors are shown: web tension error ($e_1$), carriage position error ($e_2$), carriage velocity error ($e_3$), exit velocity error ($e_e$), and process velocity error ($e_p$). The control signals of accumulator carriage, exit-side driven roller, and process-side driven roller for both controllers are also shown.

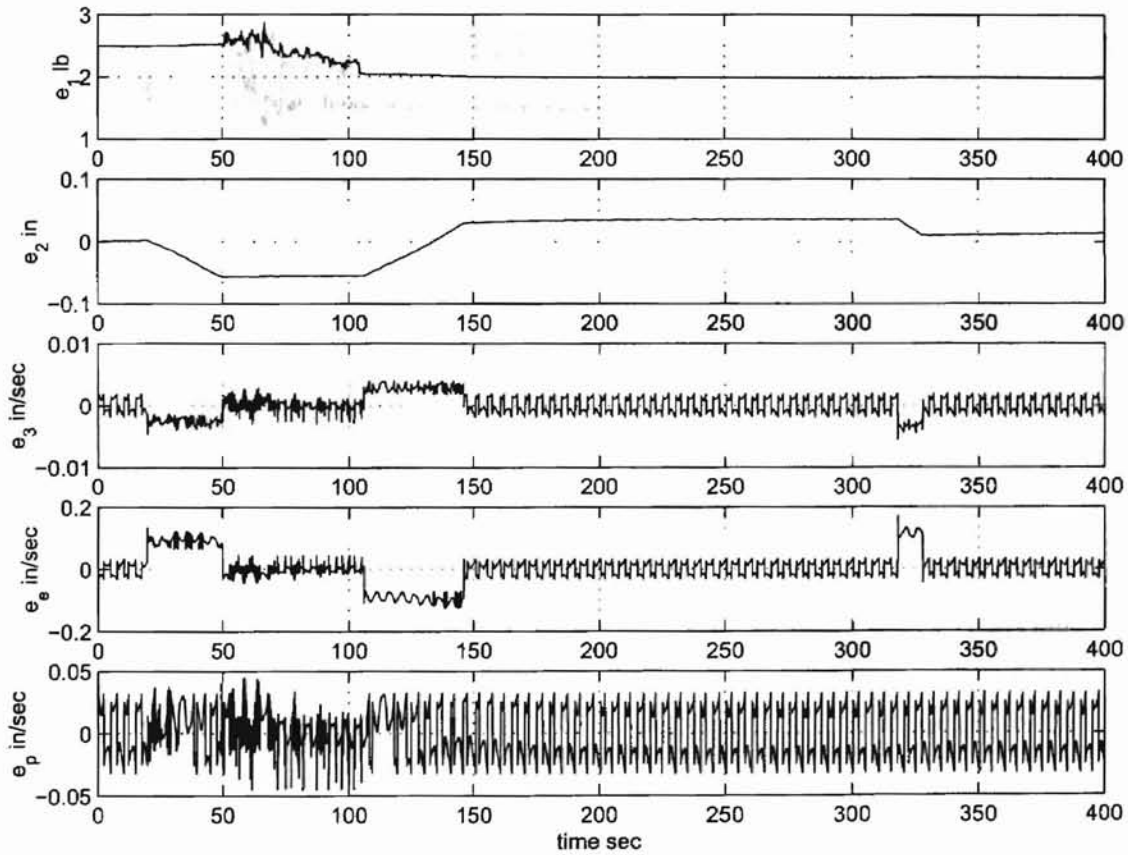


Figure 4.15: State errors of the proposed controller with adaptation law: Disturbance 1.

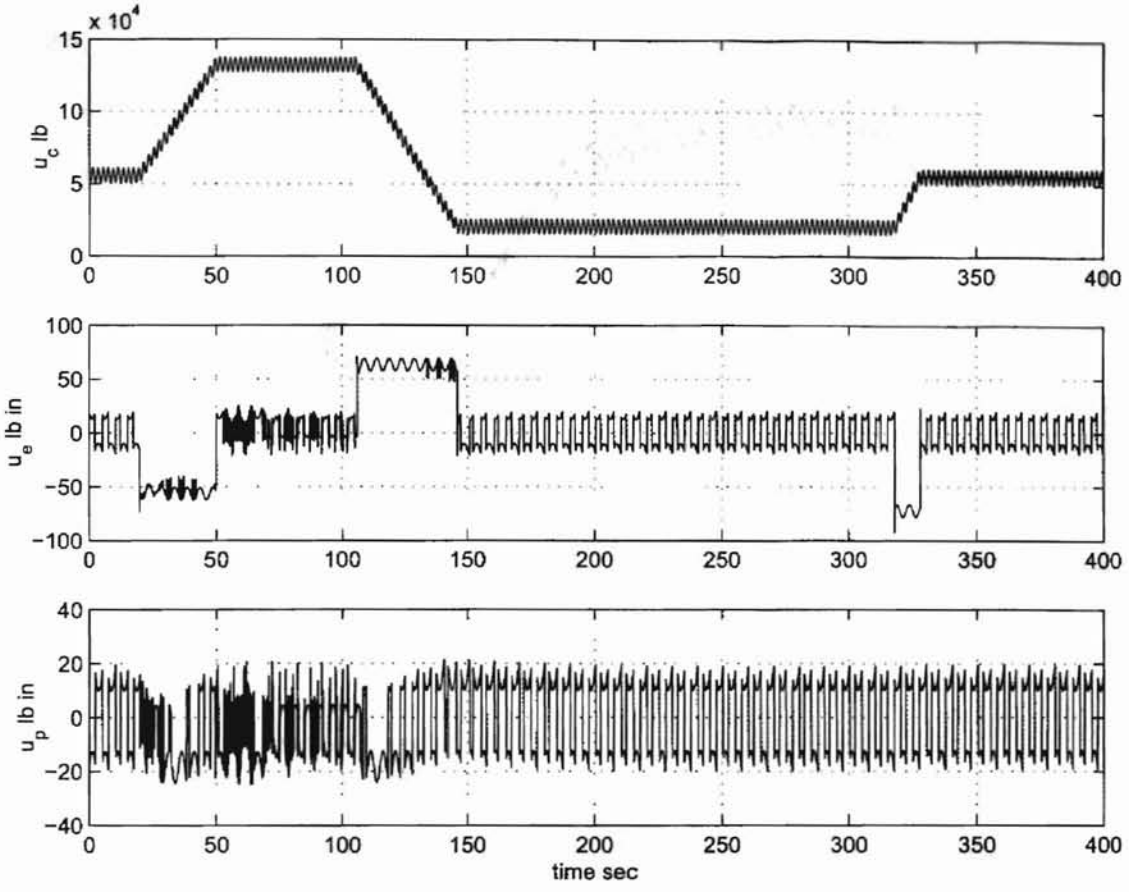


Figure 4.16: Control inputs for the proposed controller with adaptation law: Disturbance 1.

All the state errors are very low. The results are similar to what is earlier shown. Figure 4.17 shows how the estimate of viscous friction coefficient is behaving.

### 4.3 Simulation Study Considering Web Span Weight Acting on the Carriage

In section 3.1.3, the change in web span weight acting on carriage is discussed, as the carriage is in motion. In metal industry, if the thickness of web material is in the range of 1/8th of an inch, the change in web span weight acting on carriage is considerable as shown in Figure 3.2. In this section the effect of this weight change is studied with simulations for the proposed controller and for industrial control scheme. The simulations are performed

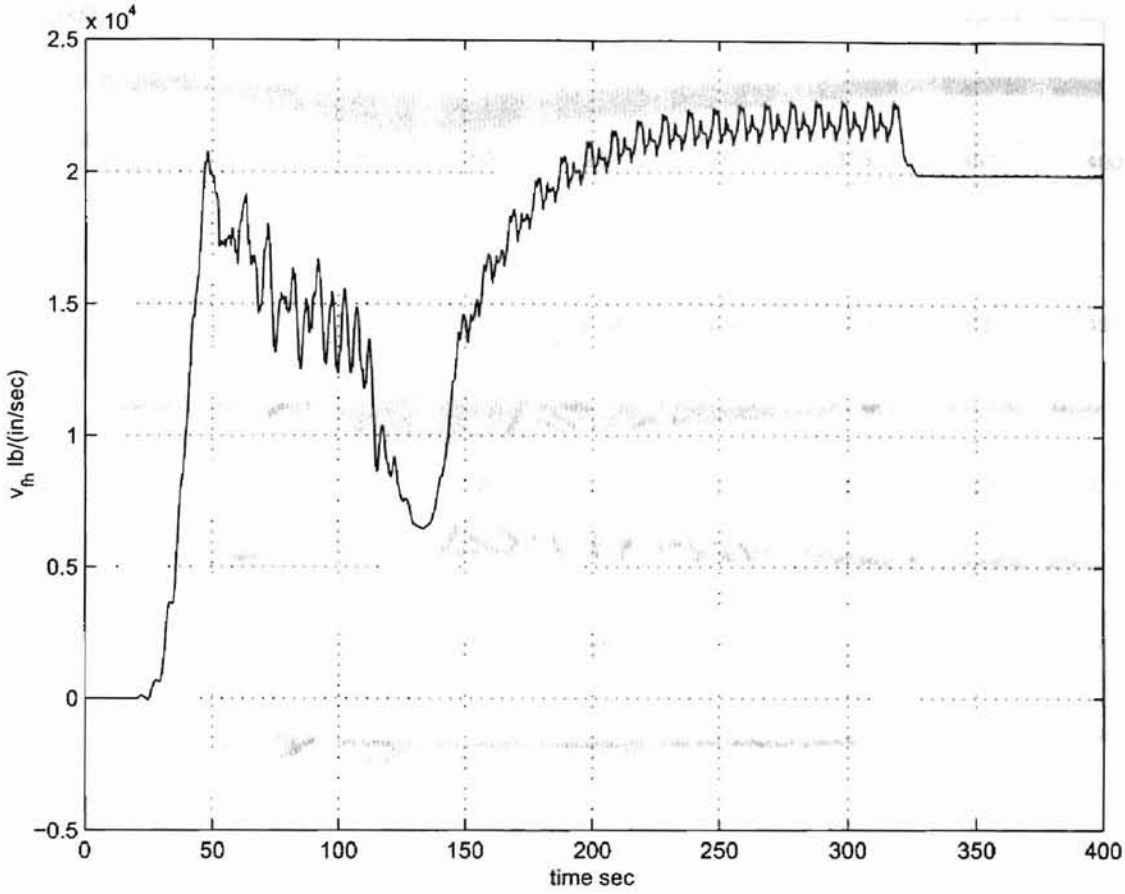


Figure 4.17: Viscous friction coefficient estimation for the proposed controller: Disturbance 1.

for first case of disturbance used in section 4.1. Figures 4.18 through 4.21 are corresponding to case when in the actual model the effect of varying mass is considered by replacing $M_c$ with $M_c + NA\xi_2\rho$ and there is no compensation for this varying mass in the controller. In case of industrial controller the variations in tension are very high. If no compensation is being used for varying mass the tension is dropping to a low value, i.e., a part of control effort is being used to compensate for weight change and there is not enough effort to account for average total tension required in all the web spans. The proposed controller is performing well in this case also. Even though there is no compensation for weight change in controller, the control algorithm is accounting for weight change as the control effort

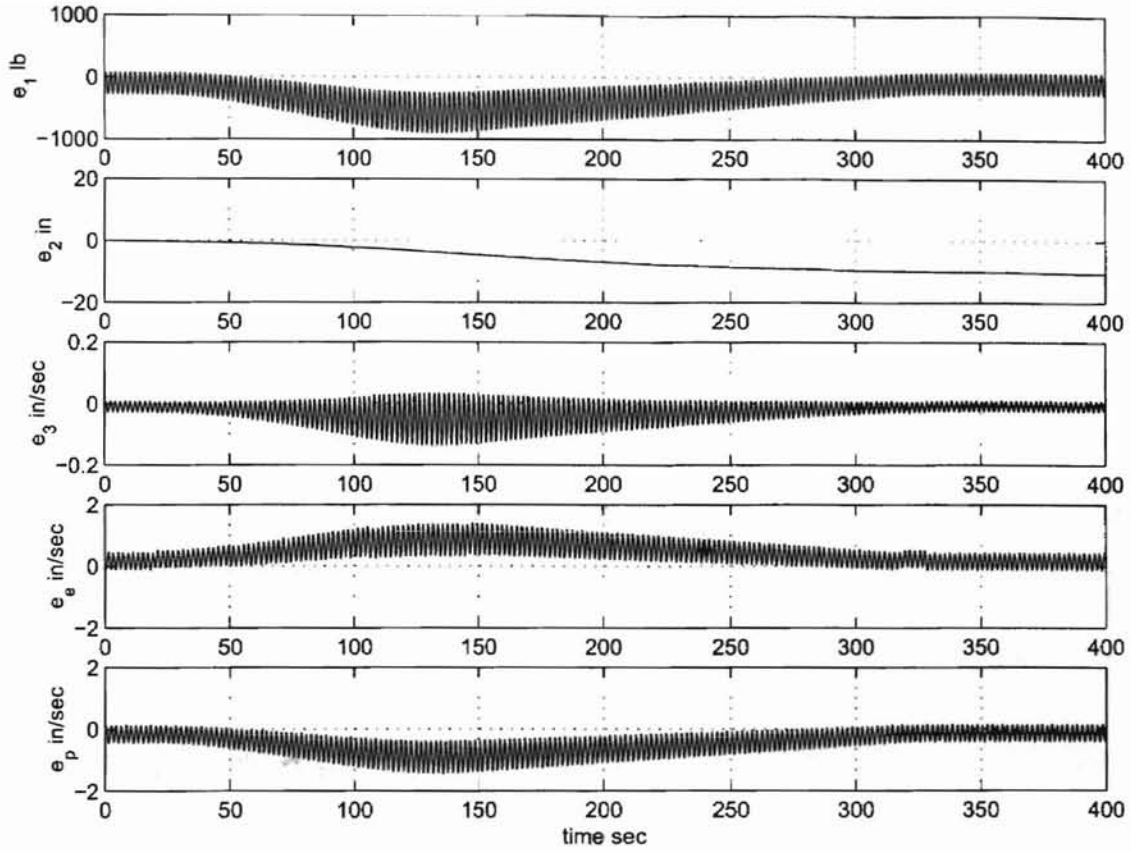


Figure 4.18: State errors of the industrial controller: No compensation for varying mass.

required in the case of proposed controller is much higher than the industrial controller. Figures 4.23 through 4.25 are for the case when compensation for varying mass is considered in the process of controller design. Performance is improved in case of both type of controllers. Overall the proposed controller is showing more promising results.

## 4.4 Synopsis

In this chapter, design of a control algorithm for web tension regulation in an accumulator, in web processing lines, is considered. A feedback controller together with an observer for web tension is proposed. It is shown that the proposed feedback controller results in a stable closed-loop system. Simulation results on an industrial continuous web processing line are given and discussed for the proposed controller/observer and compared with a

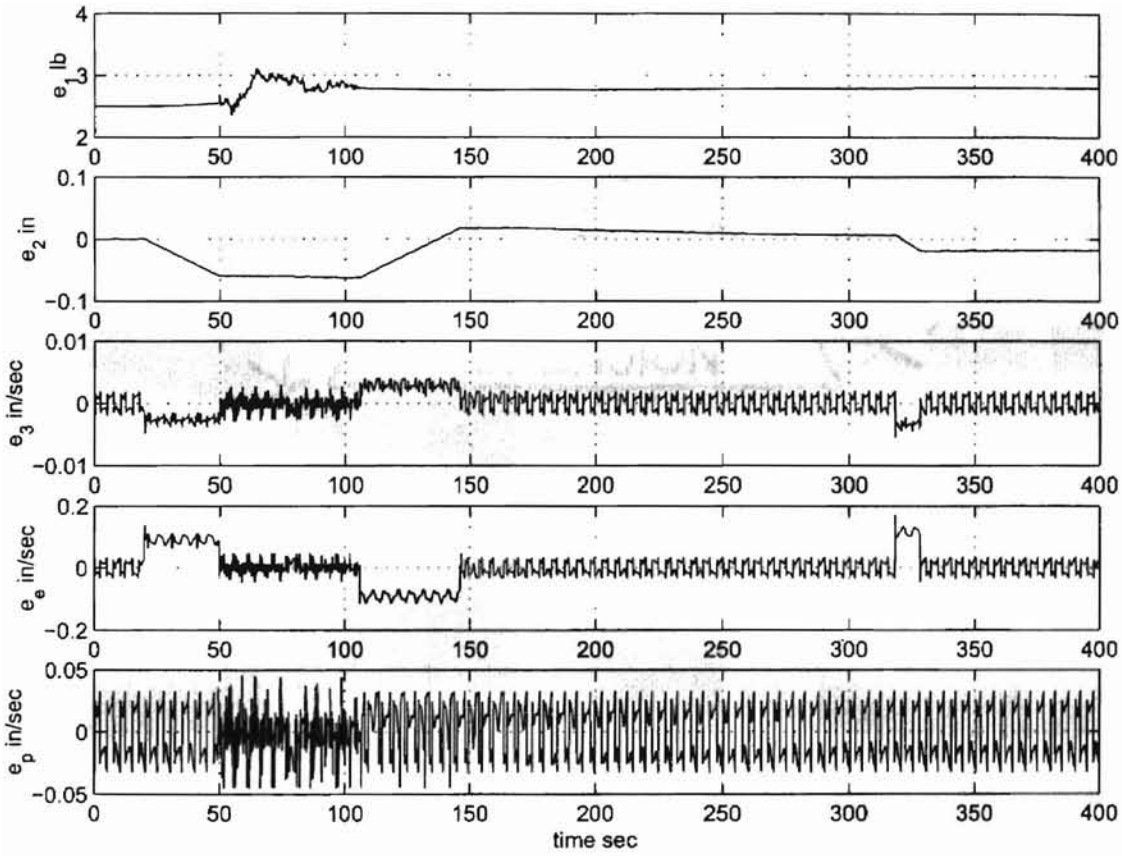


Figure 4.19: State errors of the proposed controller: No compensation for varying mass.

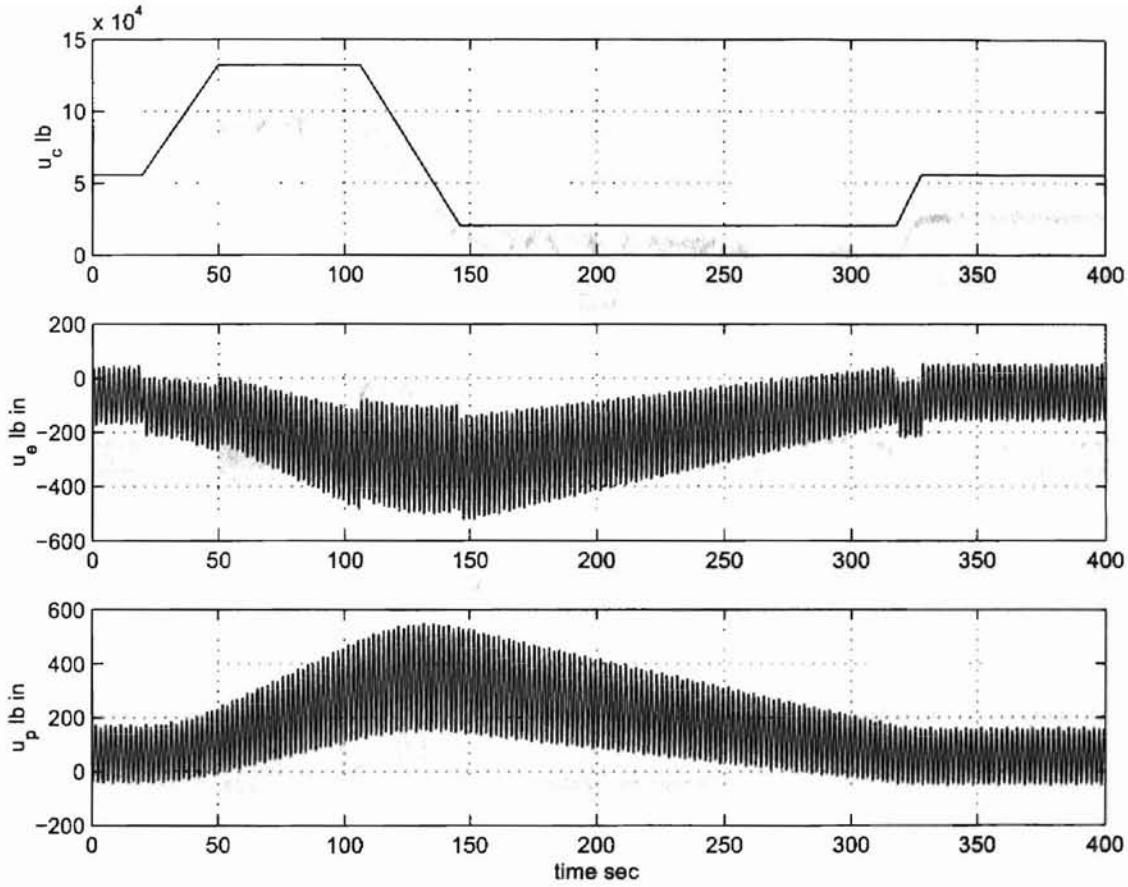


Figure 4.20: Control inputs for the industrial controller: No compensation for varying mass.

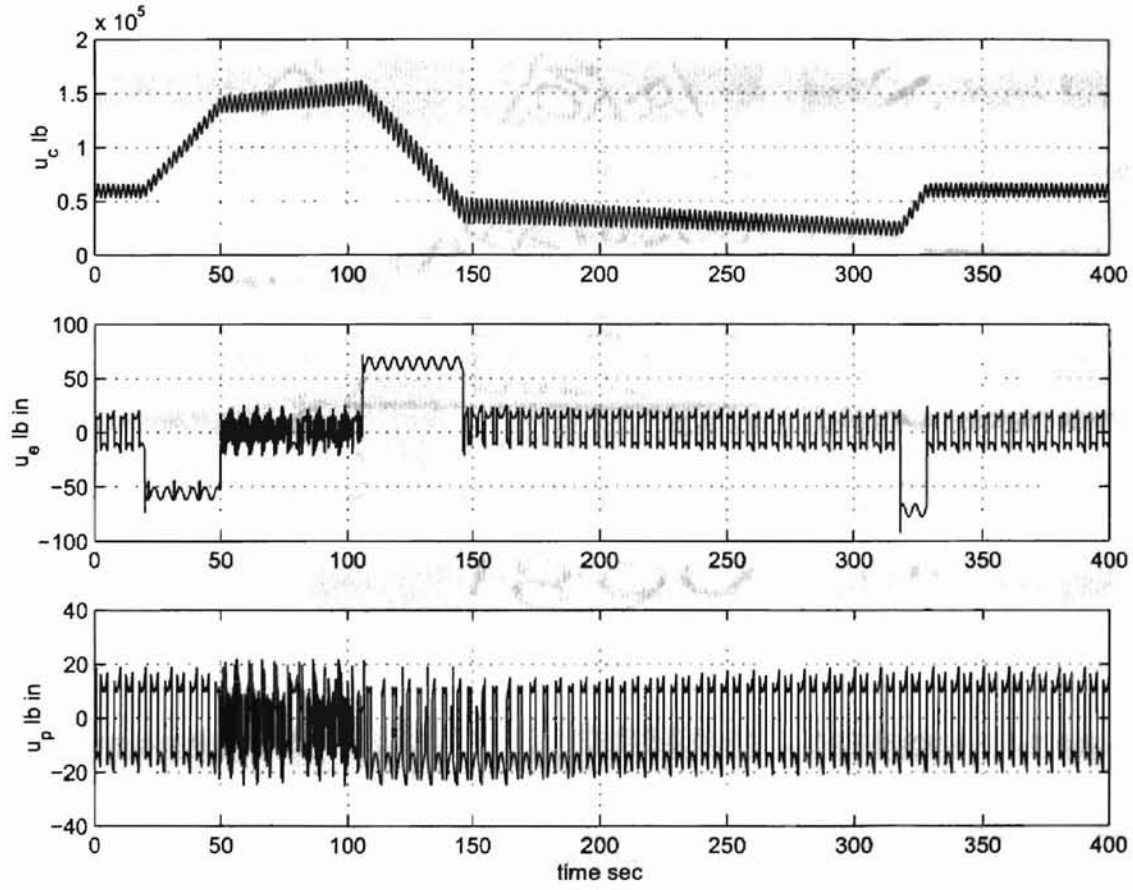


Figure 4.21: Control inputs for the proposed controller: No compensation for varying mass.

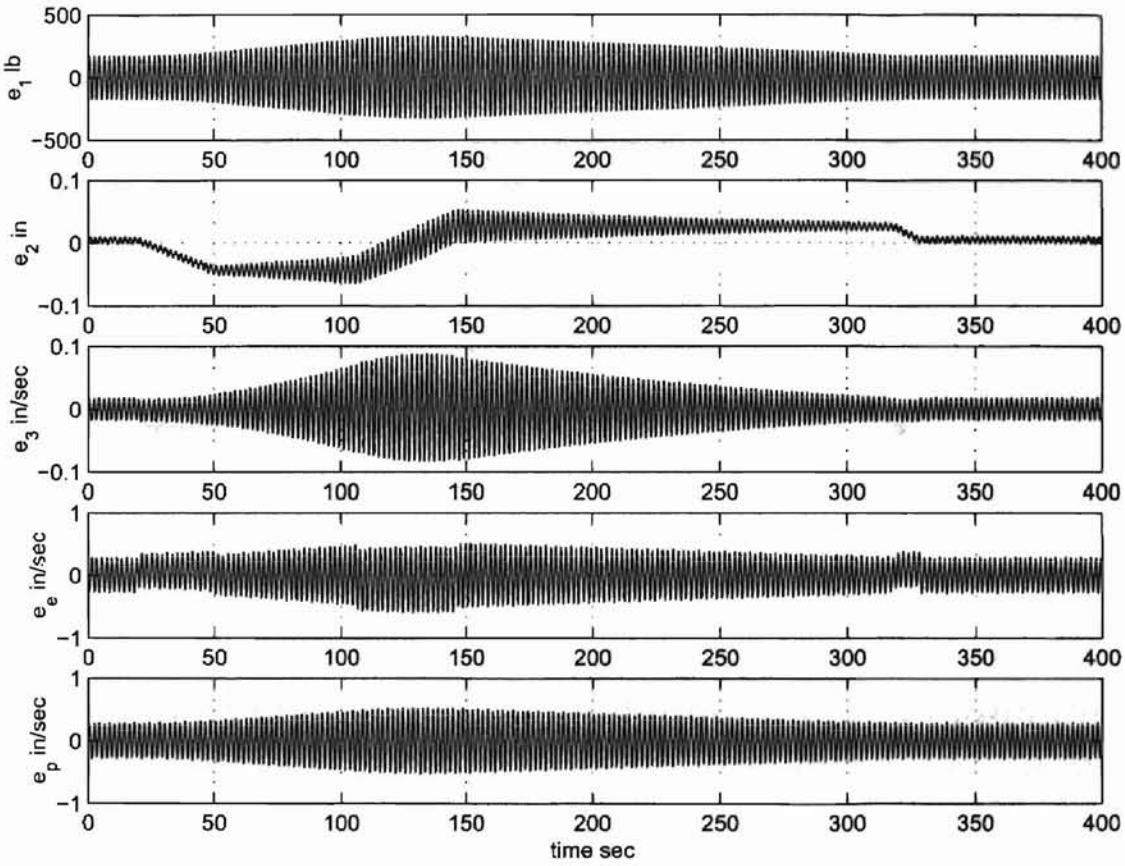


Figure 4.22: State errors of the industrial controller with compensation for varying mass.

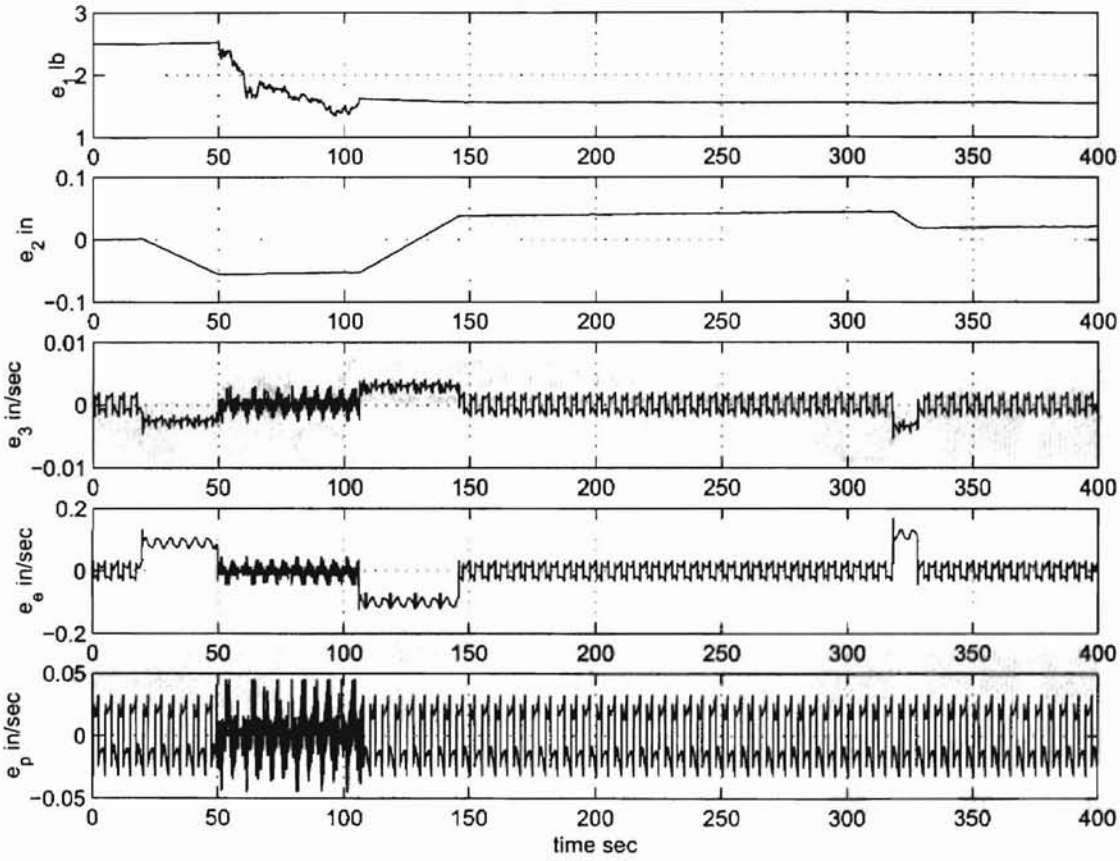


Figure 4.23: State errors of the proposed controller with compensation for varying mass.

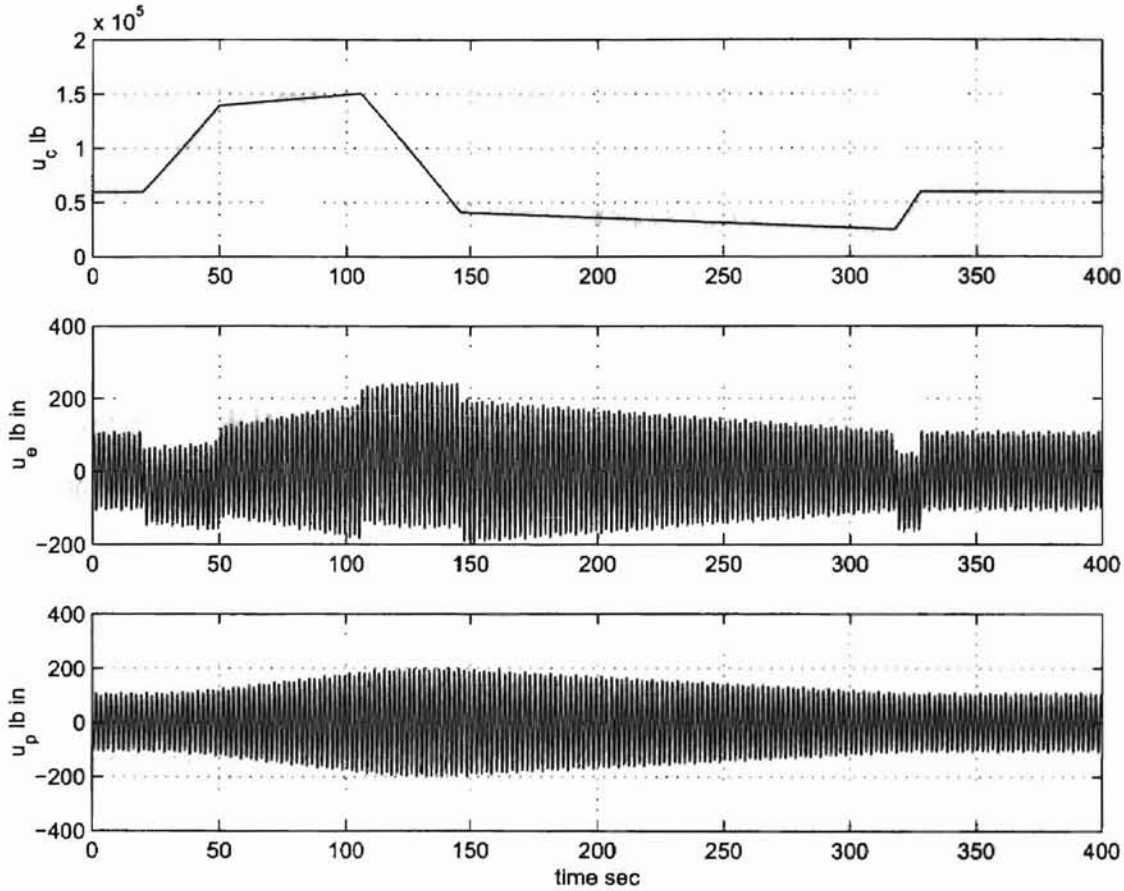


Figure 4.24: Control inputs for the industrial controller with compensation for varying mass.

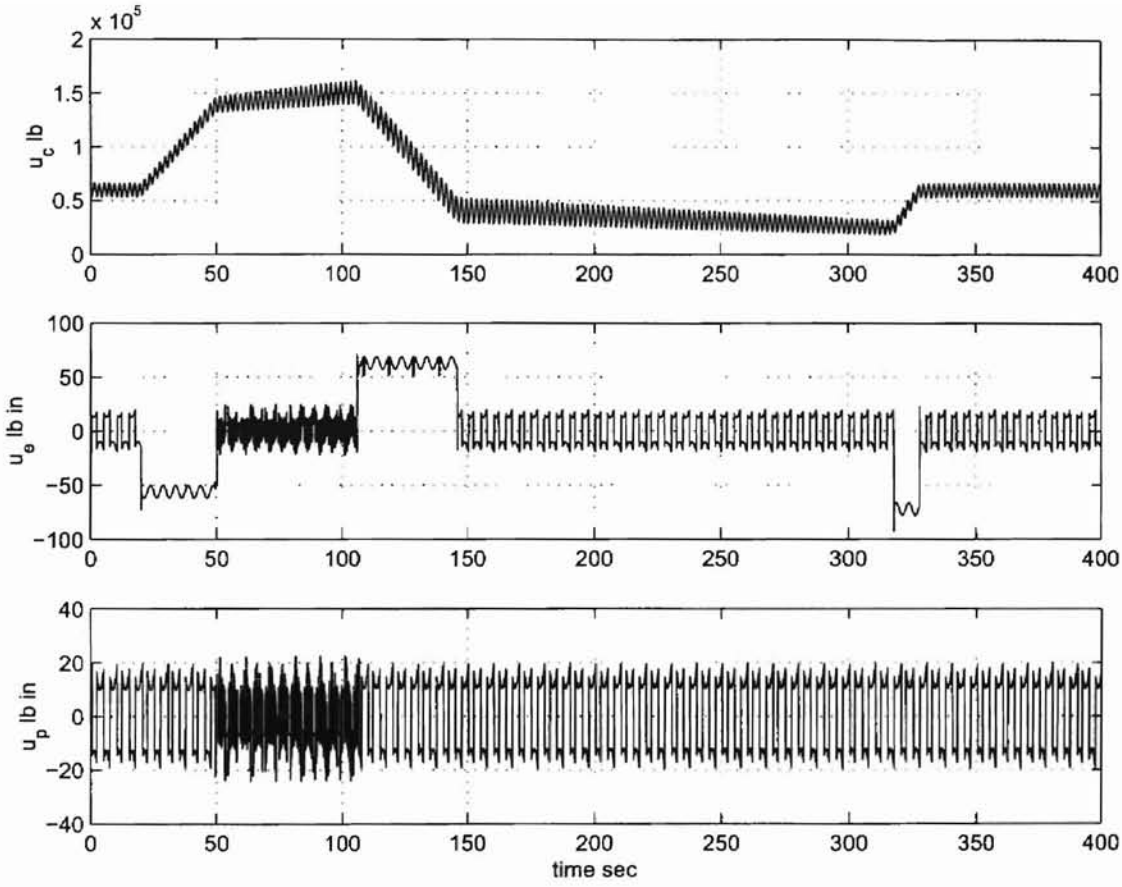


Figure 4.25: Control inputs for the proposed controller with compensation for varying mass.

currently used industrial controller. The effect of change in web spans weight acting on the carriage and adaptation law for viscous friction coefficient in case of uncertainties is also considered. Simulations are performed for these cases also.

# CHAPTER 5

## CONCLUSIONS AND FUTURE RESEARCH

Feedback control algorithms for the accumulator carriage, and for the upstream and downstream driven rollers to the accumulator, are designed for tracking the desired exit and process web velocities, and to maintain the web tension at the desired level. It is common in the web handling industry to just apply a desired force on the carriage using a hydraulic system in opposition to the carriage weight and the force required to produce desired tension in all the accumulator web spans; thus, ignoring the dynamics of the carriage motion. This strategy often leads to large tension variations not only in the accumulator web spans but also in web spans in the entire process line due to tension disturbance propagation both upstream and downstream of the accumulator. Simulation results comparing the proposed control algorithm with the currently used control scheme in industry show that the proposed control algorithm results in much less web tension variations.

Friction is a complicated phenomenon, which exists in all mechanical systems. Knowledge of the friction coefficients is essential for a stable controller design, which may not be practically feasible. High accuracy control cannot be achieved if friction effect is not considered properly. Therefore, an adaptation law is designed for friction coefficient along with a stable closed loop controller. The control scheme along with this adaptation law shows the same performance. Estimating the friction coefficient is a more practical approach, which has been attained in this dissertation.

The weight of the web spans acting on the carriage changes with the carriage motion. The effect of the weight of the web on the accumulator carriage can effect the tension in the web spans in a substantial way. The weight of the web on the carriage can be substantial in

metal process lines where the thickness of the web can be as high as 0.2 inches. The effect of this time-varying weight is also investigated in this dissertation. The proposed controller is accounting for this weight change, with minimal variations in tension in web spans.

## 5.1 Future Research

This research also provides a solid background for some further advanced study on accumulators. Instead of assuming that the force on the carriage is directly accessible as an input, future work should include the dynamics of the actuator, either electro-hydraulic or electro-mechanical, coupled with the dynamics of the carriage and the web spans. Although a friction model that includes linear viscous friction is proposed, better friction modeling may be required for accumulators as these have some of the peculiar friction characteristics. There is a need to conduct experiments on a processing line with a well designed experimental procedure. This can better validate the concepts developed and provide directions to iterate on these concepts to better model and control the dynamic behavior.

## BIBLIOGRAPHY


[1] D.P. Campbell, Dynamic Behavior of the Production Process, Process Dynamics. *John Wiley and Sons, Inc.*, New York, 1958.

[2] K.P. Grenfell, "Tension control on paper-making and converting machinery," *Proc. of the 9th IEEE Annual Conf. on Electrical Engineering in the Pulp and Paper Industry*, Boston, MA, June, 1963.

[3] D. King, "The mathematical model of a newspaper press," *Newspaper Techniques*, December, 1969.

[4] G. Brandenburg, "New mathematical models for web tension and register error," *Proc. of the 3rd Intl. IFAC Conf. on Instrumentation and Automation in the Paper, Rubber, and Plastics Industry*, vol. 1, pp. 411-43, 1977.

[5] W. Wolfermann, & D. Schroder, "New Decentralized Control in Processing Machines with Continuous Moving Webs," *Proc. of the Second Intl. Conf. on Web Handling*, June 6-9, 1993.

[6] G.E. Young and K.N. Reid, "Lateral and longitudinal dynamic behavior and control of moving webs," *ASME Journal of Dynamic Systems, Measurement, and Control*, vol. 115, pp. 309–317, June, 1993.

[7] W. Wolfermann, "Tension control of webs – A review the problems and solutions in the present and future," *Proc. of the Third Intl. Conf. on Web Handling*, Stillwater, OK, June, 1995.

[8] J.J. Shelton, "Limitations to sensing of web tension by means of roller reaction forces," *Proc. of the Fifth Intl. Conf. on Web Handling*, Stillwater, OK, June, 1999.

[9] P.R. Pagilla, S.S. Garimella, L.H. Dreinhoefer, and E.O. King, "Dynamics and control of accumulators in continuous strip processing lines," *IEEE Transactions on Industry Applications*, vol. 37, no. 3, pp. 934–940, 2001.

[10] P.R. Pagilla, E.O. King, L.H. Dreinhoefer, and S.S. Garimella, "Robust observer-based control of an aluminium strip processing line," *IEEE Transactions on Industry Applications*, vol. 36, no. 3, pp. 835–840, 2000.

VITA

Inderpal Singh

Candidate for the Degree of

Master of Science

Thesis: A STUDY ON CONTROL OF ACCUMULATORS IN CONTINUOUS WEB PROCESSING LINES

Major Field: Mechanical Engineering

Biographical:

Personal Data: Born in India, on April 3, 1977, the son of Balwant Singh and Jaswant Kaur.

Education: Received the B.S. degree from Thapar Institute of Engineering & Technology, Punjab, India, in 1998, in Mechanical Engineering; Completed the requirements for the Master of Science degree with a major in Mechanical Engineering at Oklahoma State University in December, 2002.

Experience: Research Assistant at Oklahoma State University from August 2000 to December 2002; Teaching Assistant at Oklahoma State University from August 2000 to August 2002; Design Engineer at ISGEC, Haryana, India from July 1998 to July 2000.

Professional Memberships: American Society of Mechanical Engineers, Honorary Society of Phi Kappa Phi.